THE UNIVERSITY OF ADELAIDE

DEPARTMENT OF MECHANICAL ENGINEERING

TRANSIENT MODELLING

OF FINNED TUBE

HEAT EXCHANGERS

by

Gijsbertus J. Van Aken

Dip.Mech.Eng. (RMIT)
Grad.Dip.Auto.Control (RMIT)
M.I.E.Aust.

THESIS FOR THE DEGREE OF

MASTER OF ENGINEERING SCIENCE

March 1993

Awarded 1993

TRANSIENT MODELLING OF FINNED TUBE HEAT EXCHANGERS

CONTENTS

CONTENTS

LIST OF APPENDICES

A. FLOW INSIDE SMOOTH TUBES AND DUCTS - HEAT TRANSFER EQUATIONS

B. NORMAL AND ENHANCED HEAT TRANSFER AREAS OF FIN ELEMENTS

C. CORRELATION OF AIR SIDE HEAT TRANSFER WITH TEST DATA

D. SOFTWARE LIBRARIES

LIST OF FIGURES

LIST OF FIGURES *(continued)*

ABSTRACT

A complete performance evaluation of a heat exchanger includes an analysis of full load heat and mass transfer, part load performance, and its dynamic response.

Traditionally, heat and mass transfer calculations have been based on steady state overall heat transfer coefficients and the logarithmic mean temperature difference between the working fluids. This involves guessing the fin and tube surface temperatures and adjusting these until a balance is achieved between the heat fluxes inside the tubes and the external surface of the heat exchanger. Tube and fin temperatures are assumed to be uniform throughout with the fin area reduced by a factor to account for the temperature gradient along the fin to the tube. Heat exchanger time constants are approximated from empirical equations and tabulations.

The logarithmic mean temperature difference applies strictly to counter flow and parallel flow configurations only, and although it has been shown that it can be applied to cross flow systems, it cannot accommodate diverse coil circuit arrangements without use of 'correction' factors. The assumption of uniform fin and tube temperatures precludes the analysis of coils which are partially wet and partially dry.

A transient modelling technique is described in which the heat storage capacities of the working fluids, the tubes and the fins are recognised. The technique establishes the temperature gradients throughout the fluids and those within the tubes and fins for a number of heat exchanger sections. It can therefore be used to establish the true surface temperatures for each section.

Besides computing the rate of heat and mass transfer, the modelling procedure also simulates all the time lags associated with heat storage and fluid flow and it is therefore suitable for establishing the required characteristics for control of the heat exchanger.

STATEMENT

This thesis contains no material which has been accepted for the award of any other degree or diploma in any University and, to the best of the author's knowledge and belief, it contains no material previously published or written by another person, except where due reference is made in the text.

Gijsbertus J. Van Aken
March 1993

ACKNOWLEDGEMENTS

LIST OF SYMBOLS

The following list only shows those symbols that are common
to all sections of this thesis. Sections 5.0, 6.0, 8.0, and
Appendices A, B, and C have their own symbol definitions and
are therefore listed in their respective Sections. The
symbols defined throughout the thesis are also used in the
same format within the computer programs.

a	channel width = (Ct - Do)/1000	- m
Ac	minimum free flow area	- m²
Acr	total internal area / row for fluid flow	- m²
Af	face area of coil	- m²
Api	inside surface area of tubes per row	- m²
At(e)	heat transfer area for fin element(e)	- m²
Ato(e)	total heat tran. area of fin el(e)/row	- m²
B()	data storage vector in COILSIM	
C$	coil circuiting: <D>ouble serpentine	
	<S>ingle serpentine	
	<H>alf circuit	
	<T>hird circuit	
	<Q>uarter circuit	
Cc	heat capacity of coil material	- J/cc K
Cfin	specific heat of fin material	- kJ/kg K
Clht	coil height, at right angles to tubes	- mm
Clwi	coil width, parallel to tubes	- mm
Cm(e)	heat capacity of coil element(e) per row	- J/K
Cm1	heat capacity of tubes per row	- J/K
Cm2	heat capacity of fin component in el.(1)	- J/K
CNT%	simulation count	
Cp	specific heat for moist air	- kJ/kg K
Cr	centre distance between rows	- mm
Ct	centre distance between tubes	- mm
Cw	specific heat of water	- kJ/kg K
Cwr	heat capacity of water per row	- J/K
Da$	computer date	
Df	water vapour diffusion coefficient	- m²/s
Dh	hydraulic diameter	- m
Di	tube inside diameter	- mm
Do	effective tube outside diameter	- mm
Dp	tube outside diameter	- mm
DT	integration interval	- sec
DTmax	maximum permissable integration interval	- sec
Fg$	Fin Geometry:	
	<R>ectangular continuous plate fins	
	<C>oncentric circular plate fins	
Fm$	fin material: <A>luminium	
	<C>opper	
	<O>ther, def'd in COILPAR	
Fr	water flow rate inside tubes	- *l*/sec
FP	fin pitch	- mm

h(n)	air enthalpy entering row n	— kJ/kg air
ha	moist air enthalpy approaching fin el.	— kJ/kg air
hfg	latent heat of vaporisation for water	— kJ/kg water
hfin	heat capacity of fin material	— J/cc K
hfw	enthalpy of saturated liquid water	— kJ/kg water
hg	enthalpy of saturated water vapour	— kJ/kg water
hi	heat transfer coefficient inside tubes	— W/m² K
hn	standard convection heat transfer coeff.	— W/m² K
ho(e,c)	heat transfer coefficient for fin element(e) within configuration(c)	— W/m² K
hoc(e)	convection heat transfer coefficient for outside surface	— W/m² K
how	heat transfer coefficient for wet fins	— W/m² K
hp	heat capacity of tube material	— J/cc K
hs	enthalpy of saturated moist air on fins	— kJ/kg air
k	thermal conductivity	— W/m K
ka	thermal conductivity of air	— W/m K
kc	thermal conductivity of tubes	— W/m K
Ke	vortex enhancement factor	
kfin	thermal conductivity for fins	— W/m K
Km(e,c)	mean heat tran. enhancement for el.(e,c)	
Kr	reduced heat transfer factor for fins	
kw	thermal conductivity for water	— W/m K
Le	Lewis number (dimensionless)	
Ma	mass flow rate of dry air	— kg/sec
Mu	μ - dynamic viscosity (also Pa s or N s/m²)	— kg/m s
Nc%	number of coil sections per row	
Ncirc%	number of parallel circuits per row	
Nfin%	total number of fins over coil width	
Nrow%	number of rows in coil	
Nt%	number of tubes per row in use	
Ntc%	maximum number of tubes per row section	
Ntub%	number of tubes installed per row	
Nu	Nusselt number = h Dh / k	
Nu(H)	Nusselt number for constant heat rate	
Num	mean Nusselt number	
Nu∞	Nusselt number for fully developed laminar or turbulent flow	
Nu(T)	Nusselt number for constant surface temp.	
Nv%	Number of variables stored by COILSIM	
Pm$	tube material: <A>luminium <C>opper <O>ther, def'd in COILPAR	
Pr	Prandtl number = Cp μ/k (dimensionless)	
Pat	atmospheric pressure	— kPa
Pw	vapour pressure	— kPa
Pws	saturation vapour pressure	— kPa
Qa	air to fin heat transfer rate	— Watt
Qe(e)	el.(e+1) to el.(e) heat transfer rate	— Watt

R0	tube outside radius plus fin thickness	— m
R1	outer boundary rad. for inner fin element	— m
R2	outer boundary rad. for interm. fin el.	— m
R3	outer radius of equivalent circular fin	— m
Re	Reynolds number = Dh G/μ (dimensionless)	
Rea	air side Reynolds number (channel flow)	
Rent	air side Reynolds number (entering fins)	
Rer	water side Reynolds number	
Rfi	fouling resistance inside tubes	— m²K/W
Rfo	gas side fouling resistance	— m²K/W
RH	relative humidity	— %
rho	density of moist air	— kg/cu.m
Rm(e)	mean radius for fin element(e)	— m
s	space between fins = Channel height	— m
Sb	enthalpy slope dhs/dtw at saturation	— kJ/kg air K
Sfin	specific gravity of fin material	— g/cc
Sp	specific gravity of tube material	— g/cc
Sx	enthalpy/temperature ratio (ha-hs)/(Ta-tw)	
Ta	db temperature of air	— C
Ta(n)	db temp. of air entering nth coil row	— C
TA$	Tube arrangement: <I>n line <S>taggered	
tde	dew point temperature	— C
Td(n)	dp temp. of air entering nth coil row	— C
Tf(e)	temperature of fin element(e)	— C
Ti$	computer time	— hh:mm
TIME	time lapsed since start of simulation	— sec
Tr(n)	water temperature entering nth coil row	— C
Tr	mean temperature of fluid inside tube	— C
Tw	wet bulb temperature of air	— C
Ui	modified heat transfer coef. inside tubes	— W/m² K
Uf	face velocity	— m/s
Uod	overall ext. heat tran.coef. for dry fins	— W/m² K
Uow	overall ext. heat tran.coef. for wet fins	— W kg/kJ m²
v	specific volume	— cu.m/kg
Vcc	volume of fluid inside tubes per row	— cu.cm
VN$()	names of variables stored by COILSIM	
Vr	mean water velocity inside tubes	— m/sec
W	moisture content of air or humidity ratio	— kg/kg dry air
W(n)	hum. ratio of air entering nth coil row	— kg/kg dry air
Ws	moisture content of sat. air at wb temp.	— kg/kg dry air
xf	fin thickness	— mm
xp	tube wall thickness	— mm
xtub%	number of tubes per row in use	
yv	width of vortex	— m
yw	film thickness of water	— mm

Greek Symbols

α	thermal diffusivity	$-$ m^2/s
μ	dynamic viscosity of fluid	$-$ kg/m s
δ	density of fluid	$-$ kg/cu.m
τ	time constant	$-$ seconds

Array Dimensions

c	tube configuration number
e	fin element identification,
	1 = inner element
	2 = intermediate fin element
	3 = outer fin element
n	coil row identification

1.0 SUMMARY

A modelling procedure for finned tube heat exchangers is described which predicts transient responses to changes in fluid flow and temperatures as well as the steady state performance. It does this by taking all the thermal storage capacities of the tubes, fins and working fluids into consideration and by keeping a full account of their transient temperatures.

A number of different tube and circuit arrangements can be modelled for counter and parallel flow. Plate fins are divided into a number of elements to allow the actual temperature gradients within the fins to be modelled and to allow the application of local heat transfer coefficients.

All heat transfer parameters are derived from the coil dimensions and parameters, and the physical properties of fluids are derived from a library of algorithms.

A novel technique is described which optimises the integration interval while maintaining stable and accurate integration.

The simulation program is described with logic flow diagrams and the computed results are compared with test results.

The emphasis of this thesis is on cooling coils, since that area is the most challenging, but the procedure applies equally as well to heating coils.

1.0   INTRODUCTION

Historically, cooling and dehumidifying coils have been selected from manufacturers' tabulated performance data. These were usually interpolated and extrapolated from a few test data using the ANSI/ARI Standard 410-81[2]. This Standard has been the widely accepted method for rating air coils and has also been used as the basis of a number of coil selection programs.

The wide range of conditions that have often been accepted for comfort air conditioning has made selection from tabulated data for that purpose rather forgiving and the ARI Standard has been found adequate within those wide design constraints.

With the desire to design more energy efficient systems and the greater expectations in air conditioning performance there was a need to re-evaluate the selection procedures. The many assumptions and approximations upon which the ARI Standard is based apply to only a limited range of values and the validity of the fundamental formulation has been questioned[36].

During the early 1970's the author conducted extensive testing of a cooling and dehumidifying plant for a close tolerance air conditioning system. The sprayed cooling coil was initially selected on the basis of the Goodman[15] charts and then evaluated for its dynamic performance in a test rig. The selection procedure was by trial and error, and the testing, including the setting up of a data recorder, was conducted over a period of four weeks. From this experience it became clear that a reliable method for predicting heat and moisture transfer combined with the dynamic characteristics of the coil would be highly desirable.

The air handling system was successfully simulated at that time on an analogue computer[7] but the author's attempt to model the sprayed cooling coil as a dynamic system, by using the Goodman equations combined with the time constants derived from BSIRA Technical Note TN 6/77[1], was not satisfactory. Hence alternative methods have been sought.

A literature search on numerical methods for evaluating cooling and dehumidifying coil performance yielded a number of publications[2,9,15,26,40]. All the methods described solved for steady state performance only and are based on logarithmic mean temperature differences between the working fluids. The implication is that only the mean coil surface temperature can be solved. This is then uniformly applied to the primary and secondary (fin) surface areas. The fin area being reduced by a factor, referred to as fin efficiency[10], to account for reduction in heat transfer due to the temperature gradient within the fins.

An appreciation of the dynamic performance of heat exchangers is required to allow proper control system design and a number of workers have examined this aspect. Gartner et al[11] derived the transfer functions for a fin-and-tube cross flow heater in the frequency domain, and later[12,13] examined the effect of water velocity disturbance on serpentine circuits. Adams and Holmes[1] empirically determined the time constants for heating and cooling coils for changes in water temperature and flow rates.

Those dynamic performance data are in a format which enabled control loop analysis and control system design but are difficult to apply to a finite element method of transient modelling.

It is now clear that the classic steady state models cannot cope with partially wet and dry coil surfaces. Furthermore localised reduction or enhancement in heat transfer cannot be recognised and it is difficult to distinguish between in-line and staggered tube arrangements.

Threlkeld[40] described perhaps the most generalised method for deriving simultaneous heat and mass transfer coefficients for extended surface coils. Although the method described is for steady state solution only, it lends itself very well for finite element analysis.

In order to find a solution for partially wet and dry cooling coils and to be able to account for different tube and circuit arrangements the coil should be divided into a number of sections. Heat and mass transfer equations can then be separately applied to each of these sections.

This, however, introduces other complications. The mean fluid temperatures at any particular section will not only depend upon their entering temperatures but also upon the heat transfer that has taken place in the previous sections. Thus to arrive at a solution for a system involving counter flow, or a combination of counter flow and cross flow, a large number of trial and error estimates would be involved. This is well beyond hand calculation and computer methods have to be adopted.

Hence a modelling technique is proposed in which the heat storage capacities of the tubes, fins and working fluids, and the transient temperatures within each coil section will be considered.

2.0 MODELLING

2.1 Coil Configuration

The computer model is concerned with forced-convection heat transfer in extended surface type heat exchangers which may be applied to heating or cooling with or without dehumidification. Typically a coil consists of banks of tubes with mechanically bonded fins and configured into a number of rows in various circuit configurations as described in Section 2.3. The heating or cooling medium passes through the banks of tubes. Moist air flows across the tubes and through the fins.

2.2 Coil Divisions

In order to recognise the temperature gradients for the air and cooling fluid circuits throughout the coil, it needs to be divided into a number of elements, each one operating at its own transient conditions. The first and most obvious approach is to analyse the coil row by row. This allows the leaving fluid temperatures and air conditions to be computed for each row.

Pipe circuits in cooling coils are in some form of serpentine arrangement. Thus, except for the flow header, each tube entry is connected to a curved pipe. The combination of the pressure field associated with the curvature and the non-uniform velocity profile due to wall friction generates a secondary flow within the curved pipes [35] as shown in fig.2.1. This secondary flow will persist for some distance in the
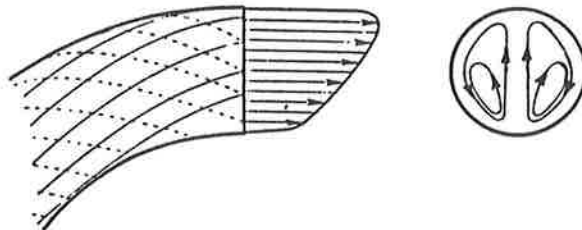
Fig.2.1 - Flow in curved pipe (Schlichting[35])

straight pipe following the bend. It is, therefore, not unreasonable to expect some heat transfer enhancement inside these pipes resulting from the secondary flow. There is also a variation in heat transfer associated with the entry region from the flow header. To allow for these heat transfer variations each coil row is divided into two equal parts in a manner as shown in fig.2.2. This also ensures that there will be a sufficient number of divisions for shallow coils to allow these to be modelled and yield a reasonably smooth process line for each working fluid. This procedure will
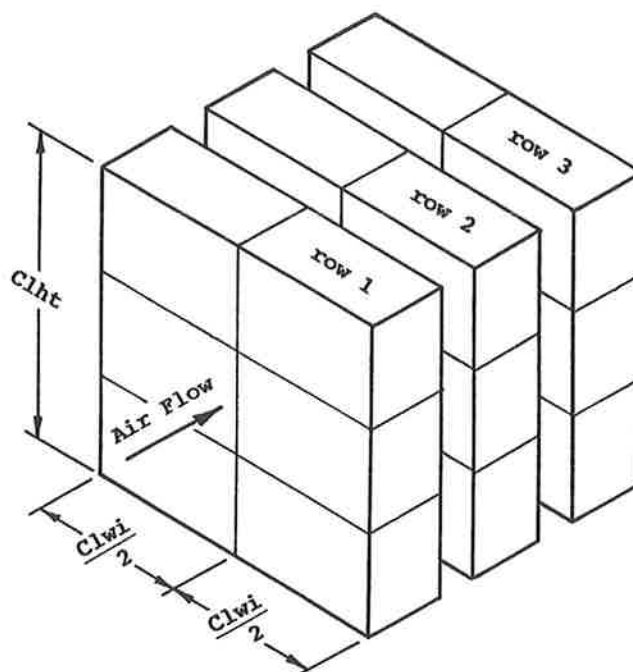
Fig.2.2 - Coil row division to allow for secondary pipe flow heat transfer enhancement.

yield two sets of conditions leaving each row. Since the coil can be modelled for a number of different fluid circuits it is not practicable to maintain a separate audit for each air stream. Furthermore, the serpentine arrangements cause the heat transfer enhancement to alternate from side to side. Therefore, after each coil row the two separately computed air streams are mixed to give the average conditions which will enter the next row.

2.3 Coil Circuits

Various circuit arrangements have been developed for cooling and heating coils. The essential operating difference between the arrangements is in their water velocities for the same water flow rates. Three common circuit arrangements[3] are shown in Fig.2.3. For the purpose of modelling, the Half Serpentine and the Standard Serpentine circuits have been modified, as shown in Figures 2.4(a) and 2.4(b) respectively, to allow for a more generalised approach.

Water velocity has a significant effect on the heat transfer characteristic. For that reason two more circuits will be modelled in addition to those shown in fig.2.4 and are referred to as Third and Quarter circuits. The Half, Third and Quarter circuits have a particular effect on the modelling strategy since the circuit re-enters each row once, twice or three times respectively. This effectively divides each half row into another two, three or four sections.
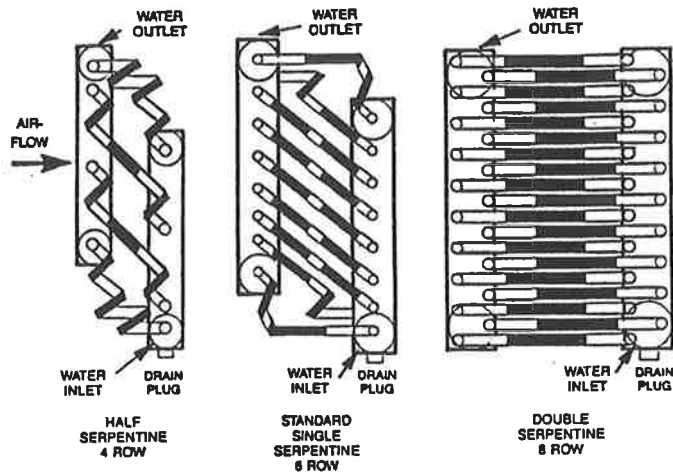
Fig.2.3 - Typical Water Circuit Arrangements
(ASHRAE 1988 Equipment Handbook[3])

(a)   (b)   (c)
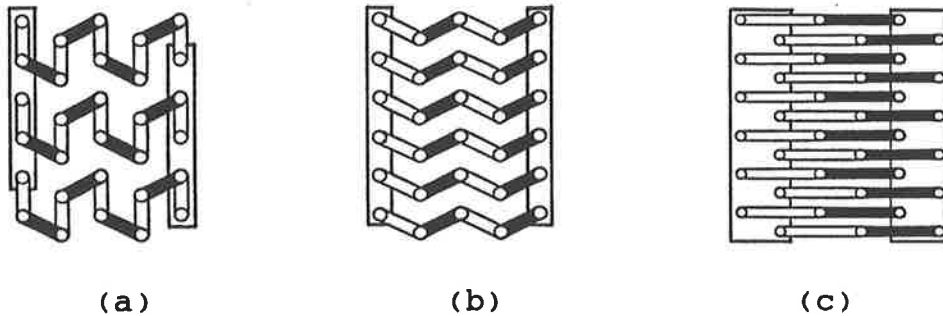
Fig.2.4 - Modified Water Circuit Arrangements
(a) Half Serpentine or two-pass   (5 row coil)
(b) Standard or Single Serpentine   (5 row coil)
(c) Double Serpentine, single pass (6 row coil)

2.4 Fin Elements

The cross sectional area for radial conduction within each
fin is very small compared with the heat transfer area on the
air side.   For this reason any extended surface will operate
with a significant temperature gradient in the radial direc-
ion.   This was recognised by Carrier and Anderson[8] and
Gardner[10] who developed the concept of fin efficiency(*) in
order to make an allowance for the reduction in heat trans-
fer. This temperature gradient is accounted for in the tran-
sient model by dividing the fins into a number of elements,
each operating at its own transient temperature and with its
own local heat transfer coefficient.   Consequently, the
limitations of the concept of fin efficiency do not apply to
the transient model.

(*) This efficiency is a factor by which an extended surface having a uniform heat transfer
    coefficient over its whole surface has to be reduced to in order to find the true heat
    transfer rate when the fin temperature at its base is applied uniformly throughout.

Since the fin's isotherms are approximately in concentric circular patterns, the fins are divided into a number of concentric rings. To facilitate such divisions, continuous plate fins are first converted into circular fins of equivalent area in the manner described in Appendix B.

Saboya[32,33,34] identified areas of high heat transfer coefficients associated with the 'horseshoe' vortices which form at the intersections of tubes and fins and trail downstream, and areas of low heat transfer in the 'shadow' behind the tubes. Gilbert[14] demonstrated the presence of the vortices by flow visualisation and on the basis of limited measurements of local heat transfer, proposed heat transfer enhancement factors for the several regions on the fin surface. Appendix B defines the fin elements and the areas affected by enhanced or reduced heat transfer.

2.5 Conventions and Assumptions

All heat transfer areas and parameters, and coil and fluid masses are computed from the coil dimensions, tube arrangeents, fin pitch, and coil circuiting.

The units within the program are in accordance with the SI convention, but data entry is in the more conveniently expressed engineering units, eg. tube diameter and fin dimensions are entered in *mm* sizes rather than *metre*.

Numerical solutions of transient heat flow are based on the following assumptions:

1. The temperature within any coil element is uniform over any given integration interval.
2. The densities of the coil materials are considered to be constant.
3. The coil materials and fluids have constant specific heats throughout the coil and over the temperature ranges encountered.
4. There is no fluid mixing in the axial direction between adjacent sections.
5. Perfect mixing occurs within each section.
6. Heat conduction in the axial direction is negligible.
7. Air has a uniform temperature and velocity across the coil face area and at entry to any subsequent coil row, i.e. the air is fully mixed across the coil section at exit from a tube row.

3.0 HEAT TRANSFER AREAS

3.1 Coil Geometry and Tube Configuration

All heat transfer areas are derived from the following coil dimensions and parameters which are interactively entered or edited into a coil data file

```
Clwi  = coil width,  parallel to tubes           - mm
Clht  = coil height, at right angles to tubes    - mm
Nrow% = number of rows
Dp    = tube outside diameter                    - mm
xp    = tube wall thickness                       - mm
Ct    = centre distance between tubes             - mm
Cr    = centre distance between rows              - mm
TA$   = tube arrangement, <S>taggered
                          <I>n-line
Fg$   = fin geometry, <R> continuous plate fins
                      <C> circular plate fins
FP    = fin pitch                                - mm
xf    = fin thickness                            - mm
C$    = coil circuiting, <D>ouble circuit
                         <S>tandard circuit
                         <H>alf serpentine
                         <T>hird circuit
                         <Q>uarter circuit
```

Allowing for half the tube centre distance at either end of each row the maximum number of tubes per row is estimated as

$$\text{Ntub\%} = \text{INT(Clht/Ct)} \ . \qquad\qquad (3.1-1)$$

In the half, third, and quarter circuit arrangements the tube circuit re-enters the same row once, twice, or three times respectively, thereby effectively dividing each row into two, three, or four separate regions or sections.

Coil circuit C$	No. of parallel circuits per row Ncirc%
<D>ouble	1
<S>ingle	1
<H>alf	2
<T>hird	3
<Q>uarter	4

Table 3.1 - Overview of Coil Circuit Arrangements.

Ncirc% is the number of parallel circuits per row and is defined in Table 3.1. The maximum number of tubes per row section is then derived as

$$Ntc\% = INT(Ntub\%/Ncirc\%) \ . \tag{3.1-2}$$

There is a facility in the computer program to select fewer tubes. In the editor this is stored as a temporary variable which is defined as

$$xtub\% <= Ntc\% \ , \tag{3.1-3}$$

and the total number of tubes per row in use is then defined as

$$Nt\% = xtub\% \cdot Ncirc\% \ . \tag{3.1-4}$$

The total number of fins

$$Nfin\% = INT(Clwi/FP - 1.) \ . \tag{3.1-5}$$

The tube outside diameters are modified by the flares of the fins so that the effective tube outside diameters become

$$Do = Dp + 2. \cdot xf \quad mm \ . \tag{3.1-6}$$
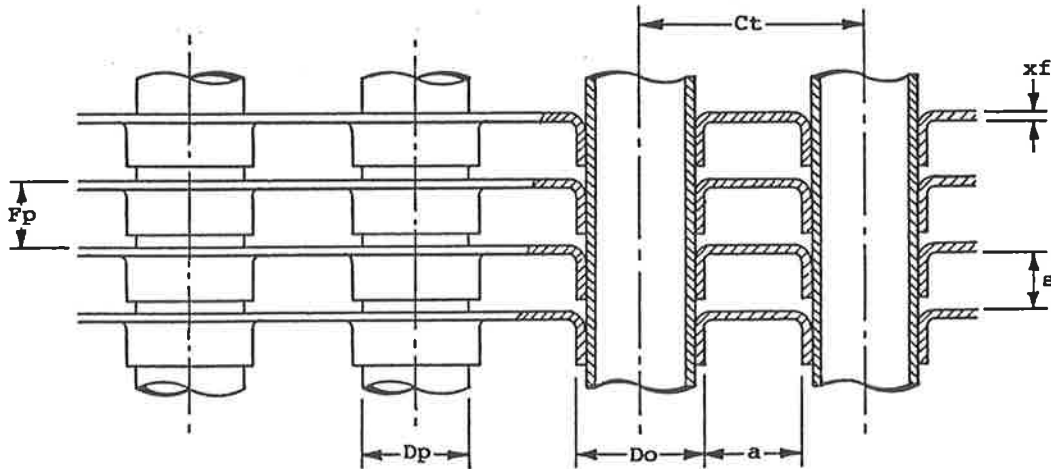
Fig.3.1 - Definition of channel dimensions a and s

The space 's' between the fins (channel height) is determined as

$$s = (FP - xf) \ / \ 1000. \quad m \ , \tag{3.1-7}$$

and the space 'a' between the tubes is determined as

$$a = (Ct - Do) \ / \ 1000. \quad m \ . \tag{3.1-8}$$

3.2 Coil Characteristic Areas

Face area of the coil is

$$Af = Clwi \cdot Clht \cdot 1.0E-06 \qquad m^2 \; . \qquad (3.2-1)$$

Dimensions for calculating free flow area Ac

Nett width = Clwi − Nfin% · xf   mm ,
Nett height = Clht − Ntub% · Do   mm .

Hence, minimum free flow area

$$Ac = (Clwi-Nfin\% \cdot xf) \cdot (Clht-Ntub\% \cdot Do) \cdot 1.0E-06 \quad m^2 \; . \quad (3.2-2)$$

3.3 Areas Inside Tubes

For the tube outside diameter Dp mm and tube wall thickness xp mm, the inside diameter of the tube is

$$Di = Dp - 2. \cdot xp \qquad mm \; . \qquad (3.3-1)$$

Hence

$$\text{Area for flow per tube} = (\pi/4) \cdot Di^2 \cdot 1.0E-06 \qquad m^2 \; ,$$

and the total area for fluid flow per row

$$Acr = Nt\% \cdot (\pi/4) \cdot Di^2 \cdot 1.0E-06 \qquad m^2 \; . \qquad (3.3-2)$$

The inside surface area for heat transfer per row

$$Api = Nt\% \cdot \pi \cdot Di \cdot Clwi \cdot 1.0E-06 \quad m^2 \; . \qquad (3.3-3)$$

3.4 External Heat Transfer Areas

The fins are divided into three elements with radii R0, R1, R2, and R3 as defined in Appendix B.   The heat transfer areas are derived as At(e) m², where (e) is the element identification.

For a coil with Nt% tubes per row and Nfin% fins, the total heat transfer area per coil row and for each fin element is then established as

$$Ato(e) = Nt\% \cdot Nfin\% \cdot At(e) \; . \qquad (3.4-1)$$

3.5 Heat Transfer between Fin Elements

For the purpose of establishing conduction path lengths, the heat in fin element(1) could be considered concentrated at R0. This is the effective tube outside radius and is also the base of the fin. Thus

$$Rm(1) = R0 \qquad m \; . \qquad\qquad (3.5\text{-}1)$$

Now let the radius at which the heat in fin element(2) could be concentrated be such that it divides that element into two equal areas, then

$$Rm(2) = \sqrt{((R1^2 + R2^2)/2.)} \qquad m \; . \qquad (3.5\text{-}2)$$

Similarly

$$Rm(3) = \sqrt{((R2^2 + R3^2)/2.)} \qquad m \; . \qquad (3.5\text{-}3)$$

The heat transfer through a flat plate is expressed as

$$Q = \frac{k\,A}{x} \cdot (t_1 - t_2) \qquad \text{Watt} \; , \qquad (3.5\text{-}4)$$

where

k	= conductivity of plate material	- W/m K
A	= area	- m^2
x	= plate thickness	- m
t_1, t_2	= plate surface temperatures	- K .

The passage of heat from one fin element to another could be compared with that through a pipe wall. When radially moving outwards, the area of the heat flow path through the fin increases with the distance of the path. Kern[22] derived the heat transfer through a pipe wall as

$$Q = \frac{2 \cdot \pi \cdot k \cdot (t_i - t_o)}{\ln(r_o/r_i)} \qquad \text{Watt per lineal m} \; . \qquad (3.5\text{-}5)$$

Applying this collectively to all the fins and tubes in one row then

$$Qe(n) = \frac{2 \cdot \pi \cdot kfin \cdot xf \cdot Nt\% \cdot Nfin\% \cdot (Tf(n+1) - Tf(n))}{1000 \cdot \ln(Rm(n+1)/Rm(n))} \qquad W \; . \qquad (3.5\text{-}6)$$

4.0 THERMAL STORAGE CAPACITIES

4.1 Heat capacity of Water

The total area for fluid flow per row, Acr m², was derived by Eq.(3.3-2). The volume of fluid per row (neglecting return bends) is then

$$Vcc = Acr \cdot 10000 \cdot Clwi / 10 \qquad cu.cm$$

or

$$Vcc = Acr \cdot Clwi \cdot 1000 \qquad cu.cm . \qquad (4.1-1)$$

For the specific heat of water, Cw in J/cc K, the heat capacity of water per row

$$Cwr = Vcc \cdot Cw \qquad J/K . \qquad (4.1-2)$$

4.2 Thermal Capacities of Coil Materials

Heat exchangers can be made from a variety of materials. Cooling coils are commonly constructed with copper tubes and the fins may be either copper or aluminium pressed onto the tubes. But even with these materials defined, there is a significant variation in published data on specific heat, specific gravity and conductivity for these materials. Hence, these parameters are not fixed in the computer program but are interactively edited and stored in a data file. Typical published data(*) are shown in Table 4.1.

Material	Temp. °C	Cond. k W/m K	Spec.Ht. J/g K	Spec.G. g/cc
Aluminium	0	202.5	0.766	2.55-2.8
	100	206.0	0.764	
Brass	0	96.9	0.551	8.4-8.7
	100	103.9	0.623	
Copper	0	387.7	0.623	8.8-8.95
	100	377.4	0.711	
Steel	0	45.0	0.446	7.83
	100	45.0	0.493	

Table 4.1 — Thermal parameters for coil materials.

(*) L.S.Marks,"Mechanical Engineers' Handbook", converted from Imp.units.

For the coil model it is more convenient to express the thermal capacities for coil metals in terms of volume rather than mass. Hence the products of specific heat and specific gravity are used in the main-line program as

Cc   for thermal capacity of tube material in   J/cc K
Cfin   for thermal capacity of fin material in   J/cc K

4.3 Heat Capacity of Fin Elements

Volume of metal in each tube

$$= \pi/4 \cdot (Dp^2 - Di^2)/100 \cdot Clwi/10 \quad \text{cu.cm}$$
$$= \pi \cdot (Dp^2 - Di^2) \cdot Clwi / 4000 \quad \text{cu.cm .}$$

For the heat capacity of tube material as Cc J/cc K the heat capacity of tubes per row

$$Cm1 = Nt\% \cdot Cc \cdot \pi \cdot (Dp^2 - Di^2) \cdot Clwi / 4000 \quad \text{J/K .} \quad (4.3\text{-}1)$$

Volume of fin flare

$$= \pi/4 \cdot (Do^2 - Dp^2)/100 \cdot s \cdot 100 \quad \text{cu.cm}$$
$$= \pi/4 \cdot (Do^2 - Dp^2) \cdot s \quad \text{cu.cm .}$$

Volume of fin section(1)

$$= \pi \cdot (R1^2 - R0^2) \cdot 1.0E+04 \cdot xf/10 \quad \text{cu.cm}$$
$$= \pi \cdot (R1^2 - R0^2) \cdot xf \cdot 1000 \quad \text{cu.cm .}$$

For the heat capacity of fin material as Cfin J/cc K the heat capacity of fin section(1) per row

$$Cm2 = Nt\% \cdot Nfin\% \cdot Cfin \cdot \pi \cdot ((Do^2 - Dp^2) \cdot s/4 + (R1^2 - R0^2) \cdot xf \cdot 1000) . \quad (4.3\text{-}2)$$

And the total heat capacity for fin element(1) per row

$$Cm(1) = Cm1 + Cm2 \quad \text{J/K .} \quad (4.3\text{-}3)$$

Volume of fin section(2)

$$= \pi \cdot (R2^2 - R1^2) \cdot 1.0E+04 \cdot xf/10 \quad \text{cu.cm}$$
$$= \pi \cdot (R2^2 - R1^2) \cdot xf \cdot 1000 \quad \text{cu.cm .}$$

And the total heat capacity for fin element(2) per row

$$Cm(2) = Nt\% \cdot Nfin\% \cdot Cfin \cdot \pi \cdot (R2^2 - R1^2) \cdot xf \cdot 1000 \quad \text{J/K .} \quad (4.3\text{-}4)$$

Volume of fin section(3)

$$= \pi \cdot (R3^2 - R2^2) \cdot 1.0E+04 \cdot xf/10 \qquad \text{cu.cm}$$
$$= \pi \cdot (R3^2 - R2^2) \cdot xf \cdot 1000 \qquad \text{cu.cm} .$$

And the total heat capacity for fin element(3) per row

$$Cm(3) = Nt\% \cdot Nfin\% \cdot Cfin \cdot \pi \cdot (R3^2 - R2^2) \cdot xf \cdot 1000 \qquad \text{J/K} . \quad (4.3\text{-}5)$$

5.0 THERMO-PHYSICAL PROPERTIES OF FLUIDS

The full text and algorithms, developed by the present author, are listed in ACS Mechanical Engineering Report No.39, "Numerical Methods on the Properties of Gases, Vapours and Liquids". This Report is referenced elsewhere as [42]. For convenience the features relevant to the thesis are extracted into this Section.

Symbols used in Section 5.0

Cp	specific heat at constant pressure		- kJ/kg K
Cpm$_t$	mean spec.heat at t°C (reference 0°C)		- kJ/kg K
Cv	specific heat at constant volume		- kJ/kg K
Df	coefficient of diffusion		- m²/s
gamma	specific heat ratio Cp/Cv		
h	specific enthalpy		- kJ/kg
k	Boltzmann constant	1.380622E-23	- J/K
kt	thermal conductivity		- W/m K
M	molecular weight		
p	pressure on gas mixture		- atm
Psat	saturation vapour pressure		- kPa
R	universal gas constant	82.0562	- cc atm/K mol
		1.98717	- cal/K mol
		8.31441	- J/K mol
T	absolute temperature		- K
t	temperature		- °C
T*	reduced temperature kT/Є		- K
Tc	critical temperature		- K
Tr	reduced temperature T/Tc		- K
Tsat	temperature at saturation pressure		- K

Є	force constant	°
σ	force constant or molecular diameter	- Å
μ	coefficient of viscosity (dynamic)	- kg/m s
	(alternative units are Pa s and N s/m²)	
Ω$^{(x,s)*}$	reduced collision integrals for calculating the transport coefficients	

subscripts

f	saturated water
fg	transition from saturated water to steam
g	saturated steam
n	Lennard-Jones parameters for non-polar molecules
p	Stockmayer parameters for polar molecules

5.1 Vapour Pressure of Saturated Steam

The solution for the vapour pressure of saturated steam is the basis for psychrometric calculations. A number of empirical equations have been examined[42] and the best known of these is the Keenan and Keyes[21] equation which has been converted[39] for SI units as

$$Psat = \cfrac{22105.8416}{EXP\left[\cfrac{2.302585X \ (3.2437814 + 3.26014E\text{-}03X + 2.00658E\text{-}09X^3)}{((1165.09 - X) \ (1.0 + 1.21547E\text{-}03X)}\right]},$$

$$(5.1\text{-}1)$$

where Psat is in kPa and

$$X = 673.4 - 1.8 \cdot Tsat \text{ in } °C \qquad (5.1\text{-}2)$$

This equation gives the saturation vapour pressure for steam from 0°C to the critical temperature of 374.15°C with an accuracy to three significant digits and is the equation used in sub-program PSKEEKEY. A more accurate result can be obtained for the same temperature range with the ASME[6] equation:

$$\ln\left[\frac{Psat(atm)}{218.3074}\right] = \left[\frac{1}{Tr} * \frac{F_1}{F_2}\right] - \left[\frac{1 - Tr}{F_3}\right], \qquad (5.1\text{-}3)$$

where

$$Tr = Tsat/Tc$$
$$Tc = 647.3 \text{ K}$$
$$F_1 = \sum_{n=1}^{n=5} k_n \ (1 - Tr)^n$$
$$F_2 = 1. + k_6 \ (1.- Tr) + k_7 \ (1.- Tr)^2$$
$$F_3 = k_8 \ (1.- Tr)^2 + k_9$$
$$k_1 = -7.691234564$$
$$k_2 = -26.08023696$$
$$k_3 = -168.1706546$$
$$k_4 = 64.23285504$$
$$k_5 = -118.9646225$$
$$k_6 = 4.167117320$$
$$k_7 = 20.97506760$$
$$k_8 = 1.0D+09$$
$$k_9 = 6.0$$

This equation is used in sub-program PSATASME. Hyland and Wexler[18,19] extended the range by developing an empirical equation for two temperature ranges, 173.15 to 273.15K and 273.15 to 473.15K, as:

$$Psat = \cfrac{Exp\left[a/Tsat + \sum_{n=0}^{n=4} (b_n \cdot Tsat^n) + c \cdot \ln(Tsat)\right]}{1000.} \qquad (5.1\text{-}4)$$

for which the constants are listed in Table 5.1, and is used in sub-program PSATHYWE.

| coef | Temperature range K | |
	173.15 to 273.15	273.15 to 473.15
a	-5.6745359D+03	-5.8002206D+03
b_0	6.3925247	1.3914993
b_1	-9.6778430D-03	-4.8640239D-02
b_2	6.22115701D-07	4.1764768D-05
b_3	2.0747825D-09	-1.4452093D-08
b_4	-9.4840240D-13	0.0
c	4.1635019	6.5459673

Table 5.1 - Constants for Vapour Pressure Eq.(5.1-4).

The results of equations (5.1-1), (5.1-3) and (5.1-4) together with published data[30] on saturation vapour pressures are listed in Table 5.2 for comparison.

For temperatures below 0°C only the Hyland & Wexler Equation (5.1-4) gives suitable solutions. Between 273.15K (0°C) and 450K the Keenan & Keyes (5.1-1) and the ASME (5.1-3) equations give the best solutions with little difference in accuracy. As the Keenan & Keyes equation is the simpler of the two it is recommended for this range. For temperatures above 450K the ASME equation (5.1-3) gives the best results.

Sub-program PSATH2O gives the saturation vapour pressure for water substance for the temperature range from 150K to the critical temperature of 647.3K (-120°C to 374.15°C). It does this by calling sub-programs PSATHYWE, PSKEEKEY, and PSATASME for the appropriate temperature ranges.

5.2 Diffusion of Water Vapour in Air

Ordinary diffusion is the transfer of mass from one region to another due to a gradient in concentration. For a mixture of two chemical species the coefficient of diffusion is independent of the composition. The first approximation, using the rigorous approach, is given by Hirschfelder[17] (in m²/s) as

$$[D_{12}]_1 = 2.628E{-}07 \; \frac{\sqrt{(\; T^3 (M_1 + M_2) \; / \; (2 \; M_1 \; M_2))}}{p \; \sigma_{12}^2 \; \Omega_{12}^{(1,1)*}} \qquad (5.2\text{-}1)$$

Temp. K	Vapour Pressure - bar (100 kPa)				Temp. C
	Perry's Table(a)	Hyland & Wexler Eq(5.1-4)	Keenan & Keyes Eq(5.1-1)	ASME equation Eq(5.1-3)	
150	6.30E-11	6.10E-11			-123.15
160	7.72E-10	7.73E-10			-113.15
170	7.29E-09	7.30E-09			-103.15
180	5.38E-08	5.39E-08			-93.15
190	3.23E-07	3.24E-07			-83.15
200	1.62E-06	1.63E-06			-73.15
210	7.01E-06	7.02E-06			-63.15
220	2.65E-05	2.65E-05			-53.15
230	8.91E-05	8.95E-05			-43.15
240	2.72E-04*	2.73E-04			-33.15
250	7.59E-04	7.60E-04			-23.15
260	1.96E-03	1.96E-03			-13.15
270	4.69E-03	4.70E-03			-3.15
273.15	0.00611	0.00611	0.00612	0.00611	0
280	0.00990	0.00992	0.00992	0.00991	6.85
290	0.01917	0.01920	0.01919	0.01918	16.85
300	0.03531	0.03536	0.03533	0.03532	26.85
310	0.06221	0.06230	0.06223	0.06223	36.85
320	0.1053	0.1054	0.1053	0.1053	46.85
330	0.1719	0.1721	0.1719	0.1719	56.85
340	0.2713	0.2719	0.2715	0.2715	66.85
350	0.4163	0.4168	0.4163	0.4163	76.85
360	0.6209	0.6219	0.6212	0.6213	86.85
370	0.9040	0.9054	0.9045	0.9045	96.85
373.15	1.0133	1.0142	1.0132	1.0133	100
380	1.2869	1.2886	1.2875	1.2875	106.85
390	1.794	1.797	1.795	1.795	116.85
400	2.455	2.458	2.456	2.456	126.85
410	3.302	3.305	3.303	3.303	136.85
420	4.370	4.373	4.371	4.371	146.85
430	5.699	5.703	5.701	5.701	156.85
440	7.333	7.337	7.334	7.335	166.85
450	9.319	9.323	9.318	9.320	176.85
460	11.71	11.71	11.70	11.71	186.85
470	14.55	14.55	14.54	14.55	196.85
480	17.90	17.91	17.89	17.90	206.85
490	21.83	21.84	21.81	21.83	216.85
500	26.40	26.40	26.37	26.40	226.85
510	31.66	31.67	31.63	31.66	236.85
520	37.70	37.71	37.67	37.70	246.85
530	44.58	44.60	44.55	44.59	256.85
540	52.38	52.41	52.37	52.39	266.85
550	61.19	61.22	61.20	61.21	276.85
560	71.08	71.12	71.13	71.10	286.85
570	82.16	82.19	82.26	82.18	296.85
580	94.51	94.53	94.70	94.53	306.85
590	108.3	108.2	108.5	108.3	316.85
600	123.5	123.4	123.9	123.5	326.85
610	140.3*	140.1	140.9	140.4	336.85
620	159.1	158.4	159.7	159.1	346.85
630	179.7	178.5	180.4	179.8	356.85
640	202.7	200.5	203.1	202.8	366.85
647.3	221.2	217.8	221.2	221.2	374.15

Table 5.2 - Saturated Vapour Pressures over Ice and Liquid Water, and comparison of equations.

(a) Perry's Chemical Engineers' Handbook[30], Table 3-302.
* Typographical errors in Perry's Handbook have been corrected by interpolation.

where

T	is the temperature of the gas mixture	- K
M_1, M_2	are the molecular weights of the chemical species in the mixture	
p	pressure on the mixture	- atm
σ_{12}	force constant for the mixture	- $\overset{\circ}{A}$
$\Omega_{12}{}^{(1,1)*}$	reduced collision integral	

The collision integrals are tabulated in Hirschfelder[17] as functions of the reduced temperature T^* and from these tables polynomial coefficients have been derived[42] to approximate the integrals. The polynomial coefficients for $\Omega^{(1,1)*}$ are listed in Table 5.3.

T^* Range	< 1.0	1.0 - 10.
$\Omega_{(1,1)}{}^*$	$1 / f(T^*)$	$f(1/T^*)$
Subscript 0 1 2 3 4 5 6	.18802897 .67627103 -.16955131	.59727007 1.8466139 -4.9068264 11.610331 -15.155818 10.260397 -2.8131158

Table 5.3 - Polynomial coefficients for approximating the integral $\Omega^{(1,1)*}$ (Van Aken[42])

The higher approximations for the coefficient of diffusion are given by

$$[D_{12}]_n = [D_{12}]_1 \, f_D^{(n)} \qquad m^2/s \, , \qquad (5.2-2)$$

where $f_D^{(n)} = \emptyset(T^*)$ and is given in Table 5.4 for n=2.

For water vapour in air the force constants have been established[28,42] as

$$\sigma_{np} = 3.724 \, \overset{\circ}{A}, \text{ and } \in_{np}/k = 49 \, K \, ,$$

and the molecular weights for water and air are 18.015 and 28.97 respectively. Substituting these parameters into Eq.(5.2-1) and combining this with Eq.(5.2-2) yields

$T^* = kT/\epsilon$	$f_D^{(2)}$
0.30	1.0001
0.50	1.0000
0.75	1.0000
1.00	1.0000
1.25	1.0002
1.5	1.0006
2.0	1.0016
2.5	1.0026
3.0	1.0037
4.0	1.0050
5.0	1.0059
10.0	1.0076
50.0	1.0080
100.0	1.0080
400.0	1.0080

Table 5.4 - Functions for Calculating the Higher Approximations to the Coefficient of Diffusion. (Hirschfelder[17])

Temp. C	Df_{np} cm²/s	Temp. C	Df_{np} cm²/s
-80	0.1223	70	0.3260
-70	0.1335	80	0.3422
-60	0.1450	90	0.3586
-50	0.1569	100	0.3754
-40	0.1692	120	0.4097
-30	0.1818	140	0.4451
-20	0.1948	160	0.4817
-10	0.2080	180	0.5193
0	0.2217	200	0.5580
10	0.2356	220	0.5999
20	0.2499	240	0.6407
30	0.2645	260	0.6826
40	0.2794	280	0.7255
50	0.2947	300	0.7695
60	0.3102		

Table 5.5 - Diffusion Coefficients for Water Vapour in Air computed with sub-program DFH2OAIR

$$Df_{np} = 4.020493E-09 \ \frac{T^{3/2}}{p \ \Omega_{np}^{(1.1)*}} \ f_D^{(2)} \qquad m^2/s \ , \qquad (5.2-3)$$

and for which

$$T_{np}^* = T \ / \ 49 \qquad K \ . \qquad (5.2-4)$$

Sub-program DFH2OAIR computes the Diffusion coefficient for water vapour in air by applying Equations (5.2-3) and (5.2-4) and the polynomial coefficients listed in Table 5.3. The results from this sub-program are listed in Table 5.5.

5.3 Coefficient of Viscosity for Gases

Viscosity is the transport of momentum through a fluid because of a gradient in velocity. The Newtonian definition of the coefficient of viscosity is

$$\mu = \frac{shear \ stress}{velocity \ gradient} \ .$$

Near atmospheric pressure the viscosity of a gas is quite insensitive to small pressure changes. To a first approximation the viscosity of a pure gas is given[17] by

$$[\mu]_1 = 2.6693E-06 \ \frac{\sqrt{(M \ T)}}{\sigma^2 \ \Omega^{(2,2)*}} \qquad Pa \ s \ . \qquad (5.3-1)$$

A more convenient empirical equation is given[5] as

$$\mu \cdot 10^6 = \sqrt{T} \ / \ (A + B \ T^{-1} + C \ T^{-2} + D \ T^{-3}) \qquad Pa \ s \ , \qquad (5.3-2)$$

for which the constants for water vapour and air are listed in Table 5.6.

Gas	Range K	A	B	C	D
H2O	280- 500	0.0500699	365.423	16018.	0.0
	500- 750	0.368683	490.099	-13608.	0.0
	750-1000	0.309818	575.159	-44383.	0.0
Air	85-1000	0.671692	85.22974	-2111.475	106417.

Table 5.6 - Constants for Viscosity Equation (5.3-2)
(ASHRAE[5])

5.4 Coefficient of Viscosity for Water

The viscosity of water as a liquid is given[5] as

$$\mu \cdot 10^3 = EXP\ (A + B\ T^{-1} + C\ T^{-2}) \qquad Pa\ s\ , \qquad (5.4-1)$$

for which the constants are listed in Table 5.7.

Gas	Range K	A	B	C
H_2O	273-350	0.030185	-2191.60	638605.
	350-500	-3.22950	13.18574	265531.
	500-620	-8.77361	5875.87	-1282750.

Table 5.7 - Constants for Viscosity Equation (5.4-1)
(ASHRAE[5])

5.5 Thermal Conductivity of Gases

ASHRAE[5] has published empirical Equations for refrigerant gases, including air and water vapour, in the general form

$$kt = \frac{\sqrt{T}}{A + B\ T^{-1} + C\ T^{-2} + D\ T^{-3}} \qquad W/m\ K\ , \qquad (5.5-1)$$

for which the constants are listed in Table 5.8

Gas	Range K	A	B	C	D
H_2O	373- 600	-138.818	4.80327E+05	-4.88631E+07	0.0
	600- 800	-3.40306	3.30796E+05	-7.28429E+06	0.0
	800-1000	98.3080	1.72643E+05	5.43128E+07	0.0
Air	80- 300	385.859	9.11440E+04	-2.68667E+06	5.52604E+07
	300- 600	328.052	1.67320E+05	-3.02953E+07	3.05682E+09
	600-1000	539.544	-3.32903E+05	3.59756E+08	-9.67202E+10

Table 5.8 - Constants for Thermal Conductivity Eq.(5.5-1).
(ASHRAE[5])

5.6 Thermal Conductivity of Water

The thermal conductivity of water is given[5] as

$$kt = A + B\ T + C\ T^2 + D\ T^3 \qquad W/m\ K\ , \qquad (5.6-1)$$

for which the constants are listed in Table 5.9.

Gas	Range K	A	B	C	D
H2O	273-400	-0.61694	7.17851E-03	-1.16700E-05	4.70358E-09
	400-600	-0.14532	4.02217E-03	-4.64993E-06	-4.89257E-10
	600-645	190.404	-0.94131	1.55847E-03	-8.61953E-07

Table 5.9 - Constants for Thermal Conductivity Eq.(5.6-1). (ASHRAE[5])

5.7 Specific Heat of Gases

In the case of gases the specific heat has a significant dependence upon the temperature. There is also a dependence upon pressure, but for gases far removed from saturation, this may be neglected. Thus the higher the temperature, the less the effect of pressure.

For many gases the specific heat-temperature relation may be expressed by simple empirical equations. ASHRAE[5] has collated a number of these in the general form

$$Cp = A + B\,T + C\,T^2 + D\,T^3 \quad kJ/kg\;K ,\qquad (5.7-1)$$

for which the constants are listed in Table 5.10.

These equations apply only for near atmospheric pressures but reasonable accuracies can be achieved with pressures up to 14 atm. Constants for real gas equations are listed wherever these were available. The constants for the ideal gas equations are identified by an asterisk.

Gas	Range K	A	B	C	D
H2O	290- 380‡	-.23980	2.29880E-02	-8.56702E-05	1.08197E-07
	373- 535	8.13705	-3.73435E-02	7.48227E-05	-4.95562E-08
	535-1500	1.85444	-1.19408E-04	8.30428E-07	-2.77702E-10
Air	260- 610	1.04466	-3.15967E-04	7.07909E-07	-2.70340E-10
	610- 900	1.00205	-1.62983E-04	5.69525E-07	-2.68081E-10
	600-1500*	8.73749E-01	3.22598E-04	-3.58454E-08	-1.99063E-11

Table 5.10 - Constants for Specific Heat Equation (5.7-1). (ASHRAE[5])
‡ Indicates saturated vapour equation.
* Indicates ideal gas equations.

The specific heat has been computed for air and water vapour over a wide temperature range by using the Eq.(5.7-1) and the constants in Table 5.10. A selection is listed in Table 5.11.

°C	Air	H2O		°C	Air	H2O
0	1.006	1.904		200	1.025	1.969
10	1.006	1.890		300	1.045	2.007
20	1.006	1.879		400	1.069	2.066
30	1.006	1.870		500	1.093	2.130
40	1.007	1.880		600	1.116	2.198
50	1.007	1.894		700	1.135	2.269
60	1.008	1.911		800	1.154	2.340
70	1.009	1.933		900	1.171	2.409
80	1.010	1.959		1000	1.185	2.475
90	1.010	1.992		1500	1.249	2.706
100	1.011	2.046				

Table 5.11 - Specific Heat in kJ/kg K for air and water vapour at given temperature in °C.

5.8 Specific Heat Ratio

Section 5.7 described the equations for the specific heat for gases at constant pressure. At pressures well below 10 atm and temperatures above 270 K, the specific heat at constant volume can be established with the simple relationship

$$Cv = Cp - \frac{R}{M} \quad kJ/kg \ K \ , \tag{5.8-1}$$

where

    R = universal gas constant = 8.31441 J/K mol
    M = molecular weight.

The specific heat ratio is simply defined as

$$gamma = \frac{Cp}{Cv} \ . \tag{5.8-2}$$

As an example, the specific heat of air at constant pressure and at 1000 K can be determined from Eq.(5.7-1), or from tabulated data, as Cp = 1.141. The molecular weight of air is 28.97. Now by Eq.(5.8-1)

$$Cv = 1.141 - \frac{8.31441}{28.97} = 0.854 \ kJ/kg \ K \ ,$$

and the specific heat ratio

$$gamma = \frac{1.141}{0.854} = 1.336 \ .$$

5.9 Specific Heat of Water

The specific heat equations for liquids collated by ASHRAE[5] are in the general form

$$Cp = A + B\,T + C\,T^2 + D\,T^3 + E\,T^4 \quad kJ/kg\ K\ , \qquad (5.9-1)$$

for which the constants for water are listed in Table 5.12.

Gas	Range K	A	B	C	D	E
H2O	273-450	1.76611E+01	-1.47914E-01	6.08619E-04	-1.11867E-06	7.80297E-10
	450-603	-9.66159E+01	6.35694E-01	-1.33872E-03	9.44662E-07	0.0

Table 5.12 – Constants for Specific Heat Equation (5.9-1) (ASHRAE[5])

5.10 Enthalpy

The enthalpy of a gas can be expressed as a function of specific heat, temperature, and pressure, and the change in enthalpy can be written as

$$h_T - h_0 = \int_{T_0}^{T} Cp\ dT + \int_{P_0}^{P} \frac{\delta v}{\delta T}\ dP\ , \qquad (5.10-1)$$

and for constant pressure this becomes

$$h_T - h_0 = \int_{T_0}^{T} Cp\ dT\ . \qquad (5.10-2)$$

The change in enthalpy at constant pressure could alternatively be expressed in terms of mean specific heat and temperature as

$$h_t - h_0 = Cpm_t\ (t - t_0)\ , \qquad (5.10-3)$$

where t is expressed in °C, and

$$Cpm_t = \frac{1}{t-t_0} \int\limits_{t_0}^{t} Cp \; dt \; . \tag{5.10-4}$$

For $h_0 = 0$ and $t_0 = 0$, Eq.(5.10-3) simplifies to

$$h_t = Cpm_t \cdot t \; . \tag{5.10-5}$$

The mean specific heat has been evaluated for some gases by numerical integration[42] of computed Cp values over a wide temperature range from 0°C. The results for air and dry steam are listed in Table 5.13.

°C	Air	H2O	°C	Air	H2O
0	1.006	1.904	500	1.040	2.005
10	1.006	1.896	600	1.050	2.031
20	1.006	1.890	700	1.061	2.060
30	1.006	1.884	800	1.072	2.091
40	1.006	1.882	900	1.082	2.122
50	1.006	1.883	1000	1.091	2.154
60	1.007	1.886	1500	1.134	2.304
70	1.007	1.892	2000	1.167	2.426
80	1.007	1.898	2500	1.192	2.529
90	1.007	1.907	3000	1.211	2.616
100	1.008	1.918	3500	1.227	2.692
200	1.013	1.953	4000	1.241	2.759
300	1.020	1.963	4500	1.253	2.818
400	1.029	1.982			

Table 5.13 - Mean Specific Heat in kJ/kg K between 0°C and final temperature in °C for air and dry steam. (Van Aken[42])

Polynomial equations have been fitted to Table 5.13 in the general form

$$Cpm_t = A + B t + C t^2 + D t^3 \quad kJ/kg \; K \tag{5.10-6}$$

for which the constants are listed in Table 5.14

Gas	Range °C	A	B	C	D
Air	0- 500	1.00568	4.65069E-06	1.71196E-07	-8.94002E-11
	500-4700	9.73840E-01	1.43679E-04	-2.80116E-08	2.18837E-12
H2O	0- 100	1.90429	-1.03621E-03	1.29934E-05	-1.24956E-08
	100-2000	1.91081	1.20490E-04	1.75339E-07	-5.37921E-11
	2000-4700	1.93386	2.88684E-04	-2.05111E-08	0.0

Table 5.14 - Constants for Mean Specific Heat Equation (5.10-6). (Van Aken[42])

Sub-Programs AIRGPROP, H2OGPROP, and H2OLPROP calculate the thermodynamic properties for air, steam, and water respectively.

5.11 Specific Enthalpy of Saturated Water and Steam

Eq.(5.10-6) gives the mean specific heat for air and water vapour with reference to dry air and saturated steam at 0°C respectively. Eq.(5.10-5) then gives the specific enthalpy at t°C. This is useful for combustion calculations and other applications involving dry steam.

For psychrometric calculations the properties of saturated water and steam are of greater interest. Hyland and Wexler[18] give specific enthalpy equations as functions of temperature and vapour pressure. Within the specified ranges these equations perform adequately but when considering the high degrees of polynomials used combined with the added complexity of vapour pressure correction, the performance is a little disappointing.

Polynomial equations in the form of Eqs.(5.11-1) and (5.11-2) have therefore been fitted to published steam tables. Below 150°C the accuracy is better than ±0.01%. Only when approaching the critical temperature does the discrepancy become as large as 3%.

$$h = a_0 + a_1 x + a_2 x^2 + a_3 x^3 + a_4 x^4 \qquad (5.11-1)$$

or

$$h = \frac{1.0}{a_0 + a_1 x + a_2 x^2 + a_3 x^3 + a_4 x^4} \qquad (5.11-2)$$

where

$$x = t/100 \quad . \qquad (5.11-3)$$

The coefficients for saturated water, latent heat, and saturated steam are listed in Tables 5.15, 5.16, and 5.17 respectively.

Range °C	a_0	a_1	a_2	a_3	a_4	Eq.No.
-125-0.0*	-333.887	207.38971	33.292297	0.0	0.0	5.11-1
.01-50	-1.288D-02	420.90276	-9.5934537	9.9737883	0.0	5.11-1
50-150	0.1448	419.43851	-4.0769105	3.5486064	0.0	5.11-1
150-236	-28.06	470.97310	-36.139727	10.379756	0.0	5.11-1
236-350	-1409.29	2036.1590	-627.03810	84.757637	0.0	5.11-1
350-370	-3.0079744	3.3779970	-1.4220200	.26602583	-.018662417	5.11-2
370-374.1	56.024057	-45.265173	12.191044	-1.0944619	0.0	5.11-2

Table 5.15 - Constants for computing the Specific Enthalpy h_f for saturated liquid.

* Applies to saturated ice.

Range °C	a_0	a_1	a_2	a_3	a_4	Eq.No.
.01-50	2501.47	-234.66985	-4.6764297	0.0	0.0	5.11-1
50-150	2502.32	-239.74293	9.3564359	-14.970007	0.0	5.11-1
150-236	2333.9	0.0	-98.755	0.0	0.0	5.11-1
236-350	-9776.98	17890.709	-10037.168	2466.9129	-231.61670	5.11-1
350-370	-25953943.	29126978.	-12257818.	2292889.7	-160859.36	5.11-1
370-374.1	370044720.	-299095820.	80584514.	-7237315.0	0.0	5.11-1

Table 5.16 - Constants for computing the Specific Enthalpy h_{fg} for latent heat of evaporation.

Range °C	a_0	a_1	a_2	a_3	a_4	Eq.No.
-125-0.	2501.67	185.97285	0.0	0.0	0.0	5.11-1
0.-50	2501.51	184.79196	-6.7121997	0.0	0.0	5.11-1
50-150	2502.31	180.36099	4.3888360	-11.061316	0.0	5.11-1
150-236	2402.19	330.93118	-68.309052	0.0	0.0	5.11-1
236-350	-6014.16	12718.985	-6920.6131	1692.7919	-158.16516	5.11-1
350-370	-14289414.	16039815.	-6751157.3	1263099.2	-88636.875	5.11-1
370-374.1	-50.685398	40.959233	-11.033156	.99067330	0.0	5.11-2

Table 5.17 - Constants for computing the Specific Enthalpy h_g for saturated vapour.

Sub-program ENTWATFG computes the specific enthalpies for saturated water or ice, latent heat of evaporation or sublimation, and for saturated steam as functions of temperature in °C.

6.0 PSYCHROMETRICS

Psychrometry is the study of thermodynamic properties of moist air, which could be considered as a binary mixture of dry air and super heated steam. For psychrometric calculations, at standard atmospheric pressure and in the temperature range from -50 to 50°C, the perfect gas relations may be applied with errors of less than 0.7%[40]. With decreasing pressure these errors are even smaller.

The composition of dry air is fairly constant and it may be treated as a perfect gas because the temperature applicable to heating and cooling coils is high relative to its critical temperature.

At a given temperature and pressure the amount of water vapour in moist air can vary from zero to a maximum at which the air is said to be saturated.

The following symbols are used in this section:

Cp_t	specific heat for moist air at t°C	- kJ/kg dry air K
Cpa_t	specific heat for dry air at t°C	- kJ/kg K
Cpg_t	specific heat for water vapour at t°C	- kJ/kg K
$Cpma_t$	mean specific heat for dry air at t°C	- kJ/kg K
Cw	mean specific heat for water at t °C	- kJ/kg K
fs	Enhancement factor for humidity calcs.	
h	enthalpy of moist air at t°C	- kJ/kg
ha	enthalpy for dry air at t°C	- kJ/kg
hg	enth.for saturated water vapour at t°C	- kJ/kg
hs	enth.of moist air at saturation and t	- kJ/kg dry air
hf	enthalpy of condensed water at t	- kJ/kg
Ma	mass of dry air	- kg
Mw	mass of water vapour	- kg
n	total number of moles in mixture	
na	number of moles of dry air	
nw	number of moles of water vapour	
P	total mixture pressure	- kPa
p	total mixture pressure	- Pa
pa	partial pressure of dry air	- Pa
pw	partial pressure of water vapour	- Pa
Pws	saturation pressure of water vapour	- kPa
pws	saturation pressure of water vapour	- Pa
R	universal gas constant (8314.41)	- J/kg mol K
T	absolute temperature	- K
t	dry bulb temperature	- °C
t^*	thermodynamic wet bulb temperature	- °C
td	dew point temperature	- °C
V	total mixture volume	- m^3
v	specific volume of air mixture	- m^3/kg
W	humidity ratio	- kg/kg dry air
Ws	humidity ratio at saturation	- kg/kg dry air

W_s^* humidity ratio at saturation at t^* - kg/kg dry air
x_a mole fraction for dry air
x_w mole fraction for water vapour

$\emptyset$ relative humidity   - %

6.1   Thermodynamic Properties of Water at Saturation

Between the triple point at 0.01°C and the critical tempera-
ture at 374.15°C, both the liquid and vapour states of water
may co-exist in equilibrium. These states are known as satu-
rated liquid and saturated vapour.   Before any of the moist
air properties can be determined the water vapour saturation
pressure must be established.   This can be obtained for the
temperature range of -100 to 374.15°C, by use of equation
(5.1-1),   (5.1-3),   or (5.1-4),   which equations are used in
sub-program PSATH2O.

6.2   Humidity Parameters

Specific humidity is the mass of water vapour per unit of dry
air and the Humidity ratio W of moist air is defined as the
ratio of the mass of water vapour to the mass of dry air,
thus

$$W = M_w / M_a .$$ (6.2-1)

If we let the mole fraction of dry air be x_a and that of
water vapour be x_w, then by definition $x_a + x_w = 1$. Hence
the humidity ratio can also be expressed as the mole fraction
ratio (x_w/x_a) multiplied by the ratio of molecular masses.
The molecular mass for dry air is given[4] as 28.9645, and
that for water as 18.01528.

Thus the ratio 18.01528/28.9645 = 0.62198, and

$$W = 0.62198 \; x_w/x_a .$$ (6.2-2)

The perfect equation of state for dry air is

$$p_a V = n_a R T ,$$ (6.2-3)

and that for water vapour

$$p_w V = n_w R T .$$ (6.2-4)

For the mixture this becomes

$$(p_a + p_w) V = (n_a + n_w) R T .$$ (6.2-5)

Now the mole fraction of dry air is

$$x_a = p_a / (p_a + p_w) = p_a / p ,$$ (6.2-6)

and that for water vapour

$$x_w = p_w / (p_a + p_w) = p_w / p \ . \tag{6.2-7}$$

From equations (6.2-2), (6.2-6), and (6.2-7)

$$W = 0.62198 \frac{p_w}{p - p_w} \ , \tag{6.2-8}$$

which can be re-arranged to solve for p_w as

$$p_w = \frac{W \cdot p}{(0.62198 + W)} \ . \tag{6.2-9}$$

The relative humidity is now expressed as

$$\emptyset = 100 \cdot \frac{p_w}{p_{ws}} \ \% \ . \tag{6.2-10}$$

Similarly to Eq.(6.2-8), the humidity ratio at saturation can be expressed as

$$W_s = 0.62198 \frac{p_{ws}}{p - p_{ws}} \ . \tag{6.2-11}$$

Enhancement factors can be applied to Eq.(6.2-11) to allow an exact solution for W_s. These factors account for the effect of dissolved gases, and the effect of pressure, on the properties of the condensed phase. They also allow for the effect of intermolecular force on the properties of moisture itself. Applied to Eq.(6.2-11):

$$W_s = 0.62198 \frac{f_s \cdot P_{ws}}{P - f_s \cdot P_{ws}} \ . \tag{6.2-12}$$

Solutions for factors f_s are listed in Table 6.1 as a function of temperature and pressure, where the pressures are expressed in kPa.

Temp.	Pressure, kPa					
°C	33.8	50.7	67.6	84.5	101.0	108.0
-18	1.0016	1.0025	1.0033	1.0040	1.0047	1.0051
-7	1.0016	1.0024	1.0032	1.0039	1.0045	1.0048
+4	1.0018	1.0025	1.0032	1.0038	1.0044	1.0047
16	1.0020	1.0026	1.0033	1.0039	1.0044	1.0047
27	1.0023	1.0029	1.0036	1.0041	1.0046	1.0049
38	1.0027	1.0033	1.0040	1.0045	1.0050	1.0053
49	1.0031	1.0037	1.0044	1.0050	1.0055	1.0057
60		1.0041	1.0048	1.0054	1.0059	1.0063

Table 6.1 - Enhancement Factors f_s for Humidity Calculations. (ASHRAE[4])

Table 6.1 has been fitted by empirical equations of the form

$$f_s = c_0 + c_1 \cdot t + c_2 \cdot t^2 , \tag{6.2-13}$$

where

$c_0 = 1.0004 + 3.995E-05 \cdot P$
$c_1 = (653.71/P - 6.1322) \cdot 1.0E-06 \quad \textit{(for P < 72kPa)}$
$c_1 = (26.537 - 0.32692 \cdot P) \cdot 1.0E-06 \quad \textit{(for P => 72kPa)}$
$c_2 = 1.0E-07/(.402017 - 2.583545E-03 \cdot P + 4.128112E-06 \cdot P^2)$

6.3 Specific Volume

The volume v of a moist air mixture is expressed in terms of unit mass of dry air, hence

$$v = V/M_a = V/(28.9645 \, n_a) . \tag{6.3-1}$$

By equations (6.2-3) and (6.3-1), and with the relation $p = p_a + p_w$

$$v = \frac{R \, T}{28.9645 \, (p-p_w)} . \tag{6.3-2}$$

Using equation (6.2-9),

$$v = \frac{R \, T}{28.9645 \, p} (1 + 1.6078 \, W) , \tag{6.3-3}$$

and since R = 8314.41 J/kg mol K ,

$$v = \frac{287.0552 \, T}{p} (1 + 1.6078 \, W) . \tag{6.3-4}$$

6.4 Enthalpy and Specific Heat

The enthalpy of a mixture of perfect gases equals the sum of the enthalpies of the individual components. Therefore, the enthalpy of moist air

$$h = h_a + W \, h_g . \tag{6.4-1}$$

The enthalpy for dry air at t°C is given by Eq.(5.10-5) as

$$h_a = Cpma_t \cdot t , \tag{6.4-2}$$

where $Cpma_t$ can be determined from Eq.(5.10-6) with the appropriate constants from Table 5.14, or directly from Table 5.13 which gives for t < 50°C, $Cpma_t$ = 1.006.

The specific enthalpy for saturated steam with respect to saturated steam at 0°C is given by sub-program ENTWATFG which is based on Equations (5.11-1), (5.11-2), (5.11-3) and Table 5.17. For t < 50°C the specific enthalpy for saturated steam

may be approximated as

$$h_g = 2501.8 + 1.8144 \, t \, . \tag{6.4-3}$$

Thus for $t < 50°C$, Eq.(6.4-1) can be written as

$$h = 1.006 \cdot t + W \cdot (2501.8 + 1.8144 \cdot t) \, . \tag{6.4-4}$$

Eq.(6.4-4) can be re-arranged to solve for the dry bulb temperature as

$$t = \frac{h - 2501.8 \cdot W}{1.006 + 1.8144 \cdot W} \, . \tag{6.4-5}$$

As for enthalpy, the specific heat of a mixture of perfect gases equals the sum of the specific heats of the individual components. Therefore, the specific heat of moist air

$$Cp_t = Cpa_t + W \cdot Cpg_t \, , \tag{6.4-6}$$

where Cpa_t and Cpg_t are given by Eq.(5.7-1) together with the appropriate constants listed in Table 5.10. For a restricted temperature range the specific heat of moist air can be derived from Table 5.11 as

$$Cp_t = 1.006 + 1.88 \, W \tag{6.4-7}$$

Sub-program MOISTAIR gives the wide range solution for Cp_t.

6.5 Thermodynamic Wet Bulb Temperature

When water is adiabatically evaporated into air to saturation the air temperature will be reduced to a level known as the thermodynamic wet bulb temperature. This is the principle used for the psychrometer which consists of two thermometers, one to measure the simultaneous dry bulb temperature, and the other with a wet wick to measure the wet bulb temperature.

Although this measured wet bulb temperature is not strictly the thermodynamic wet bulb temperature, the correction required is quite small.

In the above process, the humidity ratio is increased from an initial value W to the value Ws^* corresponding to saturation at t^*, the enthalpy is increased from h to hs^*, and the mass of water added is $(Ws^* - W)$. The energy added to the moist air is then $(Ws^* - W) \cdot hf^*$ kJ/kg dry air. For an adiabatic process

$$hs^* = h + (Ws^* - W) \cdot hf^* \, . \tag{6.5-1}$$

Substituting Eq.(6.4-1) into re-arranged (6.5-1) yields

$$W \cdot (h_f^* - h_g) = W_s^* \cdot h_f^* + h_a - h_s^* . \qquad (6.5\text{-}2)$$

Also by Eq.(6.4-1)

$$h_s^* = h_a^* + W_s^* \cdot h_g^*$$

and substituting this into Eq.(6.5-2) yields

$$W \cdot (h_f^* - h_g) = W_s^* \cdot h_f^* + h_a - h_a^* - W_s^* \cdot h_g^*$$

or

$$W = \frac{W_s^* \cdot (h_f^* - h_g^*) + h_a - h_a^*}{h_f^* - h_g} . \qquad (6.5\text{-}3)$$

The enthalpy of condensed water at t°C can be approximated as

$$h_f = 4.1868 \cdot t . \qquad (6.5\text{-}4)$$

Substituting the following approximations

$$h_f^* = 4.1868 \cdot t^*$$
$$h_a = 1.006 \cdot t$$

$$h_a^* = 1.006 \cdot t^*$$
$$h_g = 2501.8 + 1.8144 \cdot t$$

$$h_g^* = 2501.8 + 1.8144 \cdot t^*$$

into Eq.(6.5-3) yields the solution for the temperature range of 0.01°C to 50°C as

$$W = \frac{(4.1868 \cdot t^* - 2501.8 - 1.8144 \cdot t^*) \cdot W_s^* - 1.006 \cdot (t - t^*)}{4.1868 \cdot t^* - 2501.8 - 1.8144 \cdot t}$$

or

$$W = \frac{(2501.8 - 2.3724 \cdot t^*) \cdot W_s^* - 1.006 \cdot (t - t^*)}{2501.8 + 1.8144 \cdot t - 4.1868 \cdot t^*} . \qquad (6.5\text{-}5)$$

Many of the equations presented in this section are a function of the thermodynamic wet bulb temperature but offer no direct solution for this parameter as a function of other thermodynamic properties. Thus numeric solutions for the wet bulb temperatures from these equations are only possible by iteration.

An algorithm has been presented by Worbs[45] which approximates the wet bulb temperature as a function of dry bulb temperature and relative humidity and is given in °F as

$$(t_{db} - t_{wb}) = .3814\, t_{db} - .004\, \emptyset\, t_{db} + .03363\, \emptyset - 2.418 . $$
$$(6.5\text{-}6)$$

Since

$$t°F = 1.8 \cdot t°C + 32 ,$$ (6.5-7)

Eq.(6.5-6) can be re-arranged for °C as

$$t_1^* = .6186 \, t +.004 \, \emptyset \, t +.05243 \, \emptyset - 5.43707 .$$ (6.5-8)

Eq.(6.5-8) may be differentiated with respect to $\emptyset$ and for constant dry bulb temperature t to yield the local slope as

$$\frac{dt^*}{d\emptyset} = .004 \, t + .05243 ,$$ (6.5-9)

and the second approximation of t^* is then written as

$$t_2^* = t_1^* + (.004 \, t + .05243) \, (\emptyset_1 - \emptyset_2) .$$ (6.5-10)

6.6 Dew Point Temperature

The dew point temperature t_d is the temperature of moist air at saturation. For a perfect gas this may be defined by Eq. (6.2-9) as

$$p_{ws}(t_d) = p_w = \frac{W \cdot p}{(0.62198 + W)}$$ (6.6-1)

in which t_d can only be solved by iteration. Alternatively the dewpoint temperature can be calculated directly with the equation [ASTM E337.62]

$$t_d = \frac{3929.}{\ln (14084175./p_w)} - 231.7 \quad °C .$$ (6.6-2)

This equation is valid for the full temperature range from -125°C to the critical temperature of 374.15°C. A slightly better accuracy can be obtained with the Peppers[4] equation within the range of -50°C to 0°C

$$t_d = 6.09 + 12.608 \cdot \alpha + 0.4959 \cdot \alpha^2 ,$$ (6.6-3)

where

$$\alpha = \ln (p_w) .$$ (6.6-4)

6.7 Numerical Methods for Moist Air Properties

The application of the equations presented above and the methods used in the various sub-programs for computing the moist air properties are outlined in the present sub-section.

For wide temperature and pressure range applications the perfect gas laws are inadequate and the virial coefficients of each gas should be taken into account. This is not a simple operation[42] particularly when polar molecules, in this case water vapour, are involved. ASHRAE[4] has presented a method of using perfect gas relations with correction factors to account for the effects of pressure and dissolved gases and these are the methods adopted in the psychrometric sub-programs.

The sub-programs have been tested against published data[4] over the temperature range of -50°C to 200°C and pressure range of 84.5 kPa to 101.3 kPa with good results. However, the sub-programs for the thermophysical properties for air and water substance are valid for much wider temperature ranges and the pressure correction factors can be calculated for a pressure range of 0.1 to 5000 kPa. Thus theoretically these sub-programs cover a much wider temperature and pressure range than indicated by the ranges tested.

6.7.1 Dry and Wet Bulb Temperatures and Pressure

Sub-program DRYWETMP[b] computes the moist air properties from dry and wet bulb temperatures t and t^* and total mixture pressure P by the following method:

1. find $P_{ws}^* = f(t^*)$ with sub-program PSATH2O[a]
2. find enhancement factor $f_s = f(P, t^*)$ with sub-program ENHANCFS[b]
3. establish $W_s^* = f(P, P_{ws}^*, f_s)$ with Eq.(6.2-12)
4. find h_f^* and h_g^* at t^* with sub-program ENTWATFG[a]
5. find h_g at t with sub-program ENTWATFG[a]
6. find h_a^* at t^* with sub-program MOISTAIR[b]
7. find h_a at t with sub-program MOISTAIR[b]
8. solve for W with Eq.(6.5-3)
9. establish $p_w = f(P, W)$ with Eq.(6.2-9)
10. find $P_{ws} = f(t)$ with sub-program PSATH2O[a]
11. establish relative humidity ø with Eq.(6.2-10)
12. establish specific volume v with Eq.(6.3-4)

Within the temperature range 0.01°C to 50°C the above procedure may be simplified by deleting steps 4 to 7 and then solving for W with Eq.(6.5-5). A further simplification can be achieved by deleting step 2 and setting $f_s = 1$.

(a) Sub-program stored in Library PSYCHRO and described in Section 5.0
(b) Sub-program stored in Library PSYCHRO and described in this Section

6.7.2 Dry Bulb and Dewpoint Temperatures and Pressure

Sub-program DRYDETMP[b] computes the moist air properties from dry bulb and dewpoint temperatures t and t_d and total mixture pressure P by the following method:

1. find $P_{ws} = f(t_d)$ with sub-program PSATH2O[a]
2. find enhancement factor $f_s = f(P,t_d)$ with sub-program ENHANCFS[b]
3. establish $W = f(P,P_{ws},f_s)$ with Eq.(6.2-12)
4. establish $p_w = f(P,W)$ with Eq.(6.2-9)
5. find $P_{ws} = f(t)$ with sub-program PSATH2O[a]
6. establish relative humidity Ø with Eq.(6.2-10)
7. establish specific volume v with Eq.(6.3-4)

6.7.3 Dry Bulb Temperature, Relative Humidity and Pressure

Sub-program DRYTMPRH[b] computes the moist air properties from dry bulb temperature t, relative humidity Ø, and total mixture pressure P by the following method:

1. find $P_{ws} = f(t)$ with sub-program PSATH2O[a]
2. Solve for P_w with Eq.(6.2-10)
3. find enhancement factor $f_s = f(P,t)$ with sub-program ENHANCFS[b]
4. establish $W = f(P,P_w,f_s)$ with Eq.(6.2-12)
5. establish specific volume v with Eq.(6.3-4)

6.7.3 Other Moist Air Properties

Each of the methods described above yields the humidity ratio W from which, together with the dry bulb temperature t, the specific enthalpy of moist air can be found with sub-program MOISTAIR[b] and the dewpoint temperature t_d can be found as a function of humidity ratio and pressure with sub-program DEWPOINT[b] .

The thermodynamic wetbulb temperature can be approximated as a function of dry bulb temperature and relative humidity with Eq.(6.5-8) within ±0.5% for the comfort range. However, this equation does not perform very well for humidities less than 10% or at elevated temperatures. Furthermore it cannot account for significant departures from atmospheric pressure.

(a) Sub-program stored in Library PSYCHRO and described in Section 5.0
(b) Sub-program stored in Library PSYCHRO and described in this Section

A fast iteration method has been developed to overcome the shortcomings of Eq.(6.5-8) and is the method used in sub-program WETBULBT[b] :

1. find the first approximation of $t_1^* = f(t,\emptyset)$ with Eq. (6.5-8)

2. find $\emptyset_1 = f(t,t_1^*,P)$ with sub-program DRYWETMP[b]

3. find the second approximation $t_2^* = f(t,t_1^*,\emptyset,\emptyset_1)$ with Eq.(6.5-10)

4. find $\emptyset_2 = f(t,t_2^*,P)$ with sub-program DRYWETMP[b]

5. the final approximation for t^* can now be found as

$$t^* = t_1^* + \frac{(t_1^* - t_2^*) \cdot (\emptyset - \emptyset_1)}{(\emptyset_1 - \emptyset_2)} \ . \qquad (6.7-1)$$

(a) Sub-program stored in Library PSYCHRO and described in Section 5.0
(b) Sub-program stored in Library PSYCHRO and described in this Section

7.0 HEAT TRANSFER PARAMETERS

The equations for deriving heat transfer parameters have been described and examined in Appendix A.   The application of these parameters to the heat exchanger model and correlation of these with test data is now described.

7.1 Heat Transfer from Fluid Inside Circular Tubes

7.1.1 Fluid and Flow Parameters

Water velocities in chilled water cooling coils are normally restricted within the range of 0.25 to 2.5m/s. At a specific gravity of 1000 kg/m^3 this is equivalent to mass flow rates over the range of 250 to 2500 kg/m^{2}s.

The most common tube outside diameters are 13mm and 16mm. For a typical wall thickness of 0.65mm the corresponding inside diameters are 11.7 and 14.7mm.

Chilled water is typically supplied at 7°C and at this temperature the properties are established with Equations (5.4-1), (5.6-1), and (5.9-1) as

    viscosity μ = 1.42E-03 Pa s ,
    conductivity kw = 0.58   W/m K (or 0.58E-03 kJ/s m K),
    specific heat Cw = 4.20   kJ/kg K ,

and the Prandtl number is given by Eq.(A.2-5) as

$$Pr = \frac{\mu\ Cw}{kw} = \frac{1.42E\text{-}03 \cdot 4.20}{0.58E\text{-}03} = 10.28 \ .$$

The Reynolds number is given in Appendix A by Eq.(A.1-1) as

$$Re = Dh \cdot G \ / \ \mu \ .$$

Thus the minimum Reynolds number

$$Re_{(min)} = \frac{11.7E\text{-}03 \cdot 250}{1.42E\text{-}03} = 2060 \ ,$$

and the maximum Reynolds number

$$Re_{(max)} = \frac{14.7E\text{-}03 \cdot 2500}{1.42E\text{-}03} = 25880 \ .$$

Thus for a velocity range of 0.25 to 2.5m/s, the chilled water flow is essentially in the turbulent range.   The rationale for not exceeding 2.5m/s is to prevent excessive noise and erosion due to cavitation in the low pressure regions at the return bends.   However, the program will also compute heat transfer for water flow in the laminar and transitional ranges. In such case the program will display a

warning since, particularly for the transitional range, the results may not be reliable.

7.1.2 Well Developed Laminar Flow

For well developed laminar flow inside circular tubes the Nusselt number for constant heat rate is given as (Eq.(A.2-2))

$$Nu(H) = 4.364 \; ,$$

and for constant surface temperature as (Eq.(A.2-3))

$$Nu(T) = 3.658 \; .$$

The Nusselt number for constant heat rate is recommended[29] for heat transfer applications in which the surface temperature is greater than the fluid temperature and when the surface temperature is less than the fluid temperature the Nusselt number for constant temperature is recommended.

7.1.3 Well Developed Turbulent Flow

For well developed turbulent flow inside smooth tubes Nusselt number equations (A.3-4) and (A.3-5) are recommended[31] for Prandtl numbers less than 0.5 as

$$Nu(H) = 6.3 + .0167 \; Re^{.85} \; Pr^{.93} \; ,$$

and

$$Nu(T) = 4.8 + .0156 \; Re^{.85} \; Pr^{.93}$$

respectively and for Pr > 0.5, Eq.(A.3-10) is recommended and is given[31] as

$$Nu = 5 + 0.015 \; Re^a \; Pr^b \; ,$$

where

$$a = 0.88 - \frac{0.24}{4 + Pr} \; ,$$

$$b = 0.333 + 0.5 \exp(-0.6 \; Pr) \; .$$

Note that for Prandtl numbers greater than 0.5 the differences between Nu(H) and Nu(T) are negligible.

7.1.4 Thermal Entry Length for Circular Tube

The heat transfer for the laminar flow thermal entry length can be expressed as an enhancement ratio by equations (A.2-13) and (A.2-14) of Appendix A.

for $x^+ < 0.06$,

$$\frac{Nu_m}{Nu_\infty} = 0.55473 \ (x^+)^{-.324} \ ,$$

and for $x^+ >= 0.06$

$$\frac{Nu_m}{Nu_\infty} = 1.0 + \frac{0.027}{(x^+)} \ ,$$

where x^+ is defined by Eq.(A.2-10) as

$$x^+ = \frac{2 \ (x/Dh)}{Re \ Pr} \ .$$

In the transient model each coil row is divided into two equal parts. Thus for a coil of Clwi mm wide the thermal entry length is defined as (Clwi/2) mm. For a tube inside diameter of Di mm the entry length x^+ is derived from Eq.(A.2-10) as

$$x^+ = \frac{2 \ ((Clwi/2)/Di)}{Re \ Pr} = \frac{Clwi \ / \ Di}{Re \ Pr} \ . \qquad (7.1-1)$$

For turbulent flow the characteristic ratio,

$$\frac{x}{D} = \frac{Clwi/2}{Di} \ . \qquad (7.1-2)$$

The enhancement ratio is now given by Eq.(A.3-16) as

$$\frac{Nu_m}{Nu_\infty} = a \left[\frac{x}{D} \right]^{-b}$$

where a and b are defined by equations (A.3-18) and (A.3-19).

The heat transfer coefficients can now be established by re-arranging Eq.(A.2-1) as

$$hi = \frac{Nu \ k}{Dh} \ . \qquad (7.1-3)$$

Sub-program HTRANH2O computes the heat transfer coefficient for water inside the tubes as a function of fluid velocity, tube inside diameter, viscosity, thermal conductivity, and Prandtl number. It also returns the Reynolds and Nusselt numbers.

7.2   Heat Transfer to Finned Surfaces

Four separate zones for heat transfer have been identified at the air side and their corresponding areas have been defined for each fin element in Appendix B.   The heat transfer zones are for:

- Fully developed laminar flow   (normal heat transfer)
- Developing laminar flow
- Vortex enhancement
- Reduced heat transfer.

7.2.1   Channel Flow

It is shown in Appendix C that the heat transfer coefficient for fully developed laminar flow is best expressed in terms of channel flow for which the channel dimensions are defined by the space between the fins and the space between the tubes reduced by the vortex widths.

Tables C.9 and C.15 show that the Reynolds numbers for the two series of tests were always well within the laminar flow range.   This is in agreement with the flow visualisation experiments conducted by Gilbert[14].

For cooling applications the Nusselt numbers for constant temperature, Nu(T), are recommended[29].   These are listed in Table A.4 and may be computed with Eq.(A.2-4) for the range $0.0 < b/a < 1.0$ as

$$Nu = \exp(\emptyset(b/a))$$

for which the polynomial coefficients for $\emptyset(b/a)$ are listed in Table A.6 as

Subscript	Nu(T)
0	2.0189157
1	-2.7696340
2	2.8248030
3	-0.98764998

A similar equation has been derived for Nu(H).

7.2.2   Developing Laminar Flow

The approach side of the coil has an enhanced heat transfer zone owing to a developing laminar flow.   This has been examined in Section A.2.4 of Appendix A. Since the tubes are set back with respect to the leading fin edges the heat transfer within the thermal entry length should be determined for infinite parallel plates rather than for channel flow. This may be computed with equations (A.2-16) and (A.2-17) as

$$\frac{Nu_m}{Nu_\infty} = 0.37677 \ (x^+)^{-.304}$$

for $(x^+) < 0.02$, and for $(x^+) >= 0.02$

$$\frac{Nu_m}{Nu_\infty} = 1.0 + \frac{0.00608}{(x^+)}$$

where

$$x^+ = \frac{2 \ (x/Dh)}{Re \ Pr}$$

is given by Eq.(A.2-11).

7.2.3 Vortex Enhancement

Vortex enhancement factors have been established from experimental results as described in Appendix C and these have been fitted to the empirical equation (C.4-2) as

$$Ke = 0.22127 \cdot Re_{(channel)}^{.555} .$$

For this correlation the vortex width was defined as half the space between the fins and the Reynolds number was that for channel flow with the channel dimensions defined by the fin spacing and the space between the tubes reduced by the vortex widths. The vortex enhancement factor Ke relates to the heat transfer coefficient for fully developed laminar flow within the same channel.

7.2.4 Reduced Heat Transfer Zones

The reduced heat transfer zones were taken as having negligible heat transfer for the evaluation of the vortex enhancement factors.

7.2.5 Mean Heat Transfer Coefficients

Having defined the heat transfer coefficients for each zone and their respective areas, the mean heat transfer coefficient can be computed for each fin element. Eq.(B.3-1) shows the method adopted in sub-program FINAREAS.

7.3 Fouling Factors

After some time, heat transfer surfaces may accumulate deposits of scale, oil, or other foreign matter.   These deposits cause additional resistance to heat transfer.   The method of dealing with this resistance is through the use of the fouling factor, or fouling resistance, *Rf*.

Starting from a clean surface, fouling will increase for some time depending on the specific mechanisms involved.   In some cases an asymptotic fouling condition[27] is achieved at which time the magnitude of the deposition is equal to that of removal.   Constant fouling factors are generally used for design purposes.

For the water side fouling, resistances are recommended[40] as shown in Table 7.1.

Application	Non-Fe Tubes	Fe Tubes
Recirculated water, closed system	9E-05	18E-05
Recirculated water, open system	18E-05	35E-05

Table 7.1 - Fouling resistances, Rfi in m² K/W, for water coolers. (Threlkeld[40])

Lee and Knudsen[23] recommend a minimum water side fouling factor of 4.4E-05 m²K/W for condensers.   The heat transfer coefficient inside tubes is then modified as:

$$Ui = \frac{1}{1/hi + Rfi} ,$$

(7.3-1)

where *hi* is the internal convective heat transfer coefficient as derived by Eq.(7.1-3).

Gas-side fouling data is very limited. As a guide, Table 7.2 lists typical fouling resistances[27] for some industrial gases. For air conditioning applications air is well filtered and the fouling should be well below the factors listed in this Table. Furthermore because of the small convective heat transfer coefficient (large resistance) for the outside surace of finned tube heat exchangers, a minor deposit on this surface has little effect on the overall heat transfer coefficient *Uod*.

Gas Stream	Rfo - m² K/W
Butane	18E-05 - 53E-05
Compressed Air	35E-05
Gas Turbine	18E-05
Natural Gas	9E-05 - 53E-05
Steam	9E-05

Table 7.2 - Gas-Side Fouling resistances.
(Marner and Suitor[27])

The heat transfer coefficient for dry finned surfaces is modified as:

$$Uod = \frac{1}{1/ho + Rfo} \, , \qquad (7.3\text{-}2)$$

where *ho* is the external convective heat transfer coefficient.

8.0 HEAT AND MASS TRANSFER

Symbols used in this Section

A	heat transfer area	$- m^2$
Cp	specific heat at constant pressure	- kJ/kg K
Df	water vapour diffusivity	$- m^2/s$
h_a	enthalpy of moist air approaching coil	- kJ/kg dry air
h_c	convection heat transfer coefficient	$- W/m^2$ K
h_D	Mass transfer coefficient	
h_{fg}	latent heat of vaporisation for water	- kJ/kg water
h_{fw}	enthalpy of saturated liquid water at t_w	- kJ/kg water
h_g	enthalpy of saturated water vapour	- kJ/kg water
how	heat transfer coefficient for wet fins	$- W/m^2$ K
h_s	enthalpy of saturated moist air on fins	- kJ/kg dry air
k_a	thermal conductivity of air	- W/m K
k_w	thermal conductivity for water	- W/m K
Le	Lewis number (dimensionless)	
Ma	mass flow rate of dry air	- kg/sec
Qa	air to fin heat transfer rate	- Watt
Sb	enthalpy slope dh_s/dt_w at saturation	- kJ/kg K
Sx	enthalpy/temp. ratio $(h_a-h_s)/(T_a-t_w)$	- kJ/kg K
Ta	db temp. of air approaching coil	- C
t_w	temperature of water film	- C
Uod	overall ext. heat tran.coef. for dry fins	$- W/m^2$ K
Uow	overall ext. heat tran.coef. for wet fins	$- W$ kg/kJ m^2
W	humidity ratio of moist air	- kg/kg dry air
Ws	humidity ratio of saturated air at t_w	- kg/kg dry air
yw	film thickness of water	- mm
α	thermal diffusivity	$- m^2/s$
δ	density of air	$- kg/m^3$

8.1 Total Heat Transfer to Wet Fins

Section 7.0 dealt with sensible heat transfer coefficients which were therefore expressed in terms of temperature difference. When simultaneous cooling and dehumidification takes place then we also have to account for latent heat transfer. Therefore the total heat transfer should then be expressed in terms of enthalpy difference. Thus

$$Qa = Uow \cdot A \cdot (h_a-h_g) \quad Watt \quad . \qquad (8.1-1)$$

The external heat transfer coefficient for wet fins can be based on that for the dry fins with the added thermal resistance due to the water film(a) with thickness yw and conductivity k_w. Threlkeld[40] derived the wet fin heat transfer coefficient in terms of a dry fin heat transfer coefficient and water film thermal resistance as

(a) A uniform water film thickness is assumed whenever the fin surface temperature drops below the dew point temperature of the air stream. Much work has been done on heat transfer by dropwise condensation by Le Fevre and Rose[46,47], and many others, but the implementation to transient modelling is outside the scope of this thesis. However, heat transfer by dropwise condensation could be handled by the computer model by treating the actual droplike surface as a uniform film and then using an enhancement factor to account for the increased surface area due to the drops.

$$ how = \frac{1}{Cp/(Sb \cdot Uod) + yw/(kw \cdot 1000)} \quad W/m^2K \ , \tag{8.1-2} $$

and the overall external heat transfer coefficient for wet fins was then expressed as

$$ Uow = \frac{how}{Sb} \quad W \ kg/kJ \ m^2 \ , \tag{8.1-3} $$

where Sb is the enthalpy slope for saturated air at the fin surface temperature. This enthalpy slope differs from the specific heat of moist air since the latter parameter is determined at constant humidity ratio, whereas Sb follows the saturation line.

From Eq.(6.4-1) the enthalpy at saturation is

$$ hs = ha + Ws \cdot hg \quad . $$

Substituting the approximations for ha and hg, shown in Section 6.5, into the above equation yields

$$ hs = 1.006 \cdot t + (2501.8 + 1.8144 \cdot t) \cdot Ws \ . \tag{8.1-4} $$

Differentiating with respect to t solves for Sb as

$$ \frac{dhs}{dt} = Sb = 1.006 + 2503.614 \cdot \frac{dWs}{dt} \quad . \tag{8.1-5} $$

The saturation humidity ratio is given by Eq.(6.2-11) as a function of vapour pressure and atmospheric pressure, and the vapour pressure is given by Eq.(5.1-1), (5.1-2), or (5.1-3). These equations are not as easily differentiated, therefore a numerical solution is used to solve for

$$ Ws_0 = f(t), \quad and \quad Ws_1 = f(t+1) $$

then

$$ \frac{dWs}{dt} = Ws_1 - Ws_0 \quad . \tag{8.1-6} $$

Eq.(5.7-1) solves for Cpw, and for the temperature range of interest the specific heat for dry air is given by Table 5.11 as 1.006. Thus the specific heat for saturated air is

$$ Cp = 1.006 + Cpw \cdot Ws \quad kJ/kg \ K \ . \tag{8.1-7} $$

All parameters are now available to solve Eq.(8.1-1). Although the principal driving force for combined sensible and latent heat transfer is the enthalpy difference, it would be convenient to relate this to a temperature difference. This can be achieved by introducing the enthalpy slope Sx which is quite distinct from the slope Sb derived above. Let

$$Sx = \frac{h_a - h_s}{T_a - t_w} \quad kJ/kg\ K \quad . \tag{8.1-8}$$

Substitution into Eq.(8.1-1) yields the rate of heat transfer for wet fins in terms of temperature difference as

$$Qa = Uow \cdot A \cdot Sx \cdot (T_a - t_w) \quad Watt \ . \tag{8.1-9}$$

This equation allows the air dry bulb temperature to be iterated against the fin temperature during one integration interval.

8.2 Lewis Relation

Equations (8.1-1) and (8.1-9) express the total heat transfer and do not distinguish between sensible and latent heat load. The lewis relation is useful in determining the sensible heat ratio and is defined as the ratio of the thermal diffusivity α over the water vapour diffusivity Df. Thus

$$Le = \left[\frac{\alpha}{Df} \right]^{(1-n)} \quad or \quad \frac{h_c}{h_D \cdot Cp} \tag{8.2-1}$$

where

$$\alpha = \frac{k_a}{\delta \cdot Cp} \quad m^2/s \tag{8.2-2}$$

and Df can be derived with Eq.(5.2-3). Since α and Df have the same dimensions, the Lewis number is dimensionless. The index n varies with air velocity and surface configuration. For convective heat and mass transfer $n \approx 1/3$. Thus

$$Le \approx \left[\frac{\alpha}{Df} \right]^{(2/3)} \tag{8.2-3}$$

8.3 Dehumidification

Threlkeld[40] established the following heat and mass transfer relations

$$- Ma \cdot dh_a = dQa - Ma \cdot dW \cdot h_{fw} \tag{8.3-1}$$

where

$$dQa = h_c \cdot dA \cdot (t - t_w) + h_D \cdot dA \cdot (W - W_s) \cdot (h_g - h_{fw}) \tag{8.3-2}$$

and

$$- Ma \cdot dW = h_D \cdot dA \cdot (W - W_s) \quad . \tag{8.3-3}$$

humidity ratio

Using the Lewis relation shown in Eq.(8.2-1),

$$dQa = \frac{h_c \cdot dA}{C_p} \left[(h_a - h_s) + \frac{(W - W_s) \cdot (h_g - h_{fw} - 2501.8 \cdot Le)}{Le} \right] \qquad (8.3-4)$$

From equations (8.3-1), (8.3-3), and (8.3-4)

$$\frac{dh}{dW} = Le \, \frac{(h_a - h_s)}{(W - W_s)} + (h_g - 2501.8 \cdot Le) \qquad . \qquad (8.3-5)$$

Eq.(8.3-5) defines the process line and allows the change in air state to be determined as

$$(W_1 - W_2) = \frac{(h_1 - h_2)}{(dh/dW)} \qquad kg/kg_{\text{dry air}} \qquad . \qquad (8.3-6)$$

9.0 TRANSIENTS IN HEAT TRANSFER

Modelling a heat transfer process with finite elements does not only imply the existence of temperature gradients but it also accounts for changes of temperature within each element over a period. These changes may be caused by changes in the enthalpy of the approaching air stream, changes in water temperature, or changes in air or water flow rates. Since any coil has a certain heat storage capacity it will take some time to re-establish steady state heat transfer. Thus for transient modelling a number of time related parameters need to be considered.

9.1 Time Constants

The computer model takes a number of system time lags into consideration and in the case of a cooling application these are related to:

1. Heat gain by the coil metal from the air stream.
2. Thermal conduction within the fin material towards the tubes, causing a temperature gradient within the fins.
3. Heat transfer from the coil tubes to the chilled water.
4. Dead time lag as a function of chilled water velocity.

Consider a substance with a heat transfer area A m^2 and an initial temperature T_1°C. When this substance is surrounded by an ambient temperature T_2°C, and subjected to a heat transfer coefficient of h W/m^2K at its interface, the initial rate of heat transfer can be established as

$$Q = h \cdot (T_2-T_1) \cdot A \qquad \text{Watt.} \qquad (9.1-1)$$

If the ambient temperature T_2 can be regarded as an infinite heat sink then the temperature of the given substance will approach T_2 after some time and the rate at which its temperature changes is also dependent upon its heat storage capacity C Joules/K. Thus

$$\frac{dT_1}{dt} = \frac{Q}{C} = \frac{h \cdot A \cdot (T_2-T_1)}{C} \qquad , \qquad (9.1-2)$$

so that

$$\int dT_1 = \frac{h \cdot A}{C} \int (T_2-T_1) \, dt \quad . \qquad (9.1-3)$$

This equation represents a typical first order exponential decay for which the numeric process is represented by the flow diagram in fig.9.1 below and in which the expression $h \cdot A/C$ is the reciprocal of the time constant. Hence the time constant is given as

$$\tau = \frac{C}{h \cdot A} \qquad \text{seconds.} \qquad (9.1-4)$$
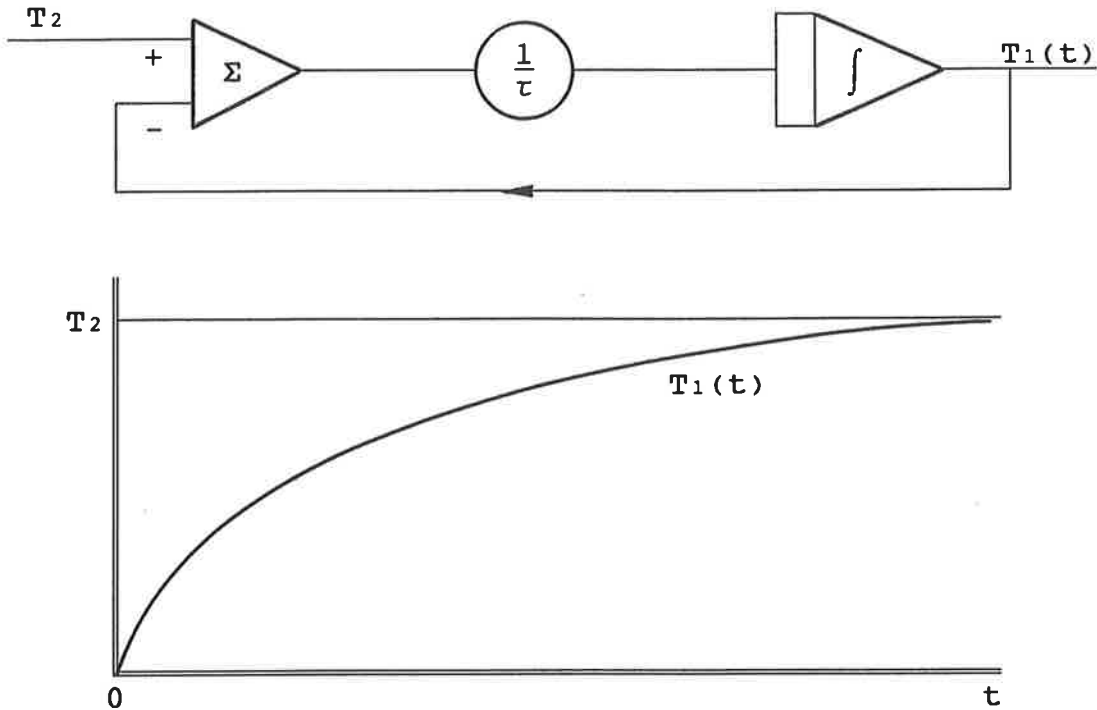
Fig.9.1 - Flow diagram for first order exponential decay.

Eq.(9.1-3) can be further developed into an exponential form for solving the temperature at time t as

$$T_{1_t} = T_2 + (T_{1_0} - T_2)/EXP\left[\frac{h \cdot A \cdot t}{C}\right] \quad °C \quad . \quad (9.1-5)$$

9.1.1 Heat Transfer between Air Stream and Coil Elements

Sub-Section 7.2 has summarised the methods developed for deriving the dry fin heat transfer coefficient for fully developed laminar flow and the enhancement factors that should be applied to compensate for the deviations from the developed laminar flow characteristics. Thus for a given fin element (e) within tube configuration (c) the heat transfer coefficient is expressed as

$$ho(e,c) = ho \cdot Km(e,c) \quad W/m^2 K \quad . \quad (9.1-6)$$

Substituting this into Eq.(7.3-2), to take account of any fouling factor, will yield the solution for the resultant heat transfer coefficient Uod(e) for dry finned surfaces.

Equations (4.3-3) to (4.3-5) give the heat storage capacities Cm(e) and Eq.(3.4-1) gives the heat transfer areas for the fin elements with the air stream, so that the time constants for dry fin elements are derived as

$$\tau_{fa_d}(e,c) = \frac{Cm(e)}{Uod(e) \cdot Ato(e)} \quad \text{seconds,} \qquad (9.1-7)$$

and by Eq.(8.1-9) the time constant for simultaneous cooling and dehumidification are

$$\tau_{fa_w}(e,c) = \frac{Cm(e)}{Uow(e) \cdot Sx \cdot Ato(e)} \quad \text{seconds .} \qquad (9.1-8)$$

9.1.2 Heat Transfer between Fin Elements

The collective rate of heat transfer Qe(e) within one coil row between all fin elements designated *(e+1)* and those designated as *(e)* is given by Eq.(3.5-6). Applying unity temperature differential, this equation will then yield the rate of heat transfer per degree K. Equating this with the heat storage capacities Cm(e) establishes the time constant for heat transfer as

$$\tau_f(e) = \frac{Cm(e)}{Qm(e)} \quad \text{seconds .} \qquad (9.1-9)$$

9.1.3 Heat Transfer between Water and Tube Material

The heat transfer coefficient Ui inside the tubes is given by Eq.(7.3-1). Taking the heat transfer in the direction from the coil material towards the chilled water as positive then its rate can be expressed as

$$Qr = Ui \cdot (Tf-Tr) \cdot Api \quad \text{Watt.} \qquad (9.1-10)$$

But the heat storage capacity Cwr of the water in the tubes is given by Eq.(4.1-2). Thus the time constant for heat transfer to or from the water inside the coil is

$$\tau_w = \frac{Cwr}{Ui \cdot Api} \quad \text{seconds .} \qquad (9.1-11)$$

The heat storage capacity of the first fin element Cm(1), which also includes the tubes, is given by Eq.(4.3-3) and the time constant is derived as

$$\tau_{fw} = \frac{Cm(1)}{Ui \cdot Api} \quad \text{seconds .} \qquad (9.1-12)$$

9.2 Transport Lag or Dead Time Lag

The foregoing sub-sections dealt with the system first order or time lags. There is one other type of lag to be considered; the time it takes for the water to progress throughout the coil, usually referred to as transport lag or dead time. This lag is therefore a function of water velocity and coil dimensions.

9.3 Numerical Integration Methods

Numerical integration involves approximating continuous differential equations with discrete finite-difference equations. The integration interval must be appropriately related to the system being modelled; too great an interval will cause unstable numeric integration, whereas a very short integration interval will be very demanding in computer resources. As a guide the optimum integration interval should be within the range of 1/10 to 1/5 of the shortest system time constant. Shorter integration intervals increase the computing time without noticeable improvement in accuracy.

The success of numerical integration does not always depend upon matching the integration interval with the shortest time constant alone, but also upon the appropriate method of numerical integration. A number of these techniques, ranging from the simple first order Euler method of integration to the higher order methods, have been developed. The higher order integration techniques, sometimes referred to as fast predictor methods, rely on the mean of a number of evaluations during any one integration interval and are most suitable for second[44] or higher order systems.

Heat transfer processes are characterised by first order time lags and can therefore be successfully computed with the first order Euler integration method. The use of higher order techniques for this application would offer very little improvement in accuracy and would be quite wasteful in computer time.

For heat transfer applications[41] an integration interval of 1/5 of the shortest time constant should give the desired stability and accuracy. However, the transfer lag mentioned in the previous sub-section should also be considered. Although non-observance of this lag will not affect the stability of the integration procedure, it can seriously affect the accuracy of the results. Since each coil row will be modelled into at least two parts, as shown in Fig.2.2, the tube length to be considered for evaluating the transport lag is Clwi/2000 m. For a water velocity Vr m/s, the transport lag can be established as

$$\tau_{trans} = \frac{Clwi}{2000 \cdot Vr} \quad \text{seconds.} \quad (9.3-1)$$

This establishes the maximum integration interval from the transport lag consideration.

Some savings in computer time could be made by using a greater integration interval, say equal to the shortest time constant, and then iterating the heat balance 5 times rather then going around the whole simulation loop 5 times.

An analysis conducted on a number of coil configurations with varying face and water velocities showed consistently great differences in time constants. The time constants for the fin elements with respect to the air stream were appreciably larger than the transport lag at all times, whereas the time constants for the fin elements with respect to each other and the chilled water in the tubes tended to be shorter than the transport lag and were therefore the governing factor. The integration interval could be increased by using the exponential equation (9.1-5).

Consider two adjacent fin elements in isolation and at temperatures T_1 and T_2. Applying Eq.(9.1-5) for a duration of several time constants produces exponential trends as depicted in Fig.9.2. Since both these elements have finite heat storage capacities, the curves overshoot the final values. Suppose that the above mentioned elements have the same time constant, then the equilibrium temperature will be midway between T_1 and T_2 and the time required to approach this equilibrium can be derived as

$$1 - e^{-(t/\tau)} = 0.5 \quad , \qquad\qquad (9.3-2)$$

therefore

$$-(t/\tau) = \ln(.5) = -0.693 \ , \quad \text{say} \ -0.7 \ ,$$

thus

$$t = 0.7 \ \tau \quad .$$

When using 5 iterations the integration could then be extended to $5 \times 0.7 \ \tau = 3.5 \ \tau$.
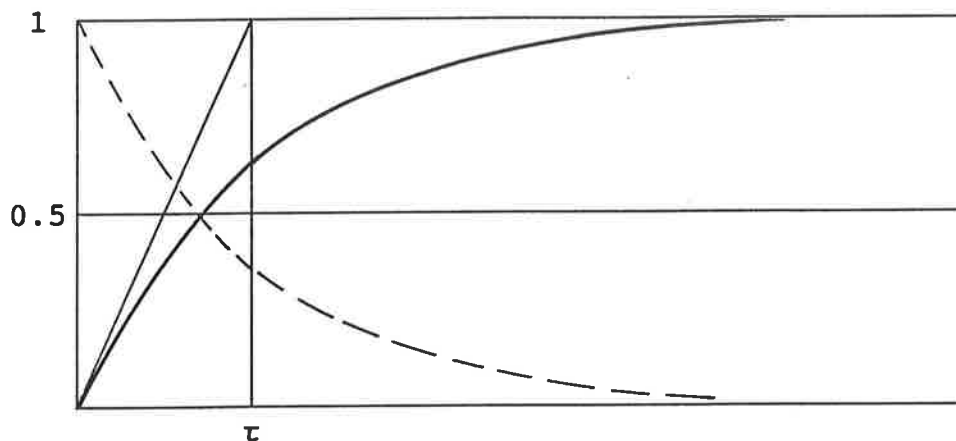
Fig.9.2 - *Derivation of optimum integration interval.*

10.0   SIMULATION PROGRAM 'COILSIM'

The methods and algorithms described in this thesis are incorporated into simulation program COILSIM for which the logic flow diagram is shown in Fig.10.1.   Main program COILSIM and auxiliary program COILPAR have been compiled with IBM Personal Computer BASIC Compiler(c) 1982-1985 and linked with the sub-program libraries listed in Appendix D.

10.1   Purpose and Application

The program models the forced convection heat transfer in any given finned tube heat exchanger and applies to heating as well as to cooling, with or without dehumidification. The program simulates the performance of any finned cooling or heating coil arrangement with up to 12 rows over a wide range of water and face velocities, water temperatures and air conditions.   A variety of water circuits are available for selection which may be arranged for either parallel or counter flow.

The program is not a replacement for coil selection procedures but is intended to simulate the performance of a given coil under a given set of conditions.   The program is particularly useful for establishing the performance of a given coil at conditions for which there are no data available. Thus it avoids the doubtful technique of interpolating or extrapolating tabulated data.

10.2   Input Data Required

All input data is interactively entered through the keyboard as prompted by the screen panels.   Generally the input data requested by the panels are:

• Coil width and height, and number of rows,
• Tube material, dimensions, spacing and row spacing,
• Fin material, thickness and spacing,
• Coil circuiting,
• Air flow rates and entering conditions,
• Water flow rates, direction of flow and entering water temperature.

The program provides default values wherever this is practical and all data entered is checked against valid ranges. Data files are maintained by the program so that data does not have to be re-entered for the same coil.   All thermophysical properties and heat transfer parameters are derived by the program on the basis of the above data.
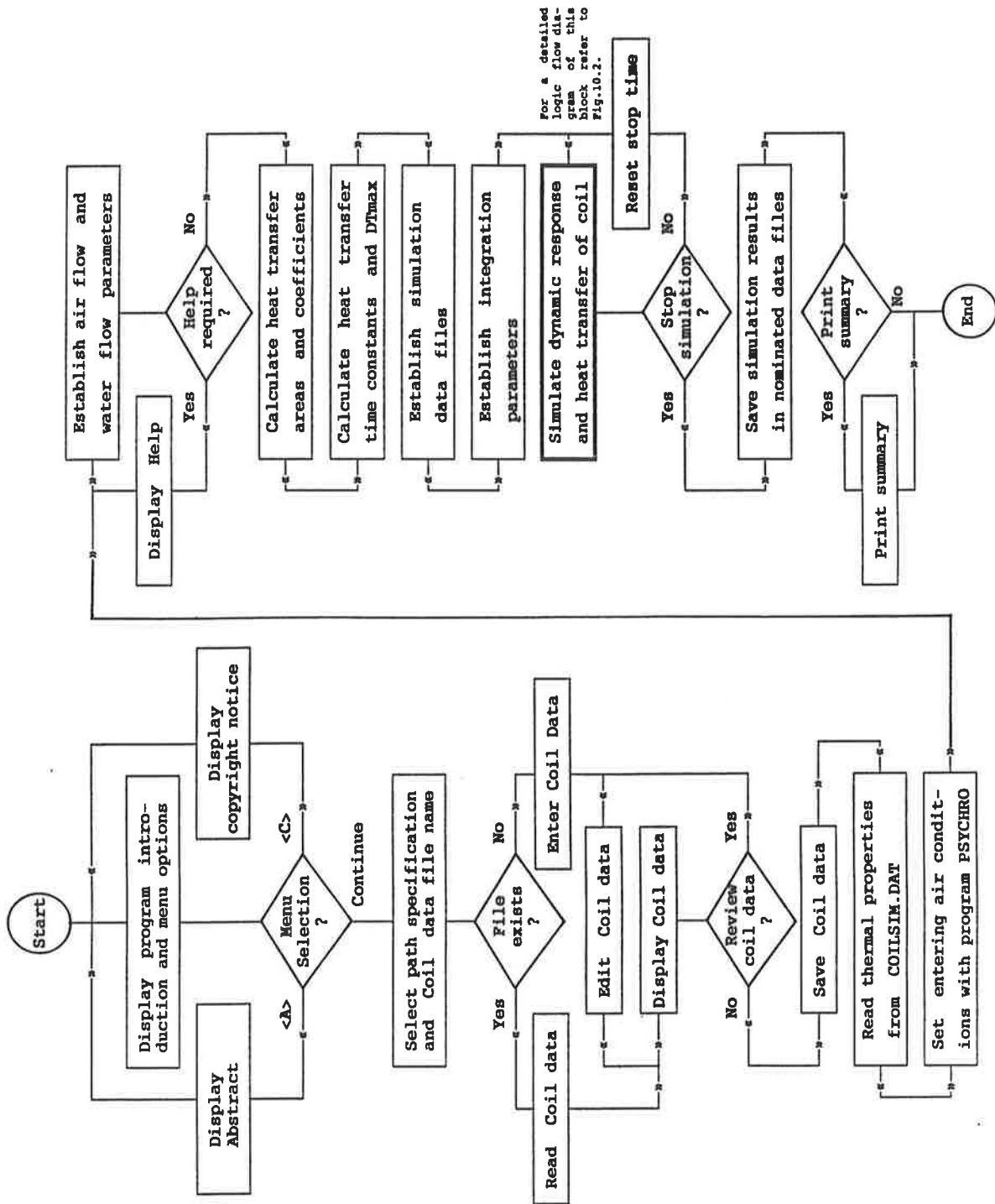
Fig.10.1 — Logic flow diagram for simulation program
COILSIM.
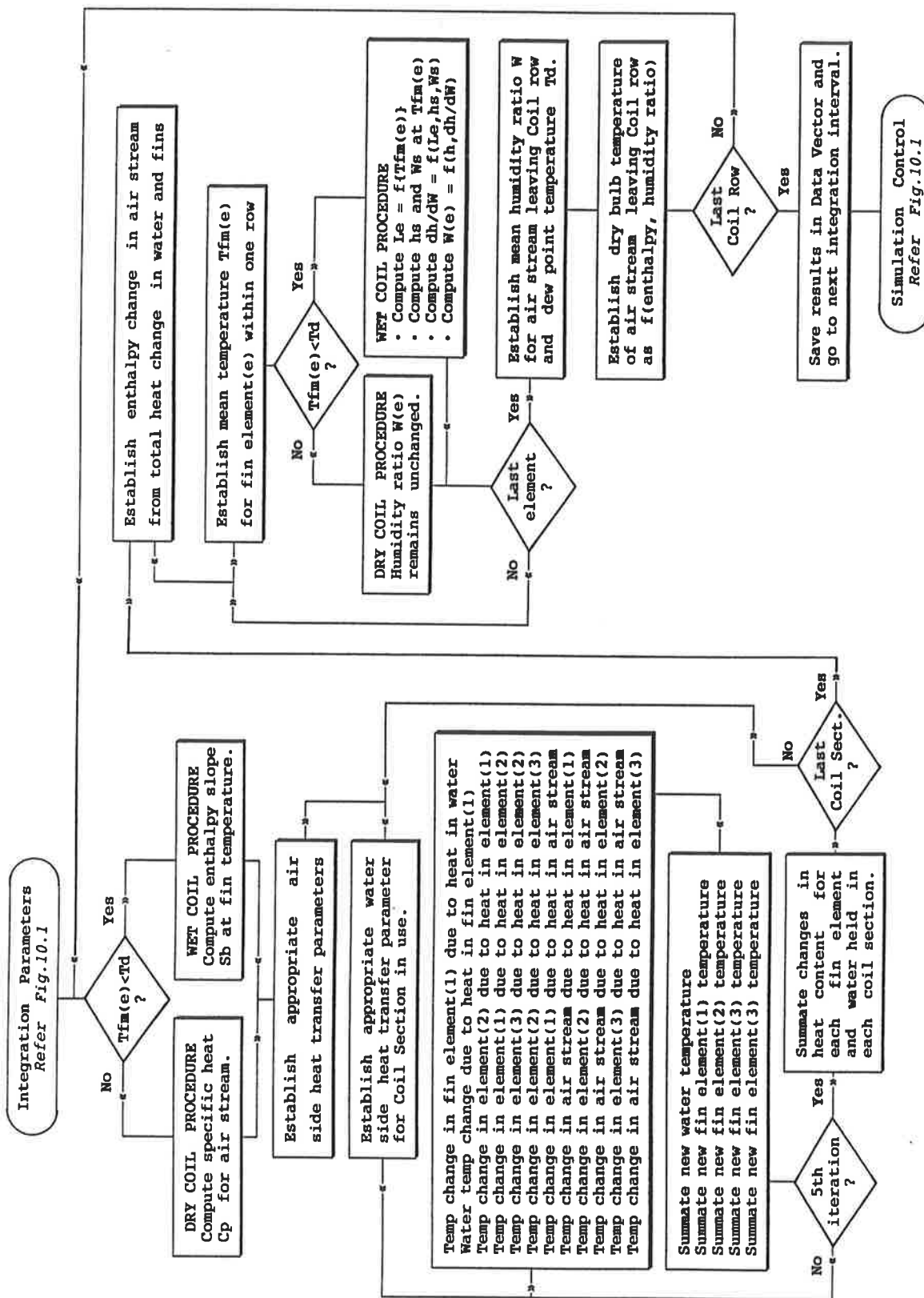
Fig.10.2 - Logic flow diagram for dynamic simulation of heat and mass transfer.

10.3 Results Obtainable

The progress of the simulation is shown on the screen in terms of heat transfer to or from the air stream and water flow, leaving air condition, and water return temperature. All initial temperatures are set to that of the entering air with a resulting initial imbalance in heat transfer shown by the air stream and return water flow. The time taken to reach equilibrium or steady state heat transfer is a function of coil materials, size and configuration, and fluid flow rates.

The steady state conditions throughout the coil are summarised at the end of the run and transient conditions throughout the simulation procedure are recorded in a data file nominated by the user for subsequent listing or plotting.

The procedure establishes the temperature gradients throughout the fluids, tubes, and fins. It consequently establishes the true surface temperatures throughout the coil and, besides computing the rate of heat and mass transfer for each row, the procedure also shows the results due to all time lags associated with heat storage and fluid flow.

10.4 Method and Limitations

The fins are divided into three elements, each operating at their individual transient temperatures which are derived by considering the heat transfer between fin elements, and between the coil material and air or water streams. Fig.10.2 shows the detailed logic flow diagram for the integration of heat and mass transfer.

The simulation procedure will run for the duration nominated by the user. During the simulation procedure the temperatures and heat flow rates for the water and air sides are displayed. Convergence of the two heat flow rates indicates the approach to steady state operation. Typically 20 to 30 seconds real time is required to reach equilibrium.

The temperature trends during the procedure will be recorded in a data file, nominated by the user, for subsequent listing or plotting these by using the DYNSIM[44] program SIMANAL.

For the practical range of face velocities, the flow between fins are always in the laminar range and the program has been modelled as such. For this reason the air flow rates are restricted by the program to a maximum Reynolds number of 2100 as determined for channel flow.

No restrictions are placed on water velocities, apart from that it must be greater than zero. Flow direction is handled in the program with the *counter flow* or *parallel flow* indicator set by the user. The program will therefore model heat transfer for water flow in the laminar as well as the turbulent region. However, warnings will be issued when the water flow is in the laminar or transient range. Good results can be expected for either the laminar or turbulent range, but for the transient range the heat transfer coefficients are averaged from those derived for laminar and turbulent flow. Therefore simulation results with water flow in the transient region must be interpreted as being INDICATIVE ONLY. In practice, coils operating in the transient flow region tend to produce unstable control.

All programs in the COILSIM suite are self explanatory and are supplemented with help panels where necessary. No external documentation is required to run these programs.

10.5 Associated Programs and Data Files

Main program COILSIM is supported by programs COILPAR and SIMANAL. Program COILPAR maintains the data file COILSIM.DAT in which the thermo-physical properties of the coil metals are stored together with the typical water film thickness for wet fins and a constant for reduced heat transfer. The DYNSIM[44] analysing program SIMANAL is used to process the data recorded by COILSIM in data files with extensions .PAR and .SIM. Program PSYCHRO[43] is linked into the main program and is used for processing the thermo-physical properties of moist air.

COILSIM uses or maintains a number of data files for the user's convenience. These can be recognised by their extensions .DAT, .CDT, .CDD, .TXT, .PAR, .SIM, .OUT, and .CTR. Apart from COILSIM.DAT, created and maintained by COILPAR, none of these files are essential for the successful execution of COILSIM. Data file PSYCHRO.DAT is created and maintained by PSYCHRO and stores the last specified entering conditions.

The coil data files are distinguished by their extension .CDT and every time a coil data file is created or modified a document file is created by the same name but with extension .CDD.

Abstracts and help files are stored in ASCII text files identified by extensions .TXT and, as such, may be sent directly to a printer if so desired. Page breaks (Ctrl-L) have been inserted for convenient formatting on A4 size sheets but are ignored by the display procedures in COILSIM, DYNSIM, and PSYCHRO, which use their own control methods.

Simulation results are stored in random access files by the name specified by the user and further identified by extensions .PAR and .SIM. These can only be read through SIMANAL. At the conclusion of the simulation procedure an overview of the simulation parameters, together with the steady state results, are summarised in a document file by the same name but with extension .OUT. Document files .CDD and .OUT may be printed through COILSIM at the time of simulation or later by sending these files directly to a printer.

COILSIM maintains registers of the current coil data file and simulation data files, with the path name where they are kept, in COILSIM.CTR and DYNSIM.CTR respectively. The DYNSIM.CTR register is also available to SIMANAL so that when this program is executed the most recently created simulation files are immediately available.

11.0 SIMULATION RESULTS

11.1 Initial Evaluation

The simulation program COILSIM has been provided with a test
mode which displays all intermediate computed parameters,
such as heat transfer areas, heat transfer coefficients, heat
storage capacities and time constants.   With this aid the
program has been validated for the processing of the coil
data in accordance with the methods and algorithms described
in this thesis.

Following the procedural validation COILSIM was run to
simulate a selection of dry coil performance tests, relevant
details of which are summarised in Tables C.3 and C.12.   The
data in Table C.3 for 6fpi were obtained by Sekhar[37] and
those in Table C.12 for 10fpi were obtained by the author.
Table 11.1 compares the simulated results with the measured
values and shows a consistent over estimation at low face
velocities. At this stage it should be noted that Eq.(C.4-2)
has been derived from the test results by using the concept
of fin efficiency which is based on a uniform heat transfer
coefficient.   However, it has been shown[14,24,32] that this is
not so and consequently four distinct heat transfer zones are
used by program COILSIM. The initial estimates, in which the

Test No. (6fpi)		D2904	D2892	D2891	D2901	D2902	D2903
Air face velocity	m/s	0.406	0.801	1.254	1.643	2.127	2.744
Re (channel flow)		260.3	539.8	811.7	1090	1535	2034
Ke = f(Re) by Eq.(C.4-2)		4.847	7.266	9.112	10.732	12.978	15.173
Num/Nu∞		1.446	1.883	2.234	2.536	2.949	3.346
Simulated ht.transf.	kW	3.794	4.421	5.598	5.715	5.466	5.312
Measured ht.transf.	kW	3.715	4.234	5.521	5.731	5.327	5.366
Deviation	%	+2.1	+4.4	+1.4	-0.3	+2.6	-1.0
Num/Nu∞ (corrected)		1.416	1.803	2.203	2.543	2.874	3.380
Ke = f(Num/Nu∞)		4.642	6.723	8.905	10.780	12.473	15.405
Test No. (10fpi)		T02	T04	T06	T08	T10	T12
Air face velocity	m/s	0.795	1.469	1.870	2.397	2.936	3.391
Re (channel flow)		362.6	684.3	891.2	1150	1406	1623
Ke = f(Re) by Eq.(C.4-2)		5.826	8.289	9.598	11.056	12.361	13.386
Num/Nu∞		1.298	1.556	1.721	1.901	2.059	2.182
Simulated ht.transf.	kW	4.813	6.226	5.613	7.085	7.428	7.573
Measured ht.transf.	kW	4.528	5.901	5.429	6.971	7.390	7.603
Deviation	%	+6.3	+5.5	+3.4	+1.6	+0.5	-0.4
Num/Nu∞ (corrected)		1.221	1.475	1.665	1.870	2.048	2.191
Ke = f(Num/Nu∞)		4.978	7.389	8.978	10.711	12.233	13.478

Table 11.1 - Initial comparison of COILSIM with test data.

concept of fin efficiencies had to be used, can now be corrected by modifying the mean enhancement ratio Num/Nu∞ by a factor of the measured over the simulated total heat transfer. From this the vortex enhancement factor Ke has been recalculated by the method described in Appendix C and the subsequent results are as listed in Table 11.1.

11.2 Comparison with Test Results

The empirical equation derived for Ke=f(Re) in Appendix C goes through the origin. It is not likely that Ke will ever be smaller than unity, hence the new values derived for Ke have been correlated as (Ke-1)=f(Re), and the results of the regressional analysis are shown in Table 11.2 which yields

$$Y = .06893 \cdot X^{.701656 \pm (.020867)} \qquad (11.1\text{-}1)$$

```
Filename: ke.dat

                    Average           Std.Dev.from Regression
Ind Var: X          1.0323E+03
Dep Var: Y          8.7246E+00        4.3278E-02

Curve 5    Y = a * X^b        a = 6.89300E-02
                              b = 7.01656E-01   se(b) = 2.0867E-02

        Number of (X,Y) pairs      =   12
        Correlation coefficient  = 0.995609
        F(1,10)                    =1131.2

Co-ord.    X              Y obs.        Y est.        Residual      % Diff

    1      2.6030E+02     3.6420E+00    3.4138E+00    -2.2818E-01    -6.27
    2      3.6260E+02     3.9780E+00    4.3077E+00     3.2971E-01     8.29
    3      5.3980E+02     5.7230E+00    5.6950E+00    -2.7969E-02    -0.49
    4      6.8430E+02     6.3890E+00    6.7263E+00     3.3730E-01     5.28
    5      8.1170E+02     7.9050E+00    7.5823E+00    -3.2266E-01    -4.08
    6      8.9120E+02     7.9780E+00    8.0961E+00     1.1811E-01     1.48
    7      1.0900E+03     9.7800E+00    9.3247E+00    -4.5526E-01    -4.65
    8      1.1500E+03     9.7110E+00    9.6820E+00    -2.8994E-02    -0.30
    9      1.4060E+03     1.1233E+01    1.1148E+01    -8.4636E-02    -0.75
   10      1.5350E+03     1.1473E+01    1.1857E+01     3.8360E-01     3.34
   11      1.6230E+03     1.2478E+01    1.2330E+01    -1.4844E-01    -1.19
   12      2.0340E+03     1.4405E+01    1.4445E+01     4.0498E-02     0.28
```

Table 11.2 - Regressional analysis for (Ke-1)=f(Re)

Since Y=Ke-1 and X=Re, Eq.(11.1-1) can be rewritten to yield the empirical equation for Ke as

$$Ke = 1 + .06893 \cdot Re^{0.7}_{\text{(Channel flow)}} \qquad (11.1\text{-}2)$$

The dry performance of a one-row, two-row, and a four-row coil has been simulated, with the vortex enhancement factor equation (11.1-2) substituted for the previous Eq.(C.4-2) in program COILSIM, and compared with experimental results[37]

as shown in Tables 11.3, 11.4, and 11.5 respectively. The simulated results for the one-row coil now show good correlation with those measured in the test rig but the simulated results for the two-row and four-row coils show an increasing deviation as the face velocity is increased. Whereas the dry coil simulations tend to be pessimistic, the wet coil simulations tend to over estimate the rates of heat transfer as shown in the next sub-section.

Test No.	Face Vel. m/s	Reynolds number	Measured H.T. kW	Simulated H.T. kW	Deviation %
D2904	0.41	260	3.715	3.677	-1.0
D2892	0.80	540	4.234	4.271	+0.9
D2891	1.25	812	5.521	5.423	-1.8
D2901	1.64	1090	5.731	5.588	-2.5
D2902	2.12	1535	5.327	5.408	+1.5
D2903	2.74	2034	5.366	5.328	-0.7

Table 11.3 - Simulation results on a one-row coil using Eq.(11.1-2).

Test No.	Face Vel. m/s	Reynolds number	Measured H.T. kW	Simulated H.T. kW	Deviation %
D6102	1.01	688	3.87	3.607	-6.8
D6101	1.68	1134	4.96	4.318	-12.9
D6103	2.08	1414	5.32	4.712	-11.4
D6111	2.41	1661	5.65	4.974	-12.0

Table 11.4 - Simulation results on a two-row coil using Eq.(11.1-2).

Test No.	Face Vel. m/s	Reynolds number	Measured H.T. kW	Simulated H.T. kW	Deviation %
D6571	1.08	776	3.70	3.523	-4.8
D6542	1.57	1098	5.18	4.771	-7.9
D6541	2.08	1443	6.33	5.554	-12.3

Table 11.5 - Simulation results on a four-row coil using Eq.(11.1-2).

11.3 Dehumidification

No rigorous capacity tests have been conducted by the author on wet coils hence published results by other workers and records from field installations have been relied upon for the initial evaluation of the performance of COILSIM for dehumidification. Example 12.7 on page 265 in Threlkeld[40] was chosen for its detailed coil data and process characteristics. One of the corresponding COILSIM data files is shown in Table 11.6.

```
========================   C O I L S I M   ==========================
DYNAMIC  SIMULATION  PROCEDURE  FOR  FINNED TUBE  HEAT EXCHANGERS
(c) G.J.Van Aken 1992,   Jul 92                        Ver. 1.0
Coil Data File:        THRELK8
24 August 1992                                         11:22 pm
====================================================================


COIL  DIMENSIONS  AND  PARAMETERS
-----------------------------------------------
Coil height (right angles to tubes)  914     mm
Coil width  (parallel to tubes) ... 1829     mm
Number of coil rows ..............    8
Tube material ....................  Copper
Tube outside diameter ............   17.170 mm
Tube wall thickness ..............    0.890 mm
Tube pitch within coil row .......   38.10  mm
Row pitch or Fin depth ...........   44.45  mm
Tube arrangement .................  Staggered
Fin Geometry .....................  Rectangular Continuous Plate
Equivalent or actual fin diameter .  46.44  mm
Fin material .....................  Aluminium
Fin thickness ....................    0.41  mm
Number of fins ...................  558
Fin pitch ........................    3.277 mm   (7.75 fpi)
Coil circuiting ..................  Double Serpentine
Number of tubes per row ( 1 x 24) .  24
Fouling resistance inside tubes ...  9.0E-05 sq.m K/W
Fouling resistance on fins .......   4.0E-05 sq.m K/W
```

Table 11.6 - COILSIM data file for Threlkeld[40] example 12.7

COILSIM can presently be modelled for water flow only. However, Threlkeld's example is based on constant temperature refrigerant. Therefore the COILSIM model was configured for double serpentine circuiting with high water velocity in an effort to minimise the water temperature rise. The simulation results are summarised for the 4-row and 8-row coils in Tables 11.7 and 11.8 respectively and the psychrometric process lines are shown in Figures 11.1 and 11.2. Unlike the pessimistic estimates observed for dry cooling coils in the previous sub-section, the results for wet cooling coils, in this example, show up as a 7.8% over estimate in heat transfer for the 4-row coil and a 3.5% over estimate for that for the 8-row coil. However, in each case the Threlkeld prediction lies very close to the simulated process line. Thus the simulation procedure for apportioning the latent and sensible heat transfer components appears to be at least as

reliable as that used by Threlkeld and any discrepancies in total heat transfer must be due to differences in estimations of the heat transfer coefficients.

```
================================ C O I L S I M =============================
DYNAMIC   SIMULATION   PROCEDURE   FOR   FINNED TUBE   HEAT EXCHANGERS
(c) G.J.Van Aken 1992,  Aug 92                              Ver. 1.0
Coil Data File:        THRELK4
Simulation Data File:  THRELK4
23 September 1992                                          11:57 pm
============================================================================


    CONDITIONS OF AIR ENTERING COIL
    -----------------------------------
    Atmospheric pressure .......... 101.325 kPa
    Dry bulb temperature ..........  27.78  C
    Wet bulb temperature .........   21.11  C
    Dew point temperature ........   18.10  C
    Relative humidity ............   55.7   %
    Air flow rate ................   4248   l/s
    Coil face velocity ...........   2.54   m/s
    Reynolds Nr (channel flow) ...   1676
    Reynolds Nr (entering fins) ..   1032

    WATER FLOW PARAMETERS
    ----------------------
    Entering temperature ..........   4.44  C
    Flow direction ............... Counter Flow
    Total flow rate ..............   22.32  l/s
    Velocity inside tubes ........    2.50  m/s
    Reynolds number ..............   25214

    INTEGRATING PARAMETERS
    -----------------------
    Integration interval ..........  0.250  seconds
    Storage interval .............   0.50   seconds
    Simulation stop time .........   30.0   seconds

    Air side heat transfer ....... 132.632  kW
    Water side heat transfer ..... 132.692  kW
    Mass transfer from air stream   18.959  g/s


Row Ch/WTemp TubeTemp  Int.Fin OuterFin  DBTemp. DewPoint HumRat.
     C         C        C        C         C       C       g/kg
--- ------- -------   ------- -------   ------- ------- -------
     5.85                                27.78   18.10   13.027
 1   6.05    10.52     12.55   13.25     22.25   16.14   11.477
 2   5.66     9.01     10.45   10.89     18.36   14.36   10.212
 3   5.05     7.78      8.96    9.31     15.29   12.69    9.142
 4   4.91     7.01      7.88    8.16     12.97   11.26    8.306
     4.44
```

Table 11.7 - Simulation results for 4-row coil in Threlkeld[40] example 12.7

Since the flow configurations and heat transfer characteristics of the cooling media in the COILSIM model were different from the example quoted above, it was desirable to compare the model's performance with operating data from chilled water cooling coils. Records from a number of projects, involving chilled water dehumidifying coils, have been investigated and their results simulated with COILSIM. The heat

transfer capacity in each one of these cases is slightly over estimated by COILSIM. However, in practice there is greater concern whether a coil can do the job rather than its performance under specific conditions. Consequently the performance data from these field installations were not sufficiently detailed to allow firm conclusions to be drawn. Some of the wet coil data from tests conducted by Sekhar[36] could be used to enhance the evaluation of the performance of COILSIM.

```
========================= C O I L S I M =========================
DYNAMIC  SIMULATION  PROCEDURE  FOR  FINNED TUBE  HEAT EXCHANGERS
(c) G.J.Van Aken 1992,   Aug 92                         Ver. 1.0
Coil Data File:          THRELK8
Simulation Data File:    THRELK8
23 September 1992                                        0:03 am
================================================================


     CONDITIONS OF AIR ENTERING COIL
     -----------------------------------
     Atmospheric pressure .......... 101.325 kPa
     Dry bulb temperature ..........  27.78  C
     Wet bulb temperature ..........  21.11  C
     Dew point temperature .........  18.10  C
     Relative humidity .............  55.7   %
     Air flow rate .................  4248   l/s
     Coil face velocity ............  2.54   m/s
     Reynolds Nr (channel flow) ...  1676
     Reynolds Nr (entering fins) ..  1032


     WATER FLOW PARAMETERS
     ----------------------
     Entering temperature ..........  4.44   C
     Flow direction ............... Counter Flow
     Total flow rate ...............  22.32  l/s
     Velocity inside tubes .........  2.50   m/s
     Reynolds number ...............  25214


     INTEGRATING PARAMETERS
     -----------------------
     Integration interval ..........  0.250  seconds
     Storage interval ..............  0.50   seconds
     Simulation stop time ..........  30.0   seconds

     Air side heat transfer ........ 180.961 kW
     Water side heat transfer ...... 183.272 kW
     Mass transfer from air stream   30.439 g/s


Row Ch/WTemp TubeTemp  Int.Fin OuterFin  DBTemp. DewPoint HumRat.
       C        C         C        C        C        C      g/kg
---  ------   ------    ------   ------   ------   ------  ------
       6.39                               27.78    18.10   13.027
 1     6.64    10.94    12.92    13.59    22.37    16.24   11.556
 2     6.15     9.42    10.83    11.26    18.55    14.53   10.330
 3     5.66     8.31     9.45     9.80    15.58    12.95    9.301
 4     5.41     7.52     8.43     8.71    13.25    11.54    8.466
 5     5.07     6.78     7.52     7.74    11.40    10.29    7.780
 6     4.93     6.29     6.88     7.06     9.94     9.23    7.235
 7     4.69     5.79     6.27     6.41     8.75     8.30    6.790
 8     4.63     5.48     5.84     5.95     7.84     7.56    6.449
       4.44
```

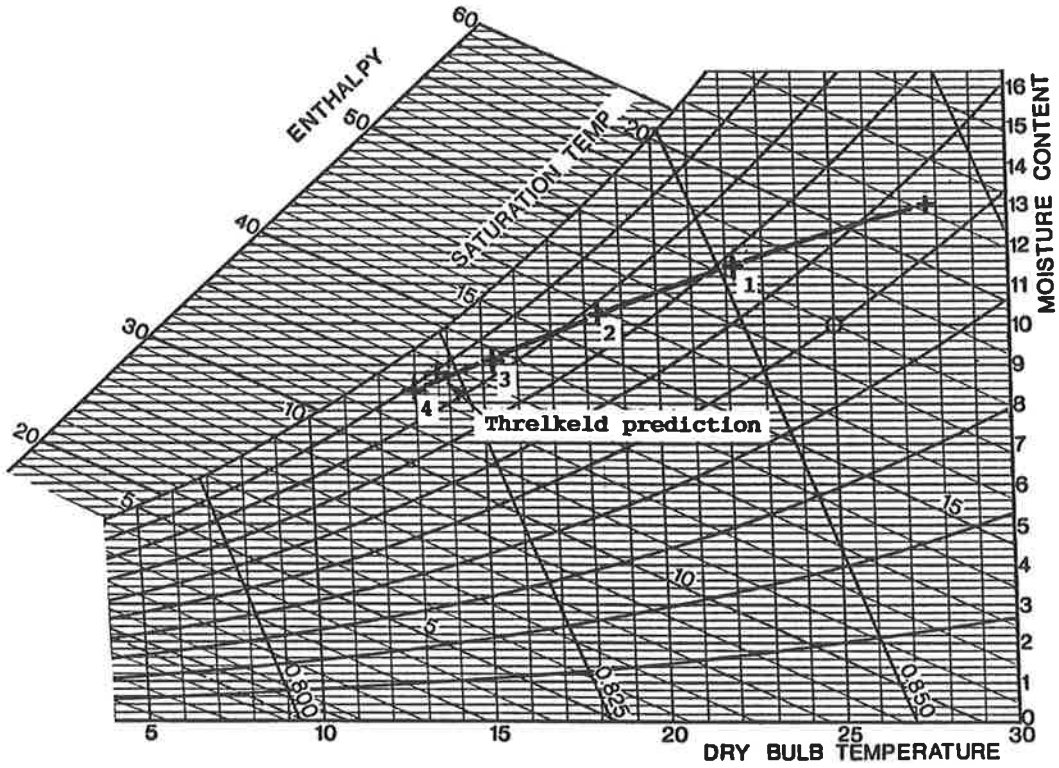*Table 11.8 - Simulation results for 8-row coil in Threlkeld[40] example 12.7*

Fig.11.1 - Psychrometric process line for 4-row coil in Threlkeld[40] example 12.7
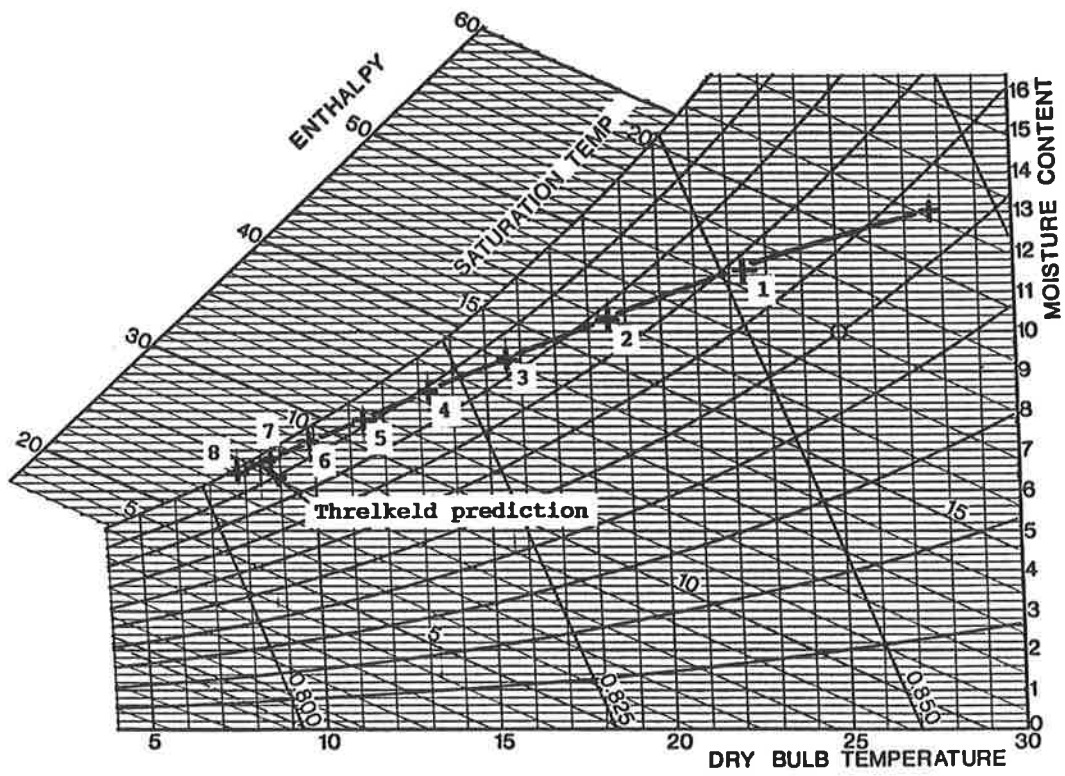

Fig.11.2 - Psychrometric process line for 8-row coil in Threlkeld[40] example 12.7

12.0 CONCLUSIONS

A transient model and computer simulation program has been developed for forced-convection heat and mass transfer in extended surface type heat exchangers. The program is intended to simulate the dynamic performance of a given heat exchanger at any given entering fluid temperature and flow rate, and is most useful for unusual applications for which operating data would otherwise have to be extrapolated or is not available. The aim of the program is to reduce or eliminate the need for expensive test rigs for performance evaluation. The program is easy to use with built in help panels; no external documentation is required to run the program.

Various circuit arrangements can be modelled and fluid flow direction can be modelled for parallel or counterflow. The program models all time lags associated with heat storage and fluid flow and will therefore also be useful for establishing the control characteristics for the heat exchanger. Although the present model assumes constant fluid flow rate as set by the user, the program can be easily adapted for transient fluid flow rate to make it interactive with automatic control algorithms.

All heat transfer areas and heat storage capacities are computed from the coil physical dimensions and parameters. The model distinguishes four different regimes for air side heat transfer and two for water side heat transfer; the location of these regimes being dependent upon the coil configuration. Heat transfer coefficients for the U-shaped vortices around the primary surfaces have been quantified as functions of Reynolds number, thus local heat transfer coefficients are calculated on the basis of fluid velocities and the thermodynamic properties of the fluids at their transient temperatures.

A finite element technique is used to establish the temperature gradients throughout each coil row and throughout the fins for each coil section so that the fin efficiency factor is no longer relevant. By virtue of this, the computer model can cope with partially wet and dry cooling coils.

The modelling technique and simulation program has been designed to be valid for heating as well as for cooling with or without dehumidification. However, owing to the lack of test data for heating applications, the program has at this stage been tested for cooling only.

In an effort to minimise temperature gradients and the number of variables in the test specimen, the simulation model was in the first instance developed on the basis of tests conducted on single row dry cooling coils. Consequently the model's correlation with these tests is quite good and is within ±2.5% for a wide range of face velocities and two different fin spacings. For the two-row and four-row coils

tested the simulation program under estimates the coil capacities by about 12% at the higher face velocities. But comparing the simulated performance with field data for dehumidifying coils the program tends to over estimate the rate of heat transfer.

There are still a number of uncertanties and simplifications in the model. Heat transfer in the reduced heat transfer zones has been ignored, condensate film thicknesses are assumed to be constant and uniform, vortex trajectories are idealised to allow geometric solutions, and vortex widths and their heat transfer coefficients have been established by regressional analysis on test results from only two different fin spacings.

Although the presence of vortices and their importance in heat transfer has been previously demonstrated[14,24,32], their heat transfer coefficients have not, to the authors knowledge, been quantified prior to this thesis. Owing to the restricted number of test samples that were available this information is still sketchy and further work is needed to gain a more detailed knowledge of the behaviour of the vortices for different face velocities, tube diameters, and fin geometries.

Although it has been shown[14,32] that the heat transfer coefficients in the reduced heat transfer zones are very small, their close proximity to the primary surface may make these more significant than has been allowed for in this thesis. In particular they may enhance the ratio of latent to sensible heat transfer above that given by the COILSIM model.

Overall heat transfer coefficients for wet cooling coils have been simplified by assuming uniform condensate films. Heat transfer calculations may be improved by considering the more realistic mechanism of "droplike" condensation which topic is being actively studied by other workers within the research program of which the present work forms part. However, the above mentioned discrepancy in dry coil heat transfer must be resolved prior to seeking improvements in wet coil operation since both cases are based on the same air side heat transfer coefficients.

Presently only flat continuous plate fins are properly modelled. Circular plate or spiral fins create a new region of developing laminar flow for each row and it can also be expected that the vortex will be interrupted by each new row. A similar situation exists for "vented fins". The computer program can be readily extended to model these different surfaces but further test results will be required to validate the program for this mode.

Heat transfer by direct expansion of refrigerants is outside the scope of this thesis, but once the appropriate numerical methods are known these would not be difficult to implement into the simulation program.

13.0 REFERENCES

1. Adams,S. and Holmes,M., "Determining Time Constants for Heating and Cooling Coils", BSIRA Technical Note TN 6/77, (1977).
2. ANSI/ARI STANDARD 410-81, "Forced Circulation Air-Cooling and Air-Heating Coils", Air Conditioning and Refrigeration Institute, American National Standard, (1981).
3. ASHRAE Handbook - Equipment, American Soc. of Heating, Refrig. and Air Cond. Engineers, (1988).
4. ASHRAE Handbook - Fundamentals, American Soc. of Heating, Refrig. and Air Cond. Engineers, (1989).
5. ASHRAE, "Thermophysical Properties of Refrigerants",1973.
6. Atwood,T., "Steam Vapour Pressure Tables with a Programmable Calculator", Heating/Piping/Air Cond., Nov.1982.
7. Brown,M.R., "Design of the National Standards Laboratory for CSIRO", AIRAH Conference, Vic. Division, March, 1975.
8. Carrier,W.H. and Anderson,S.W., "The Resistance to Heat Flow Through Finned Tubing", Heating, Piping and Air Conditioning, May, 1944.
9. Ellul,W.M.J., "A Numerical Approach to the Performance of Dehumidifying Coils", I.E.Aust. Thermofluids Conference, Hobart, December 1976.
10. Gardner,K.A., "Efficiency of Extended Surfaces", A.S.M.E.Trans, Vol.67, pp.621-631, (1945).
11. Gartner,J.R. and Harrison,H.L., "Frequency Response Transfer Functions for a Tube in Crossflow", ASHRAE Transactions Vol.69, (1963).
12. Gartner,J.R. and Daane,L.E., "Dynamic Response Relations for a Serpentine Crossflow Heat Exchanger with Water Velocity Disturbance", ASHREA Trans. Vol.75 Pt.1, (1969).
13. Gartner,J.R., "Simplified Dynamic Response Relations for Finned-Coil Heat Exchangers", Research Report No.2250 RP-92, presented at ASHRAE Annual Meeting, Nassau, Bahamas, June 25-29, 1972.
14. Gilbert,G.P., "Flow Through a Model Fin and Tube Heat Exchanger and its influence on Mass and Heat Transfer", M.Eng.Sc.Thesis, Faculty of Eng., Univ. Adelaide, (1988).
15. Goodman,W., "Performance of Coils for Dehumidifying Air", Heating, Piping and Air Conditioning, Vol.10, 1938-39, (8 articles).
16. Guillory,J.L. and McQuiston,F.C., "An Experimental Investigation of Air Dehumidification in a Parallel Plate Exchanger", ASHRAE Trans. Vol.79 part 2, (1973).
17. Hirschfelder J.O., Curtiss C.F. and Bird R.B., "Molecular Theory of Gases and Liquids", J.Wiley & Sons, 1964.
18. Hyland,R.W. and Wexler,A., 1983a. "Formulations for the thermodynamic properties of the saturated phases of H_2O from 173.15 K to 473.15 K.", ASHREA Trans.89(2A):500-513.
19. Hyland,R.W. and Wexler,A., 1983b. "Formulations for the thermodynamic properties of dry air from 173.15 K to 473.15 K, and of saturated moist air from 173.15 K to 372.15 K, at pressures to 5 MPa.", ASHREA Trans.89(2A): 520-535, (1983).

20. Kays,W.M., "Convective Heat and Mass Transfer", McGraw-Hill, 1966.
21. Keenan,J.H. and Keyes,F.G., "Thermodynamic Properties of Steam", Wiley, New York, 1936.
22. Kern,D.Q., "Process Heat Transfer", McGraw-Hill, 1986.
23. Lee,S.H. and Knudsen,J.G., "Scaling Characteristics of Cooling Tower Water", ASHRAE Trans. V.85, pt.1, 1979.
24. Luxton,R.E., "Prediction and Management of Flow in Ducts and Pipes", ESAA Summer School in Mechanical Engineering, Vol.II, Adelaide, 1984.
25. McAdams,W.H., "Heat Transmission", McGraw-Hill, 1954.
26. McElgin,J and Wiley,D.C., "Calculation of Coil Surface Areas for Air Cooling and Dehumidification", Heating, Piping and Air Conditioning, March, 1940.
27. Marner,W.J. and Suitor,J.W., "Survey of Gas-Side Fouling in Industrial Heat Transfer Equipment", JPL Publication 83-74; NASA-CR-173469, (1983).
28. Mason E.A. and Monchick L., "Survey of the Equation of State and Transport Properties of Moist Gases", Int.Symp. on humidity and moisture, Washington DC, May 20-23, 1963.
29. Mathur,G.D., "Calculating Single-Phase Heat-Transfer Coefficient", Heating/Piping/Air Cond., March 1990.
30. Perry H., "Chemical Engineers' Handbook", 6th ed., McGraw-Hill, 1988.
31. Rohsenow,M.R. Hartnett,J.P. Ganic,E.N., Handbook of Heat Transfer Fundamentals, Chapter 7, 2nd ed., McGraw-Hill, (1985).
32. Saboya,F.E.M. and Sparrow,E.M., "Local and Average Transfer Coefficients for One-Row Plate Fin and Tube Heat Exchanger Configuration", J. Heat Transfer, Trans. ASME, Vol.96, pp.265-272, 1974.
33. Saboya,F.E.M. and Sparrow,E.M., "Transfer Characteristics of Two-Row Plate Fin and Tube Heat Exchanger Configurations", Int.J. Heat Mass Transfer, Vol.19, pp.41-49, 1976.
34. Saboya,F.E.M. and Sparrow,E.M., "Experiments on a Three-Row Fin and Tube Heat Exchanger", J.Heat Transfer, Trans. ASME, Vol.98, pp.520-521, 1976.
35. Schlichting,H., "Boundary Layer Theory", 6th ed., McGraw-Hill, Sydney, 1968.
36. Sekhar,S.C., Luxton,R.E. and Shaw,A., "Some Problems in the Rating of Cooling Coils - ARI Standard 410 Revisited", International Congress of International Institute of Refrigeration, Brisbane, September 1988.
37. Sekhar,S.C., "Life Cycle Design of Humidifiers in Air Conditioning", Ph.D.Thesis, Faculty of Engineering, University of Adelaide, (1990).
38. Shaw,A., "Exploration of Air Velocity across Air-Conditioning System Dehumidifiers - An Energy Conservation Project", ASHRAE Trans. Vol.88, (1982).
39. Sutherland,J.W., "The Solution of Psychrometric Problems Using a Digital Computer", Aust. Refr., Air Cond. and Heating, April, 1971, pp.43-48.
40. Threlkeld,J.L., Thermal Environmental Engineering, Chapt.12, Prentice-Hall, 1962.

41. Van Aken,G.J.,   "Transient Modelling of the Dynamic Performance of Heat Exchangers", Proceedings of AIRAHFAIR 88 Conference, Sydney, 1988.
Reprinted AIRAH Journal pp.46-54, April, 1989.
42. Van Aken,G.J., "Numerical Methods on the Properties of Gases, Vapours and Liquids", ACS Mech.Eng.Report No.39, February 1990.
43. Van Aken,G.J.,   "Computer Methods for Psychrometric Problems", ACS Mech.Eng.Report No.41, May 1990.
44. Van Aken,G.J.,   "DYNSIM   General Purpose Dynamic System Simulation Procedure",   ACS Mech. Eng. Report No.43, August 1990.
45. Worbs,P.E.,   "A Friendly Microprocessor Approach to the Determination of the Thermodynamic Properties of Moist Air", ASHRAE Trans.90(1A): 2804, pp.46-57, (1984).
46. Le Fevre,E.J. and Rose,J.W.,   "A Theory of Heat Transfer by Dropwise Condensation", Proc.3rd Int.HT Conf., Am.Inst. Chem.Engrs.,Vol.2,362-375 (1966).
47. Rose,J.W., "Further Aspects of Dropwise Condensation Theory", Int.J.HMT 19, 1363-1370 (1976).

APPENDIX A

FLOW INSIDE SMOOTH TUBES AND DUCTS – HEAT TRANSFER EQUATIONS

CONTENTS

A.1 FRICTION FACTORS

A.1.1 Characteristic Equations for Fluid Flow

The flow of fluid in ducts or pipes can be readily character-
ised by the non-dimensional group of variables known as the
Reynolds number which is defined as

$$Re = Dh \cdot G / \mu \ , \qquad\qquad (A.1-1)$$

where

    Dh = hydraulic diameter   - m
    G = mass flow rate of the fluid - kg/m² s
    μ = dynamic viscosity of the fluid - kg/m s .

For circular tubes the hydraulic diameter is the same as the
tube inside diameter.   To study flow in non-circular tubes
with the same characteristic non-dimensional group, some kind
of equivalent tube diameter should be defined.   From experi-
mental evidence[20] the hydraulic radius, defined as

$$rh = \frac{flow\ area}{wetted\ perimeter} \ , \qquad\qquad (A.1-2)$$

appears to be most appropriate. For a circular tube

$$rh = \frac{\pi/4\ Di^2}{\pi\ Di} = \frac{Di}{4} \ ,$$

thus

$$Dh = 4 \cdot rh \ . \qquad\qquad (A.1-3)$$

For flow between parallel planes of large aspect ratio

$$rh \approx \frac{width \times spacing}{2 \times width} \approx \frac{spacing}{2}$$

and Dh becomes twice the plate spacing.

Laminar flow will be obtained for Reynolds numbers less than
about 2100[25], regardless of tube cross-sectional shape.
Above this number and up to about 4000 the flow is transitio-
nal.   Although laminar flow may persist it becomes unstable
to small disturbances.   Above 4000 the flow is generally
regarded as turbulent, but turbulent flow may not be fully
established until a Reynolds number of about 10,000[20].

The transitional range should be avoided in design since the
rate of heat transfer is unpredictable and stable capacity
control would not be possible.

The pressure drop due to fluid flow in a pipe or duct is
given by the Fanning equation as

$$dpf = \frac{f\ G^2\ v\ dL}{2\ rh} \qquad Pascal \qquad\qquad (A.1-4)$$

where

```
f  = Fanning friction factor
G  = mass velocity of fluid     -   kg/m² s
v  = specific volume of fluid   -   cu.m/kg
L  = length of pipe or duct     -   m
rh = hydraulic radius           -   m .
```

Since rh = Dh/4 and letting dL = unit length then

$$dpf = \frac{2\ f\ G^2\ v}{Dh} \qquad Pascal/m\ . \qquad\qquad (A.1-5)$$

A.1.2 Fully Developed Laminar Flow in Circular Tubes

The Hagen-Poiseuille law of isothermal streamline motion in well developed incompressible flow in round tubes is given by

$$\frac{-dpf}{dL} = \frac{32\ \mu\ V}{Dh^2}\ . \qquad\qquad (A.1-6)$$

Equating this with Eq.(A.1-4) yields the Fanning friction factor for laminar flow in circular pipes as

$$f = 16/(Dh\ G/\mu) = 16/Re\ . \qquad\qquad (A.1-7)$$

Well developed laminar flow can only occur at points far removed from the tube entrance. For an entry condition with uniform velocity the combined effects of surface shear and momentum flux are expressed as

$$\overline{f}_{app} \cdot Re = \emptyset(\frac{Re}{x/Di}) \qquad\qquad (A.1-8)$$

and is graphically represented in fig.(A.1). Polynomial coefficients have been fitted to $\emptyset(\frac{Re}{x/Di})$ as listed in Table A.1.

Subscript	Coefficient
0	1.7257224D+01
1	2.6624830D-01
2	-6.4066518D-04
3	7.3150477D-07

Table A.1 - Polynomial coefficients for $\emptyset(\frac{Re}{x/Di})$ in Eq(A.1-8).
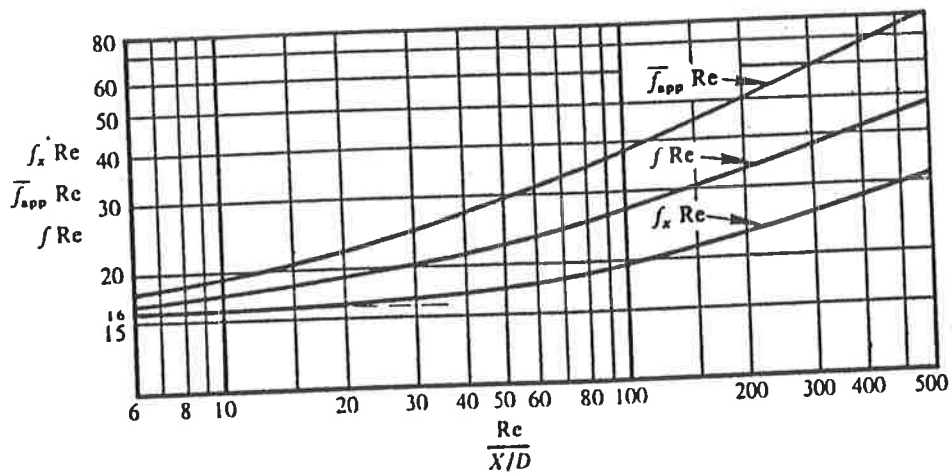
Fig.A.1 - *Friction coefficients for laminar flow in the hydrodynamic entry length of a circular tube. (Langhaar[20])*

This solution is also a valid approximation for sharp-cornered or abrupt-contraction entrances as found in flow headers of cooling and heating coils.
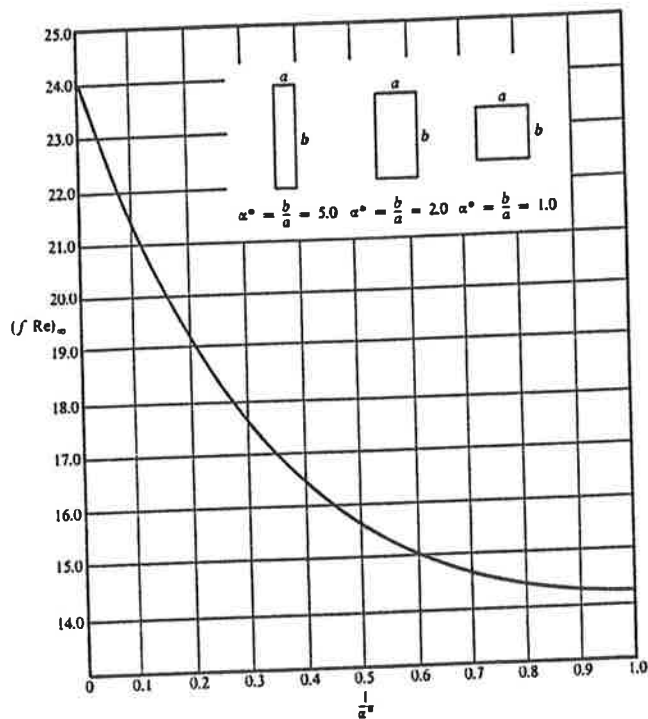
Fig.A.2 - *Friction coefficients for fully developed laminar flow in rectangular tubes (Kays[20])*

A.1.3 Fully Developed Laminar Flow in Rectangular Tubes

For rectangular tubes the Fanning friction factor for well developed laminar flow is defined in fig.A.2 as

$$f \cdot Re = \phi(1/\alpha^*) \; , \tag{A.1-9}$$

for which a fifth degree polynomial equation has been fitted by Shah and London[31] as

$$f \cdot Re = 24.0 \cdot \phi(\alpha^*) \; . \tag{A.1-10}$$

The polynomial coefficients for $\phi(\alpha^*)$ are listed in Table A.2.

Subscript	Coefficient
0	1.0
1	-1.3553
2	1.9467
3	-1.7012
4	0.9564
5	-0.2537

Table A.2 - Polynomial coefficients for $\phi(\alpha^*)$ in Eq.(A.1-10).

A.1.4 Fully Developed Turbulent Flow in Tubes and Ducts

For fully developed turbulent flow in smooth circular tubes the friction factor is given by the Karman-Nikuradse[20] relation

$$\frac{1}{\sqrt{4f}} = -0.8 + 0.87 \ln(Re \sqrt{4f}) \; , \tag{A.1-11}$$

which is graphically represented in fig.A.3. This equation also works well for smooth rectangular ducts. However, it can only be solved for f by iteration. Therefore simpler and directly usable expressions have been sought. The Blasius equation[20]

$$f = 0.079 \, Re^{-0.25} \tag{A.1-12}$$

is based on direct pipe pressure drop measurements, and has been recommended for the Reynolds number range of 5,000 to 30,000. It correlates with the Karman-Nikuradse equation over a much wider range and is within ±4% for Reynolds numbers between 2,000 and 200,000.
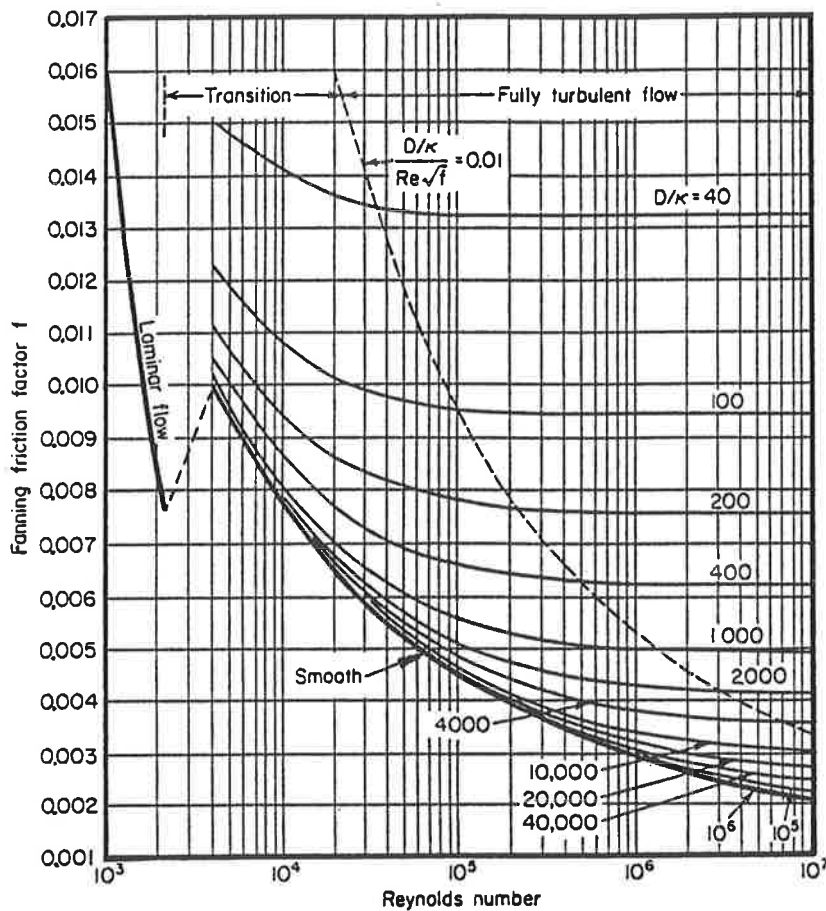
Fig.A.3 - Fanning friction factor plot for smooth and rough tubes (Rohsenow[31])

For the Reynolds number range of 30,000 to 1,000,000, an approximation to the Karman-Nikuradse equation is given[20] as

$$f = 0.046 \, Re^{-0.2} \; . \tag{A.1-13}$$

A wide range equation is given by Kays[31] as

$$f = (1.58 \ln(Re) - 3.28)^{-2} \; , \tag{A.1-14}$$

and McAdams'[25] wide range equation is given as

$$f = 0.00140 + 0.125/Re^{0.32} \; . \tag{A.1-15}$$

Equations (A.1-12) to (A.1-15) are compared with the Karman-Nikuradse relation, Eq.(A.1-11), in Table A.3 from which it is concluded that for Reynolds numbers below 9,000 Equation (A.1-12) gives the best correlation and for Reynolds numbers of 9,000 and greater Eq(A.1-14) is the best choice.

Re	Eq.(11)	Eq.(12)	Eq.(13)	Eq.(14)	Eq.(15)
1.0E+03	0.01560	0.01405	0.01155	0.01716	**0.01511**
2.0E+03	0.01233	0.01181	0.01006	0.01312	**0.01238**
3.0E+03	0.01085	**0.01067**	0.00928	0.01139	*0.01104*
4.0E+03	0.00995	**0.00993**	0.00876	0.01036	*0.01020*
5.0E+03	0.00932	**0.00939**	0.00837	0.00965	*0.00959*
6.0E+03	0.00885	**0.00898**	0.00807	0.00913	*0.00913*
7.0E+03	0.00848	**0.00864**	0.00783	*0.00872*	0.00875
8.0E+03	0.00817	**0.00835**	0.00762	*0.00839*	0.00845
9.0E+03	0.00792	0.00811	0.00745	**0.00811**	0.00819
1.0E+04	0.00770	0.00790	0.00729	**0.00787**	0.00796
2.0E+04	0.00645	0.00664	0.00635	**0.00654**	0.00666
3.0E+04	0.00585	0.00600	**0.00585**	*0.00591*	0.00602
4.0E+04	0.00547	0.00559	0.00553	**0.00552**	0.00561
5.0E+04	0.00521	0.00528	0.00528	**0.00524**	0.00532
6.0E+04	0.00500	0.00505	0.00509	**0.00503**	0.00510
7.0E+04	0.00484	**0.00486**	0.00494	*0.00486*	0.00492
8.0E+04	0.00470	**0.00470**	0.00481	0.00472	0.00477
9.0E+04	0.00458	0.00456	0.00470	**0.00460**	0.00465
1.0E+05	0.00448	0.00444	0.00460	**0.00450**	0.00454
2.0E+05	0.00390	0.00374	0.00400	**0.00390**	0.00392
3.0E+05	0.00360	0.00338	0.00369	**0.00361**	0.00361
4.0E+05	0.00342	0.00314	0.00349	*0.00342*	**0.00341**
5.0E+05	0.00328	0.00297	0.00333	*0.00328*	**0.00328**
6.0E+05	0.00317	0.00284	0.00321	*0.00318*	**0.00317**
7.0E+05	0.00309	0.00273	0.00312	*0.00309*	**0.00308**
8.0E+05	0.00302	0.00264	0.00303	*0.00302*	**0.00301**
9.0E+05	0.00296	0.00256	0.00296	*0.00296*	**0.00295**
1.0E+06	0.00290	0.00250	**0.00290**	*0.00291*	*0.00290*
2.0E+06	0.00259	0.00210	0.00253	**0.00259**	0.00260
3.0E+06	0.00242	0.00190	0.00233	**0.00243**	0.00246
4.0E+06	0.00232	0.00177	0.00220	**0.00233**	0.00236
5.0E+06	0.00224	0.00167	0.00210	**0.00225**	0.00230
6.0E+06	0.00218	0.00160	0.00203	**0.00219**	0.00225
7.0E+06	0.00213	0.00154	0.00197	**0.00214**	0.00221
8.0E+06	0.00209	0.00149	0.00191	**0.00210**	0.00217
9.0E+06	0.00205	0.00144	0.00187	**0.00206**	0.00214
1.0E+07	0.00202	0.00140	0.00183	**0.00203**	0.00212
2.0E+07	0.00183	0.00118	0.00159	**0.00184**	0.00198
3.0E+07	0.00173	0.00107	0.00147	**0.00175**	0.00191
4.0E+07	0.00167	0.00099	0.00139	**0.00168**	0.00186
5.0E+07	0.00162	0.00094	0.00133	**0.00164**	0.00183
6.0E+07	0.00158	0.00090	0.00128	**0.00160**	0.00181
7.0E+07	0.00155	0.00086	0.00124	**0.00157**	0.00179
8.0E+07	0.00152	0.00084	0.00121	**0.00154**	0.00177
9.0E+07	0.00150	0.00081	0.00118	**0.00152**	0.00176

Table A.3 - Comparison of Fanning friction factor equations.
Bold figures indicate the best correlation
Italic figures indicate a good correlation

These equations are for most of their ranges within ±1% and at the extremes of these ranges still within ±2.5% from the Karman-Nikarudse relation.

A.1.5 Flow in Curved Tubes or Pipes

In curved tubes a secondary flow increases the pressure drop per unit length. A number of curves have been published[31] giving the Loss coefficient as a function of radius of curvature, tube inside diameter, and angle of bend as shown in figures A.4 and A.5. For computer methods a numeric algorithm is more convenient. For fully developed laminar flow the friction coefficient is given[20] as

$$\frac{f}{f_{straight\ tube}} = \left[1 - \left[1 - \left[\frac{11.6}{Re\ \sqrt{(r_o/R)}} \right]^{0.45} \right]^{2.22} \right]^{-1} \quad (A.1-16)$$

for $11.6 < Re\ \sqrt{(r_o/R)} < 2000$, and where

ro = radius of the tube inside diameter
R = radius of curvature at the centreline.
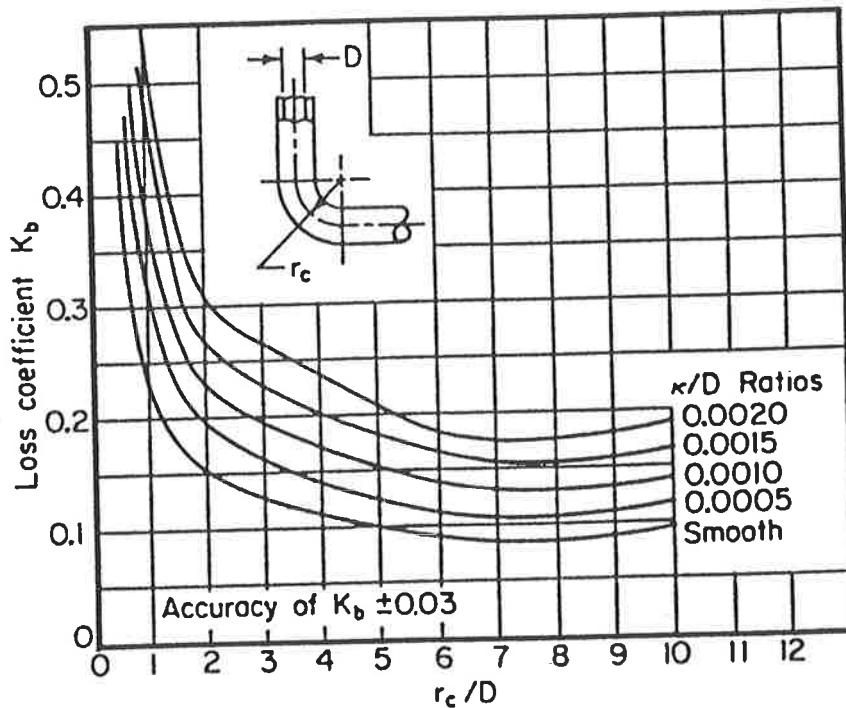
Fig.A.4 - *Loss coefficients for 90 degree bends* (Rohsenow[31])

Turbulent flow in curved circular tubes is correlated[20] by

$$\frac{f}{f_{straight\ tube}} = \left[Re\ (r_o/R)^2 \right]^{0.05} \qquad (A.1-17)$$

for $Re\ (r_o/R)^2 > 6$.

The curves in fig.A.5 indicate that by 90° the Loss coefficients level off to constant values thereby suggesting that for bend angles greater than 90° these angles do not need considering other than for calculating the tube length.
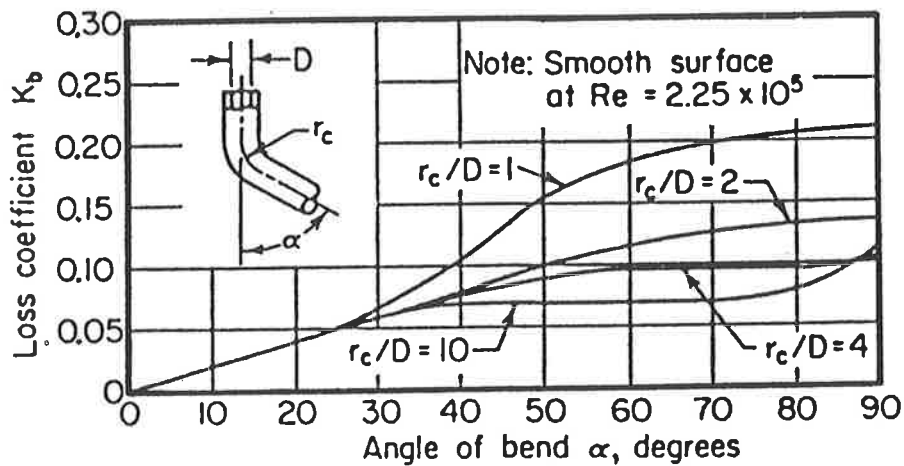
Fig.A.5 - Loss coefficients for bends vs angle of bend in smooth tubes. (Rohsenow[31])

A.2 HEAT TRANSFER: LAMINAR FLOW INSIDE SMOOTH TUBES

A.2.1 Circular Tubes with Fully Developed Velocity and Temperature Profiles

Heat transfer parameters are conveniently related in terms of the non-dimensional Nusselt number

$$Nu = \frac{h\ Dh}{k} \ . \qquad\qquad (A.2-1)$$

For a fully developed laminar flow the heat transfer coefficient h depends only on k and Dh.   For constant heat rate

$$Nu(H) = 4.364 \qquad\qquad (A.2-2)$$

and for constant surface temperature

$$Nu(T) = 3.658 \ . \qquad\qquad (A.2-3)$$

The difference in heat transfer coefficient is illustrated by the different temperature profiles in fig.A.6.
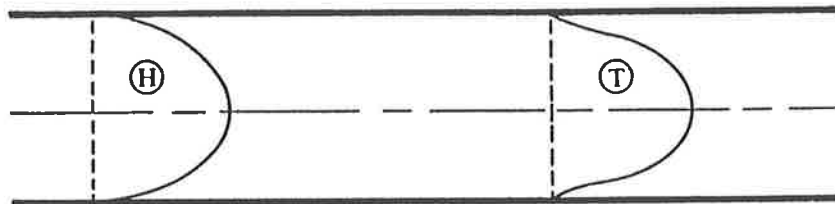
Fig.A.6 - *Temperature profiles for fully developed laminar flow   (Kays[20])*
(H) Constant heat rate
(T) Constant surface temperature

These are the two extremes met in heat exchanger analysis. Constant heat rate can be applied to electric resistance heating, radiant heating, and in counterflow heat exchangers with approximately equal fluid capacity.   Whereas constant surface temperature can be applied to evaporators, condensers, heat exchangers where one fluid has a very much higher capacity rate than the other.

The temperature variations with tube length are shown in fig.A.7 for the two cases.
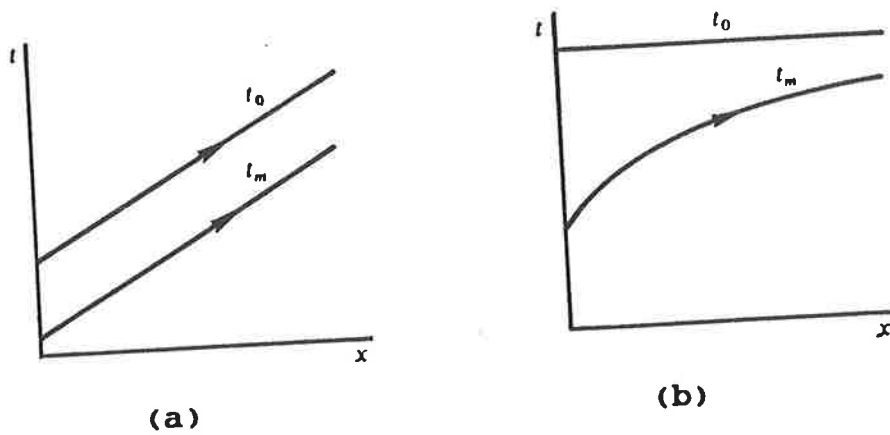
Fig.A.7 – *Temperature variations with tube length (Kays[20])*
(a) Constant heat rate
(b) Constant surface temperature

A.2.2 Rectangular Tubes with Fully Developed Velocity and Temperature Profiles

The local heat transfer coefficient varies around the periphery of non-circular tubes and approach zero at the corners; this means that beside the usual heat transfer parameters the heat flux also depends on the proportions of the rectangular section. Tables A.4 and A.5 list the Nusselt numbers for rectangular tubes with various width to height ratios.

$\dfrac{2b}{2a}$	Nu				
0.0	7.541	7.541	7.541	0	4.861
0.1	5.858	6.095	6.399	0.457	3.823
0.2	4.803	5.195	5.703	0.833	3.330
0.3	4.114	4.579	5.224	1.148	2.996
0.4	3.670	4.153	4.884	1.416	2.768
0.5	3.383	3.842	4.619	1.647	2.613
0.6	3.198	—	—	—	2.509
0.7	3.083	3.408	4.192	2.023	2.442
0.8	3.014	—	—	—	2.401
0.9	2.980	—	—	—	2.381
1.0	2.970	3.018	3.703	2.437	2.375
1.43	3.083	2.734	3.173	2.838	2.442
2.0	3.383	2.602	2.657	3.185	2.613
2.5	3.670	2.603	2.333	3.390	2.768
3.33	4.114	2.703	1.946	3.626	2.996
5.0	4.803	2.982	1.467	3.909	3.330
10.0	5.858	3.590	0.843	4.270	3.823
∞	7.541	4.861	0	4.861	4.861

Table A.4 – *Nusselt numbers for fully developed laminar flow in rectangular ducts, for constant surface temperature, one or more walls transfering heat. (Rohsenow[31])*
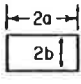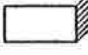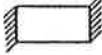
$\dfrac{2b}{2a}$	Nu				
0.0	8.235	8.235	8.235	0	5.385
0.1	6.700	6.939	7.248	0.538	4.410
0.2	5.704	6.072	6.561	0.964	3.914
0.3	4.969	5.393	5.997	1.312	3.538
0.4	4.457	4.885	5.555	1.604	3.279
0.5	4.111	4.505	5.203	1.854	3.104
0.6	3.884	—	—	—	2.987
0.7	3.740	3.991	4.662	2.263	2.911
0.8	3.655	—	—	—	2.866
0.9	3.612	—	—	—	2.843
1.0	3.599	3.556	4.094	2.712	2.836
1.43	3.740	3.195	3.508	3.149	2.911
2.0	4.111	3.146	2.947	3.539	3.104
2.5	4.457	3.169	2.598	3.777	3.279
3.33	4.969	3.306	2.182	4.060	3.538
5.0	5.704	3.636	1.664	4.411	3.914
10.0	6.700	4.252	0.975	4.851	4.410
∞	8.235	5.385	0	5.385	5.385

Table A.5 - Nusselt numbers for fully developed laminar flow in rectangular ducts, for constant heat rate, one or more walls transfering heat. (Rohsenow[31])

The second columns in Tables A.4 and A.5 can be expressed for the range 0.0 < b/a < 1.0 by Eq.(A.2-4) for which the polynomial coefficients for $\emptyset(b/a)$ are listed in Table A.6.

$$Nu = \exp(\emptyset(b/a)) , \qquad\qquad (A.2-4)$$

where $\emptyset(b/a) = f_0 + f_1(b/a) + f_2(b/a)^2 + f_3(b/a)^3$

Subscript	Nu(T)	Nu(H)
0	2.0189157	2.1081446
1	-2.7696340	-2.2225976
2	2.8248030	1.9538238
3	-0.98764998	-0.55786151

Table A.6 - Polynomial coefficients for $\emptyset(b/a)$ in Eq.(A.2-4).

A.2.3 Circular-Tube Thermal-Entry-Length

Characteristic equations used for establishing the thermal entry length includes the Prandtl number which is a non-dimensional group of fluid transport properties defined as

$$Pr = \frac{\mu \; Cp}{k} . \qquad\qquad (A.2-5)$$

Now the kinematic viscosity

$$v = \mu \, / \, \delta \, , \qquad\qquad\qquad (A.2-6)$$

and the thermal diffusivity

$$\alpha = \frac{k}{\delta \; Cp} \; . \qquad\qquad\qquad (A.2-7)$$

Therefore by multiplying the numerator and denominator by density, the Prandtl number becomes

$$Pr = \frac{v}{\alpha} \; . \qquad\qquad\qquad (A.2-8)$$

The kinematic viscosity is a diffusivity for momentum down a momentum gradient. Thus at unity Prandtl number the momentum and heat are diffused through the fluid at the same rates. If the Prandtl number is greater than 1 the velocity profile develops more rapidly than the temperature profile.

The Prandtl number for any particular fluid varies slightly with temperature. Gases are in the range from 0.5 to 1 and the Prandtl number for water ranges from 1 to 10 depending mainly on temperature. Algorithms for fluid parameters are given in Section 5.0.

Now consider a uniform fluid temperature over the flow cross section at a point where the velocity profile is fully established. The boundary conditions will be such that the temperature gradient is infinite at x+ = 0, or Nu = ∞. Further down the tube the Nusselt number will approach the fully established condition in a manner shown in fig.A.8.
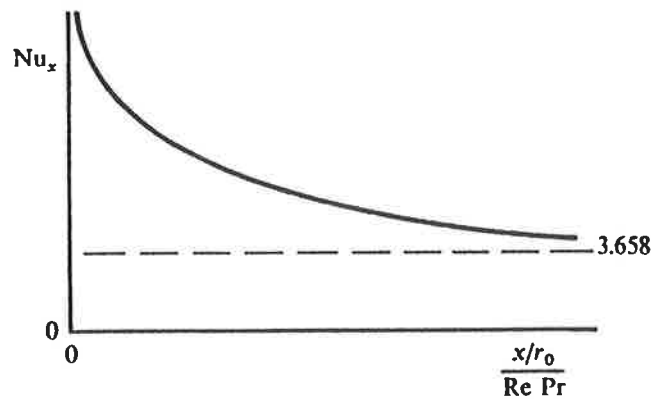
Fig.A.8 - Variation of local Nusselt number in the thermal entry region of a tube with constant surface temperature. (Kays[20])

The local and mean Nusselt numbers for constant surface temperature were evaluated[31] as

$$Nu(T)_x = \frac{\Sigma\ Gn\ \exp\ (-\Gamma n^2\ x^+)}{2\ \Sigma\ (Gn/\Gamma n^2)\ \exp\ (-\Gamma n^2\ x^+)} \tag{A.2-9}$$

and

$$Nu(T)_m = \frac{1}{2\ x^+}\ \ln\left[\frac{1}{8\ \Sigma\ (Gn/\Gamma n^2)\ \exp\ (-\Gamma n^2\ x^+)}\right], \tag{A.2-10}$$

where

$$x^+ = \frac{2\ (x/Dh)}{Re\ Pr}, \tag{A.2-11}$$

and for which the constants and eigenvalues for these series are given in Table A.7.

n	Γn^2	Gn
0	7.312	0.749
1	44.62	0.544
2	113.8	0.463

For n>2, $\Gamma n = 4n + \frac{8}{3}$; $Gn = 1.01276\Gamma n^{-1/3}$

Table A.7 - *Infinite-series solution functions for the circular tube; constant surface temperature; thermal entry length.* (Kays[31])

The local Nusselt number for constant heat rate is given[31] as

$$Nu(H)_x = \left[\frac{1}{Nu_\infty} - \frac{1}{2}\ \Sigma\ \frac{\exp(-\Phi m^2\ x^+)}{Am\ \Phi m^4}\right]^{-1} \tag{A.2-12}$$

for which the eigenvalues and constants are given in table A.8.

Local Nusselt numbers $Nu(T)x$ and $Nu(H)x$ have been computed for various values of x^+ with equations (A.2-9) and (A.2-12) for n and m = 0 to 15 and the results are listed in Table A.9. These equations were also numerically integrated to yield the mean Nusselt numbers $Nu(T)m$ and $Nu(H)m$. Compared with the analytical results of Eq.(A.2-10) the results are slightly low for low values of x^+ as could be expected since when $x^+ \rightarrow 0$, $Nux \rightarrow \infty$.

m	Φm^2	Am
1	25.68	7.630E-03
2	83.86	2.058E-03
3	174.2	0.901E-03
4	296.3	0.487E-03
5	450.9	0.297E-03

For m>5, $\Phi m = 4m + \frac{4}{3}$; $Am = 0.416\Phi m^{-7/3}$

Table A.8 - Infinite-series solution functions for the circular tube; constant heat rate; thermal entry length (Kays[31])

The mean Nusselt numbers have also been calculated as ratios over $Nu\infty$. Comparing columns 4 and 9 in Table A.9, there is very little difference between these ratios. It is therefore not unreasonable to use the solutions shown in column 6 to calculate the mean Nusselt numbers for constant surface temperature as well as those for constant heat rate. However, the infinite series equation (A.2-10) is not very convenient for continuous transient modelling and a simpler solution has been sought. The Nusselt number ratios can be adequately expressed by the two equations below:

for $x^+ < 0.06$

$$\frac{Nu_m}{Nu\infty} = 0.55473 \ (x^+)^{-.324} \quad , \quad\quad\quad (A.2-13)$$

and for $x^+ >= 0.06$

$$\frac{Nu_m}{Nu\infty} = 1.0 + \frac{0.027}{x^+} \quad . \quad\quad\quad (A.2-14)$$

Since a fully developed temperature profile is approached at a thermal entry length of $x^+ \approx 0.1$ we can say that the entry length is approximated by

$$(x/D) = 0.05 \ Re \ Pr \ . \quad\quad\quad (A.2-15)$$

(A.2-11)	Equation (A.2-9)			Eq.(A.2-10)		Equation (A.2-12)		
x^+	$Nu(T)_x$	$Nu(T)_m$	$\dfrac{Nu(T)m}{Nu(T)\infty}$	$Nu(T)_m$	$\dfrac{Nu(T)m}{Nu(T)\infty}$	$Nu(H)_x$	$Nu(H)_m$	$\dfrac{Nu(H)m}{Nu(H)\infty}$
0.001	12.78	15.56	4.25	19.30	5.28	15.73	19.39	4.44
0.002	10.12	13.27	3.63	15.27	4.18	12.53	16.48	3.78
0.003	8.83	11.95	3.27	13.32	3.64	10.97	14.83	3.40
0.004	8.03	11.04	3.02	12.09	3.31	9.99	13.71	3.14
0.005	7.47	10.37	2.83	11.22	3.07	9.30	12.88	2.95
0.006	7.04	9.84	2.69	10.56	2.89	8.77	12.23	2.80
0.007	6.70	9.41	2.57	10.03	2.74	8.36	11.70	2.68
0.008	6.43	9.05	2.47	9.60	2.62	8.02	11.26	2.58
0.009	6.20	8.74	2.39	9.23	2.52	7.74	10.88	2.49
0.010	6.00	8.48	2.32	8.92	2.44	7.49	10.55	2.42
0.020	4.92	6.92	1.89	7.14	1.95	6.15	8.62	1.98
0.030	4.44	6.16	1.68	6.31	1.73	5.55	7.68	1.76
0.040	4.17	5.69	1.56	5.81	1.59	5.20	7.10	1.63
0.050	4.00	5.37	1.47	5.46	1.49	4.97	6.70	1.53
0.060	3.89	5.13	1.40	5.21	1.42	4.82	6.40	1.47
0.070	3.82	4.95	1.35	5.02	1.37	4.70	6.16	1.41
0.080	3.77	4.80	1.31	4.86	1.33	4.62	5.97	1.37
0.090	3.73	4.69	1.28	4.74	1.30	4.56	5.82	1.33
0.100	3.71	4.59	1.26	4.64	1.27	4.51	5.69	1.30
0.110	3.69	4.51	1.23	4.55	1.24	4.48	5.58	1.28
0.120	3.68	4.44	1.21	4.48	1.22	4.45	5.49	1.26
0.130	3.67	4.38	1.20	4.42	1.21	4.43	5.41	1.24
0.140	3.67	4.33	1.18	4.36	1.19	4.42	5.34	1.22
0.150	3.66	4.29	1.17	4.32	1.18	4.40	5.28	1.21
0.160	3.66	4.25	1.16	4.28	1.17	4.40	5.22	1.20
0.170	3.66	4.21	1.15	4.24	1.16	4.39	5.17	1.19
0.180	3.66	4.18	1.14	4.21	1.15	4.38	5.13	1.18
0.190	3.66	4.16	1.14	4.18	1.14	4.38	5.09	1.17
0.200	3.66	4.13	1.13	4.15	1.14	4.38	5.05	1.16
∞	3.66	3.66	1.00	3.66	1.00	4.36	4.36	1.00

Table A.9 - *Solutions for Local and Mean Nusselt numbers
for circular tube and thermal entry length.
(T) for constant surface temperature
(H) for constant heat rate.*

A.2.4 Thermal Entry Length for Rectangular Cross Section

Flow between parallel plates is a special case of the rect-
angular family.   The constant surface temperature solutions
are presented with equations (A.2.9) and (A.2.10) using
eigenvalues and constants given in Table A.10.

n	Γn^2	Gn
0	15.09	1.717
1	171.3	1.139
2	498	0.952

$$\text{For } n>2, \quad \Gamma n = \frac{16\,n}{\sqrt{3}} + \frac{20}{3\sqrt{3}}; \quad Gn = 2.68\ \Gamma n^{-1/3}$$

*Table A.10 - Infinite-series solution functions for the
parallel planes system; constant surface
temperature; thermal entry length (Kays[20])*

Table A.11 lists the solutions to equations (A.2-9) and
(A.2-10) for the local and mean Nusselt numbers respectively.
The mean Nusselt number can be expressed as a ratio over Nu_∞
by the following empirical equations:

for $(x^+) < 0.02$

$$\frac{Nu_m}{Nu_\infty} = 0.37677\ (x^+)^{-.304} \quad , \tag{A.2-16}$$

and for $(x^+) >= 0.02$

$$\frac{Nu_m}{Nu_\infty} = 1.0 + \frac{0.00608}{(x^+)} \quad . \tag{A.2-17}$$

(A.2-11)	(A.2-9)	(A.2-10)	
x^+	$Nu(T)_x$	$Nu(T)_m$	$\dfrac{Nu(T)m}{Nu(T)\infty}$
0.001	15.84	23.43	3.11
0.002	12.83	18.76	2.49
0.003	11.42	16.53	2.19
0.004	10.55	15.13	2.01
0.005	9.96	14.15	1.88
0.006	9.52	13.42	1.78
0.007	9.18	12.83	1.70
0.008	8.92	12.36	1.64
0.009	8.70	11.97	1.59
0.010	8.52	11.63	1.54
0.020	7.75	9.83	1.30
0.030	7.59	9.10	1.21
0.040	7.55	8.72	1.16
0.050	7.55	8.48	1.13
0.060	7.55	8.33	1.10
0.070	7.55	8.22	1.09
0.080	7.55	8.13	1.08
0.090	7.55	8.07	1.07
0.100	7.55	8.02	1.06
0.110	7.54	7.97	1.06
0.120	7.55	7.94	1.05
0.130	7.54	7.91	1.05
0.140	7.55	7.88	1.05
0.150	7.55	7.86	1.04
0.160	7.55	7.84	1.04
0.170	7.55	7.82	1.04
0.180	7.55	7.81	1.04
0.190	7.55	7.79	1.03
0.200	7.55	7.78	1.03

Table A.11 - Solutions for Local and Mean Nusselt numbers for flow between parallel plates; constant surface temperature; thermal entry length.

There is no infinite series solution available as yet for the remainder of the rectangular tube family. Table A.12 lists the mean Nusselt numbers for a number of different aspect ratios and corresponding solutions for $Nu_m/Nu\infty$.

| | $Nu(T)_m$ | | | | | $\dfrac{Nu_m}{Nu_\infty}$ | | | | |
| | b/a | | | | | b/a | | | | |
x^+	1	2	4	6	∞	1	2	4	6	∞
0.01	8.63	8.58	9.47	10.01	11.63	2.91	2.54	2.10	1.92	1.54
0.02	6.48	6.84	7.71	8.17	9.83	2.18	2.02	1.71	1.57	1.30
0.05	4.83	5.24	6.16	6.70	8.48	1.63	1.55	1.37	1.28	1.13
0.10	4.04	4.46	5.44	6.04	8.02	1.36	1.32	1.21	1.16	1.06
0.20	3.53	3.95	5.00	5.66	7.78	1.19	1.17	1.11	1.08	1.03
∞	2.97	3.38	4.51	5.22	7.54	1.00	1.00	1.00	1.00	1.00

Table A.12 - Nusselt numbers for rectangular-tube family;
constant surface temperature; thermal entry
length. (Kays[31])

Empirical equations have been fitted as

$$\frac{Nu_m}{Nu_\infty} = 1.0 + A\,(x^+)^{-1} + B\,(x^+)^{-2} + C\,(x^+)^{-3} \qquad\qquad (A.2\text{-}18)$$

where

$$A = \emptyset_a\,(a/b), \qquad B = \emptyset_b\,(a/b), \qquad C = \emptyset_c\,(a/b), \qquad (A.2\text{-}19)$$

for the range of a/b = 0 to 1 and for which the polynomial
coefficients for $\emptyset(a/b)$ are listed in Table A.13.

Subscript	A	B	C
0	3.5715565D-03	3.8857180D-05	-2.4752562D-07
1	8.7831804D-02	-1.1895281D-03	5.8502316D-06
2	-5.2205294D-02	7.2501809D-04	-3.3587069D-06

Table A.13 - Polynomial coefficients for Eq.(A.2-19).

A.3 HEAT TRANSFER: TURBULENT FLOW INSIDE SMOOTH TUBES

A.3.1 Fully Developed Turbulent Flow in Tubes and Ducts

In a turbulent flow the velocity profile is characteristically very flat. From the assumed similarity this must also be true of the temperature profile. It has been shown[20] that when the Prandtl number is close to unity the Stanton number may be approximated as

$$St = \frac{f}{2} \qquad \text{(A.3-1)}$$

and where the friction factor f is as defined in Section A1 and is usually calculated by equations (A.1-15) and (A.1-17).

For Prandtl numbers in the range 0.5 to 30 the Stanton number is given[20] as

$$St = \frac{\sqrt{(f/2)}}{0.833\left[5Pr + 5\ln(5Pr+1) + 2.5\ln\dfrac{Re\,\sqrt{(f/2)}}{60}\right]} \qquad \text{(A.3-2)}$$

Since Nu = St Pr Re,

$$Nu = \frac{Re\,Pr\,\sqrt{(f/2)}}{0.833\left[5Pr + 5\ln(5Pr+1) + 2.5\ln\dfrac{Re\,\sqrt{(f/2)}}{60}\right]} \qquad \text{(A.3-3)}$$

This equation shows that for turbulent flow Nu = $\emptyset$(Re,Pr) rather than being a mere constant as for laminar flow. It gives good results over a wide range of Reynolds numbers for the Prandtl numbers specified.

Nusselt numbers for fully developed turbulent flow have been solved and compared[20] with experimental data for a range of Reynolds and Prandtl numbers and are listed in Table A.14. Good correlation was found for the medium and high Prandtl numbers but the accuracy at very low Prandtl numbers (liquid metals) remains in some doubt. For Prandtl numbers greater than 0.5 the values given in Table A.14 compare sufficiently closely with experimental data to be taken as datum for comparison of other equations.

The dimensionless temperature profiles plotted in Fig.A.9 show that at higher Prandtl numbers the temperature profile becomes quite 'square,' whereas at low Prandtl numbers much more rounded profiles, similar to that for laminar flow, are obtained. Various refinements have been developed in an attempt for a complete solution.

Re	10^4	3×10^4	10^5	3×10^5	10^6
Pr					
0.0	6.30	6.64	6.84	6.95	7.06
0.001	6.30	6.64	6.84	7.08	8.12
0.003	6.30	6.64	7.10	8.14	12.8
0.01	6.43	7.00	8.90	14.2	30.5
0.03	6.90	9.10	15.9	32.4	80.5
0.5	26.3	57.3	142	340	895
0.7	31.7	70.7	178	430	1150
1.0	37.8	86.0	222	543	1470
3.0	61.5	149	404	1030	2900
10	99.8	248	690	1810	5220
30	141	362	1030	2750	8060
100	205	522	1510	4030	12000
1000	380	975	2830	7600	22600

Table A.14 - Nusselt numbers for fully developed turbulent flow in a circular tube with constant heat rate. (Kays[20])
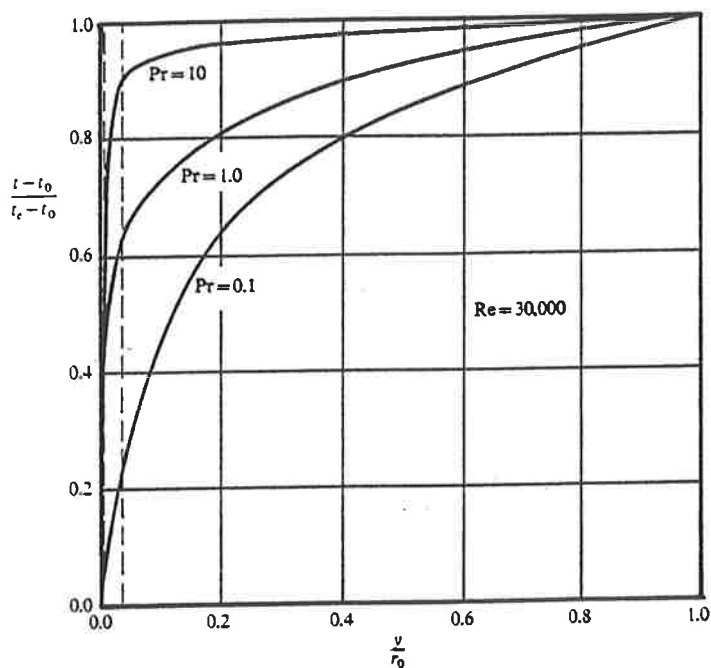
Fig.A.9 - Effect of Prandtl number on turbulent flow temperature distribution

Kays[31] presented a number of empirical algebraic equations for fully developed turbulent flow. These are applicable to circular tubes and to tubes of noncircular cross section. For $Pr \leq 1$, separate equations are given for constant heat rate and constant surface temperature. For higher Prandtl numbers no such distinction is made since there is very little difference.

For $Pr < 0.03$ (liquid metals)

$$Nu(H) = 6.3 + 0.0167\ Re^{0.85}\ Pr^{0.93} , \qquad (A.3-4)$$

$$Nu(T) = 4.8 + 0.0156\ Re^{0.85}\ Pr^{0.93} . \qquad (A.3-5)$$

For very pure liquid metals

$$Nu(H) = 5.6 + 0.0165\ Re^{0.85}\ Pr^{0.86} , \qquad (A.3-6)$$

$$Nu(T) = 4.5 + 0.0156\ Re^{0.85}\ Pr^{0.86} . \qquad (A.3-7)$$

For $0.6 < Pr < 0.8$ (gases) and $Re < 10^5$

$$Nu(H) = 0.022\ Pr^{0.5}\ Re^{0.8} , \qquad (A.3-8)$$

$$Nu(T) = 0.021\ Pr^{0.5}\ Re^{0.8} . \qquad (A.3-9)$$

For $0.1 < Pr < 10^4$ and $10^5 < Re < 10^6$

$$Nu = 5 + 0.015\ Re^a\ Pr^b \qquad (A.3-10)$$

where
$$a = 0.88 - \frac{0.24}{4 + Pr} ,$$

$$b = 0.333 + 0.5\ \exp(-0.6\ Pr) .$$

A wide range equation was proposed by Gnielinski[31] for $0.5 < Pr < 2000$ and $2300 < Re < 5.0E+06$;

$$Nu = \frac{(Re - 1000)\ Pr\ f/2}{1.0 + 12.7\ (Pr^{2/3} - 1)\ \sqrt{(f/2)}} , \qquad (A.3-11)$$

where f is defined by Eq.(A.1-15) for $Re < 9000$ and Eq. (A.1-17) for $Re => 9000$.

Pr	Re	Nusselt	number	equations						Tab.
		A.3-3	A.3-4	A.3-6	A.3-8	A.3-10	A.3-11	A.3-12	A.3-13	A.14
0.0	1.0E+4	0.00	6.30	5.60	0.00	5.00	0.00	0.00	0.00	6.30
	3.0E+4	0.00	6.30	5.60	0.00	5.00	0.00	0.00	0.00	6.64
	1.0E+5	0.00	6.30	5.60	0.00	5.00	0.00	0.00	0.00	6.84
	3.0E+5	0.00	6.30	5.60	0.00	5.00	0.00	0.00	0.00	6.95
	1.0E+6	0.00	6.30	5.60	0.00	5.00	0.00	0.00	0.00	7.06
0.001	1.0E+4	0.13	6.37	5.71	1.10	5.09	0.17	2.30	3.65	6.30
	3.0E+4	0.24	6.47	5.88	2.66	5.22	0.27	5.54	8.78	6.64
	1.0E+5	0.52	6.78	6.37	6.96	5.60	0.55	14.51	23.01	6.84
	3.0E+5	1.14	7.53	7.56	16.8	6.48	1.16	35.0	55.4	7.08
	1.0E+6	2.83	9.71	11.1	43.9	8.96	2.79	91.56	145	8.12
0.003	1.0E+4	0.38	6.49	5.88	1.91	5.23	0.48	3.57	5.26	6.30
	3.0E+4	0.70	6.78	6.31	4.60	5.56	0.79	8.60	12.7	6.64
	1.0E+5	1.55	7.64	7.59	12.1	6.50	1.63	22.5	33.2	7.10
	3.0E+5	3.40	9.70	10.7	29.0	8.70	3.43	54.2	79.9	8.14
	1.0E+6	8.46	15.8	19.7	76.0	14.9	8.28	142	209	12.8
0.01	1.0E+4	1.22	6.88	6.39	3.49	5.63	1.47	5.78	7.85	6.43
	3.0E+4	2.29	7.77	7.61	8.40	6.54	2.51	13.9	18.9	7.00
	1.0E+5	5.07	10.4	11.2	22.0	9.14	5.23	36.5	49.6	8.90
	3.0E+5	11.2	16.7	19.8	53.0	15.2	11.1	87.8	119	14.2
	1.0E+6	27.9	35.3	45.2	139	32.4	27.0	230	313	30.5
0.03	1.0E+4	3.36	7.91	7.63	6.04	6.60	3.79	8.97	11.3	6.90
	3.0E+4	6.45	10.4	10.8	14.5	8.93	6.83	21.6	27.3	9.10
	1.0E+5	14.5	17.7	20.0	38.1	15.6	14.7	56.6	71.5	15.9
	3.0E+5	32.2	35.3	42.2	91.8	31.0	31.6	136	172	32.4
	1.0E+6	80.8	86.9	107	240	74.8	77.4	357	451	80.5
0.5	1.0E+4	25.7	28.3	28.4	24.7	23.7	25.1	27.6	28.9	26.3
	3.0E+4	57.5	62.3	63.7	59.4	51.3	57.6	66.5	69.7	57.3
	1.0E+5	145	162	167	156	130	143	174	183	142
	3.0E+5	345	403	417	375	316	337	420	440	340
	1.0E+6	919	1110	1150	982	845	884	1100	1152	895
0.7	1.0E+4	31.2	36.4	36.1	29.2	29.5	29.8	31.6	32.4	31.7
	3.0E+4	71.1	82.9	83.2	70.3	65.9	70.3	76.1	78.0	70.7
	1.0E+5	182	219	222	184	170	179	199	204	178
	3.0E+5	439	549	555	443	416	426	480	492	430
	1.0E+6	1180	1515	1534	1161	1220	1132	1258	1289	1150
1.0	1.0E+4	38.0	48.2	47.1	34.9	36.9	35.4	36.5	36.5	37.8
	3.0E+4	88.1	113	111	84.0	84.6	85.7	87.8	87.8	86.0
	1.0E+5	229	303	299	220	222	223	230	230	222
	3.0E+5	559	762	752	530	546	540	554	554	543
	1.0E+6	1521	2109	2083	1388	1478	1452	1451	1451	1470
3.0	1.0E+4	65.1	123	112	60.4	62.2	57.1	56.6	52.6	61.5
	3.0E+4	158	303	277	146	150	147	136	127	149
	1.0E+5	429	831	760	381	406	405	357	332	404
	3.0E+5	1086	2105	1926	918	1020	1023	860	799	1030
	1.0E+6	3051	5847	5349	2404	2815	2860	2252	2093	2900
10	1.0E+4	99.7	363	306	110	96.6	90.8	91.6	78.5	99.8
	3.0E+4	251	915	770	266	241	244	221	189	248
	1.0E+5	706	2534	2131	696	673	697	578	495	690
	3.0E+5	1842	6437	5414	1675	1728	1820	1391	1193	1810
	1.0E+6	5334	17901	15054	4390	4874	5254	3645	3126	5220
30	1.0E+4	125	998	778	191	150	135	142	113	141
	3.0E+4	320	2530	1971	460	382	369	342	273	362
	1.0E+5	918	7028	5473	1205	1083	1075	897	715	1030
	3.0E+5	2435			2902	2818	2855	2159	1721	2750
	1.0E+6	7180			7603	8052	8391	5657	4509	8060
100	1.0E+4	140			349	230	204	230	169	205
	3.0E+4	363			840	596	564	554	407	522
	1.0E+5	1050			2200	1705	1665	1451	1067	1510
	3.0E+5	2810			5298	4465	4464	3495	2571	4030
	1.0E+6	8363			13881	12836	13261	9156	6735	12000
1000	1.0E+4	149			1103	500	443	578	364	380
	3.0E+4	388			2655	1305	1235	1391	878	975
	1.0E+5	1127			6957	3754	3672	3645	2299	2830
	3.0E+5	3026			16754	9860	9914	8779	5538	7600
	1.0E+6	9047			43896	28427	29664	23000	14509	22600

Table A.15 - Comparison of equations for Nusselt numbers for fully developed turbulent flow in circular tubes Note that the equations apply to different ranges of Prandtl and Reynolds numbers.

The Dittus and Boelter equation given by McAdams[25] was based on experimental data over the ranges for $0.7 < Pr < 120$ and $10,000 < Re < 120,000$;

$$Nu = 0.023 \, Re^{0.8} \, Pr^{0.4} \, . \qquad (A.3-12)$$

This compares with the Colburn equation[31] which is

$$Nu = 0.023 \, Re^{0.8} \, Pr^{1/3} \, . \qquad (A.3-13)$$

The results from equations (A.3-3) to (A.3-13) are compared in Table A.15 with those listed in Table A.14. Inspection indicates that for the Prandtl number range of 0.5 to 100, which covers the range of interest for cooling and heating coils, Eqs.(A.3-10) and (A.3-11) give the best results.

In a later publication, Kays[31] implied a preference for equation (A.3-4) for Prandtl numbers less than 0.5 and for $Pr >= 0.5$, equation (A.3-10) was preferred.

A.3.2 Thermal Entry Length for Circular Tube

The problem of solving the thermal entry length for turbulent flow is similar to that for laminar flow described in Section A.2.3; the solutions can be put in precisely the same form. Thus Eqs.(A.2.9) and (A.2.10) for constant surface temperature and Eq.(A.2-12) for constant heat rate are directly applicable but with different eigenvalues and constants. These are now functions of both Reynolds and Prandtl numbers and are given[20] in table A.16.

If we move far enough downstream so that the local Nusselt number approaches its asymptotic value then the mean Nusselt number for constant surface temperature is given by

$$Nu_m = \frac{\Gamma o^2}{2} + \frac{1}{2x_+} \ln(\frac{\Gamma o^2}{8 \, Go}) \, . \qquad (A.3-14)$$

Note that only the first term in the infinite series solution is of importance. From Eq.(A.2-9) as $x^+ => \infty$,

$$\Gamma o^2/2 => Nu_\infty \, ;$$
thus
$$\frac{Nu_m}{Nu_\infty} = 1 + \frac{1}{x_+ \, \Gamma o^2} \ln(\frac{\Gamma o^2}{8 \, Go}) \, . \qquad (A.3-15)$$

The range of interest extends to Prandtl numbers in excess of 10. Table A.16 does not provide data for constant surface temperature for fluids with Prandtl numbers in excess of 0.7.

n,m	Pr	Re	Γn^2	Gn	Φm^2	Am
0	0.01	50,000	11.7	1.11	—	—
1			65.0	0.950	34.5	6.45E-03
2			163	0.880	113	1.81E-03
3			305	0.835	237	8.28E-04
4			491	0.802	406	4.68E-04
5			722	0.777	621	2.99E-04
0	0.01	100,000	13.2	1.30	—	—
1			74.0	1.04	40.9	5.39E-03
2			190	0.935	135	1.40E-03
3			360	0.869	284	6.25E-04
4			583	0.823	488	3.26E-04
5			860	0.788	746	2.04E-04
0	0.01	200,000	16.9	1.70	—	—
1			96.0	1.24	55.5	3.86E-03
2			247	1.07	181	9.89E-04
3			467	0.978	376	4.49E-04
4			757	0.901	642	2.52E-04
5			1116	0.847	980	1.60E-04
0	0.70	50,000	235	28.6	—	—
1			2640	5.51	1947	7.51E-05
2			7400	3.62	5230	1.97E-05
3					9875	8.00E-06
4					15900	4.02E-06
5					23270	2.28E-06
0	0.70	100,000	400	49.0	—	—
1			4430	9.12	3557	4.12E-05
2			12800	5.66	9530	1.08E-05
3					17970	4.43E-06
4					28840	2.26E-06
5					42230	1.30E-06
0	10.0	50,000			—	—
1					2.736E+04	5.021E-06
2					7.316E+04	1.21E-06
3					1.373E+05	4.36E-07
4					2.196E+05	1.87E-07
5					3.198E+05	8.79E-08
0	10.0	100,000			—	—
1					5.040E+04	2.78E-06
2					1.346E+05	6.97E-07
3					2.528E+05	2.68E-07
4					4.046E+05	1.26E-07
5					5.904E+05	6.56E-08

Table A.16 - Infinite series solution functions for turbulent flow in a circular tube; thermal entry length (Kays[20])

Therefore Nusselt numbers for constant heat rate have been
solved by using Eq.(A.2-12) in conjunction with table A.16
and integrated to yield ratios Nu_x/Nu_∞ and Nu_m/Nu_∞ as listed
in table A.17. The results compare with figs.A.10 and A.11.
Fig.A.10 shows the strong influence of the Prandtl number;
above 1 the thermal entry length becomes less important.
Fig.A.11 shows the small influence of Reynolds number for Pr
= 0.7 on the ratios Nu_x/Nu_∞, although Nu_∞ itself is a strong
function of Reynolds number. Examination of Table A.17 indi-
cates that this observation applies at least for $0.7 \leq Pr \leq 10$.

Reynolds No.		50,000		100,000	
Prandtl number	$\dfrac{x}{D}$	$\dfrac{Nu_x}{Nu_\infty}$	$\dfrac{Nu_m}{Nu_\infty}$	$\dfrac{Nu_x}{Nu_\infty}$	$\dfrac{Nu_m}{Nu_\infty}$
0.01	5	1.346	1.683	1.636	2.186
	10	1.139	1.443	1.309	1.798
	15	1.064	1.325	1.179	1.607
	20	1.031	1.254	1.110	1.489
	25	1.015	1.208	1.070	1.408
	30	1.008	1.175	1.046	1.349
	35	1.004	1.150	1.030	1.304
	40	1.002	1.132	1.020	1.269
	45	1.001	1.117	1.013	1.241
	50	1.000	1.106	1.009	1.218
0.7	5	1.151	1.261	1.152	1.255
	10	1.070	1.178	1.073	1.177
	15	1.037	1.135	1.040	1.135
	20	1.020	1.108	1.023	1.109
	25	1.012	1.089	1.014	1.090
	30	1.007	1.076	1.008	1.077
	35	1.004	1.066	1.005	1.067
	40	1.002	1.058	1.003	1.059
	45	1.001	1.051	1.002	1.053
	50	1.001	1.046	1.001	1.047
10.0	5	1.039	1.065	1.041	1.064
	10	1.019	1.045	1.020	1.045
	15	1.010	1.035	1.012	1.035
	20	1.006	1.028	1.007	1.028
	25	1.003	1.023	1.004	1.024
	30	1.002	1.020	1.002	1.020
	35	1.001	1.017	1.001	1.018
	40	1.001	1.015	1.001	1.016
	45	1.000	1.013	1.001	1.014
	50	1.000	1.012	1.000	1.013

*Table A.17 - Solutions to Eq.(A.2-12) using Table A.16
for Nusselt numbers in the thermal entry
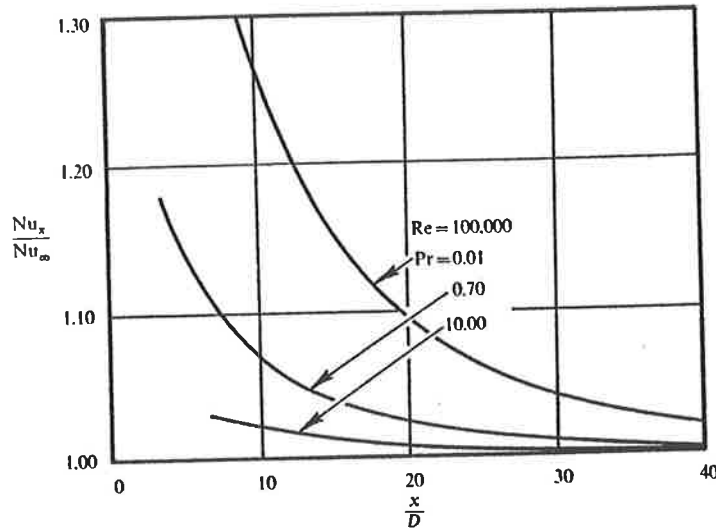length at constant heat rate.*

Fig.A.10 - Nusselt numbers in thermal entry length of a circular tube, constant heat rate. Influence of Prandtl number. (Kays[20])
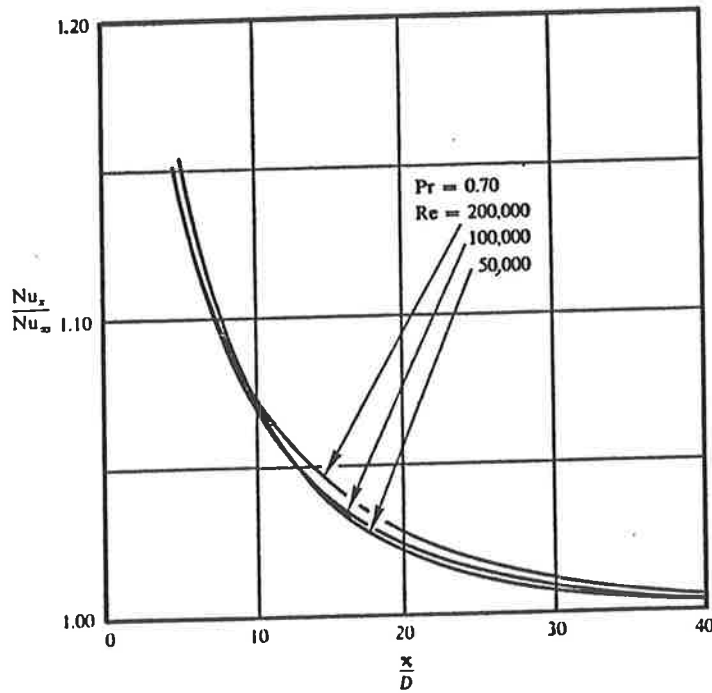

Fig.A.11 - Nusselt numbers in the thermal entry length of a circular tube, constant heat rate. Influence of Reynolds number. (Kays[20])

The results in Table A.17 fit the empirical equation

$$\frac{Nu_m}{Nu_\infty} = a \left[\frac{x}{D} \right]^{-b} , \qquad\qquad (A.3-16)$$

where for Pr = 10

$$a = 1.1, \quad b = 0.022, \qquad\qquad (A.3-17)$$

and for the ranges of Pr = 0.7 to 10 and Re = 2100 to 100,000 factors a and b in Eq.(A.3-16) may be expressed as

$$a = C_1 + C_2/Pr . \qquad\qquad (A.3-18)$$

Here

$C_1 = 1.0727 + 320.01/Re$
$C_2 = 0.23063 + 918/Re$,

and

$$b = 1 / (C_3 + C_4 \cdot Pr) , \qquad\qquad (A.3-19)$$

where

$C_3 = 9.1836 + 7.938E{-}06 \cdot Re$
$C_4 = 3.1563 + 4.256E{-}06 \cdot Re$.

A.3.3 Flow in Curved Tubes

As previously described in Section 3.2 and also shown in Fig. 3.1, secondary flows are induced in curved tubes, resulting in higher heat transfer coefficients on the outside than on the inside of the curve. From experiments conducted with water, the average peripheral heat transfer coefficients can be correlated[20] by use of the analogy relation

$$St \, Pr^{0.6} = \frac{f}{2} , \qquad\qquad (A.3-20)$$

where the friction coefficient is that given by Eq.(A.1-17). Since Nu = St Pr Re, Eq.(A.3-20) can be rewritten as

$$Nu = \frac{f}{2} Pr^{0.4} Re . \qquad\qquad (A.3-21)$$

A.3.4 Combined Hydrodynamic and Thermal Entry Length

The turbulent boundary layer development is influenced by the type of tube entrance. In heat exchangers the entrance is typically a sharp edged contraction or is preceded by a bend in the tube. In either case the heat transfer rate at the entrance is higher than that for a well developed turbulent boundary layer and the former case is expressed by Eq(A.3-16).
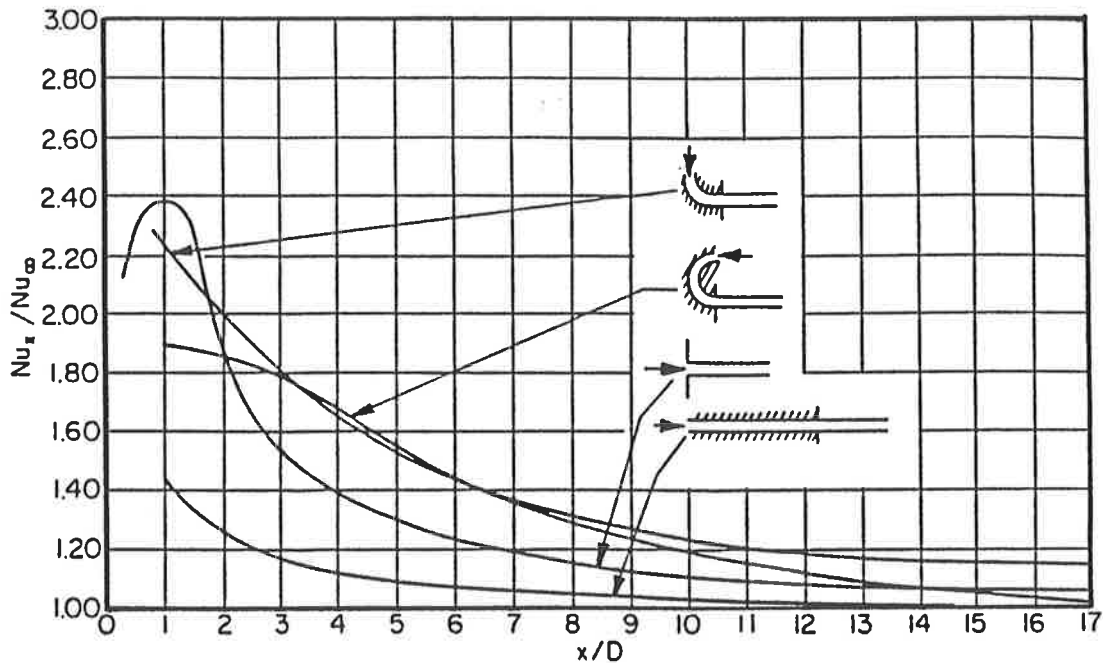
Fig.A.12 - Measured local Nusselt numbers in the entry
region of a circular tube for various entry
configurations, air with constant surface
temperature (Boelter, Young, and Iversen[20])

Experiments conducted by Boelter, Young, and Iversen[20,31]
determined the local heat transfer to air flowing through
steam heated tubes. Fig.A.12 shows the plots of the ratios
of local Nusselt number to fully developed Nusselt number as
a function of x/D. These experiments were conducted at a
Reynolds number close to 50,000. The hydrodynamic entry
length shown for the abrupt contraction corresponds to the
curves in Fig.A.11.

Applying Eq.(A.3-21) to air flow at Re = 50,000 in a curved
pipe should yield similar results to those shown in Fig.A.12
for x/D = 0. The Prandtl number for air is close to 0.7.
Now by Eq.(A.3-10) the Nusselt number for fully developed
turbulent flow is determined as

$$Nu_\infty = 98.07 \ ,$$

and from Table A.3, or Eq.(A.1-11), the Fanning friction
factor for developed flow is established as

$$f_{(straight)} = 0.00521 \ .$$

Now consider a typical tube bend in a cooling coil with a
radius of curvature R of 20 mm and a tube inside diameter of
16 mm (ro = 8 mm), then by Eq.(A.1-17) the friction factor
will increase by a factor of 1.567. Therefore

$$f_{(curved \ tube)} = 0.00817 \ .$$

By Eq.(A.3-21), the Nusselt number for the curved tube is then

$$Nu_x = \frac{0.00817}{2} \, 0.7^{0.4} \, 50000 = 177.01 \; ,$$

and the heat transfer enhancement ratio is established as

$$\frac{Nu_x}{Nu_\infty} = \frac{177.01}{98.07} = 1.805 \; ,$$

which is within 10% of that shown in Fig.A.12 for the 180° bend at x/D = 0.

The curves in Fig.A.12 refer to the local Nusselt number, but the mean Nusselt number for a given length of pipe is of greater interest. This can be expressed[20] as

$$\frac{Nu_m}{Nu_\infty} = 1 + \frac{C}{x/D} \; , \qquad\qquad (A.3-22)$$

for which C has been evaluated by integration as

Fully developed velocity profile	1.4
Abrupt contraction entrance	6
90° right angle bend	7
180° round bend	6 .

This shows that the mean Nusselt numbers for a given entry length, for which x/D > 10, are the same for the 180° round bend as for the abrupt contraction entrance.

But Eq.(A.3-22) is only valid for air at Re = 50000. It is desirable to have a more generalised equation for the mean Nusselt number which should be expressed as a function of the Reynolds and Prandtl numbers. Such an equation was developed in Section A.3.2 for the abrupt contraction entrance as Eq.(A.3-16). Because of the similarity in Nusselt number ratios as expressed by Eq.(A.3-22) for the two entry conditions under consideration, it is not unreasonable to use Eq.(A.3-16) for computing the thermal entry length Nusselt number for the 180° bend as well as for the abrupt entry.

Inspecting Table A.17, from which Eq.(A.3-16) has been derived, and considering water, which at the temperatures of interest has an approximate Prandtl number of 10, the heat transfer enhancement for a thermal entry length of x/D = 10 is only 4.5%. This rapidly diminishes further as x/D increases. Thus any differences that might exist between the two entry types will be insignificant with the low enhancement ratios and the use of Eq.(A.3-16) for expressing the mean Nusselt number for the entry from a 180° bend is therefore justified.

A.4   SYMBOLS USED IN APPENDIX A

a	channel width = Ct - Do	- m
a^*	ratio s/a	
Am	constants for calc. thermal entry lengths	
Cp	specific heat	- kJ/kg K
Dh	hydraulic diameter	- m
Di	tube inside diameter	- mm
dpf	pressure drop due to flow	- Pa
f	Fanning friction factor	
G	fluid mass flow rate	- kg/m² s
Gn	constants for calc. thermal entry lengths	
h	heat transfer coefficient	- W/m² K
k	thermal conductivity	- W/m K
L	straight length of pipe or duct	- m
Nu	Nusselt number = h Dh / k	
Nu(H)	Nusselt number for constant heat rate	
Nu(T)	Nusselt number for constant surface temp.	
Pr	Prandtl number = Cp μ/k (dimensionless)	
R	radius of curvature at centre line	- m
Re	Reynolds number = Dh G/μ (dimensionless)	
rh	hydraulic radius	- m
ro	radius of tube inside diameter	- m
s	space between fins = Channel height	- m
St	Stanton number (dimensionless)	
v	specific volume	- cu.m/kg
x	distance from pipe or duct entry	- m
x^+	entry length defined by Eq.(A.2-11)	

Greek Symbols

α	thermal diffusivity	- m²/s
δ	density of fluid	- kg/cu.m
Γn^2	eigenvalues for thermal entry length	
Φm^2	eigenvalues for thermal entry length	
μ	dynamic viscosity of fluid	- kg/m s
v	kinematic viscosity	- m²/s

APPENDIX B

NORMAL AND ENHANCED HEAT TRANSFER AREAS OF FIN ELEMENTS

CONTENTS

B.1 VORTEX ENHANCEMENT

As a result from flow visualisation and local heat transfer measurement, Gilbert[14] proposed a model of vortex trajectories with their associated heat transfer enhancement and areas of reduced heat transfer as shown in Fig.B.1. This model is the basis for computing the various heat transfer areas for the fin elements defined in this Appendix.
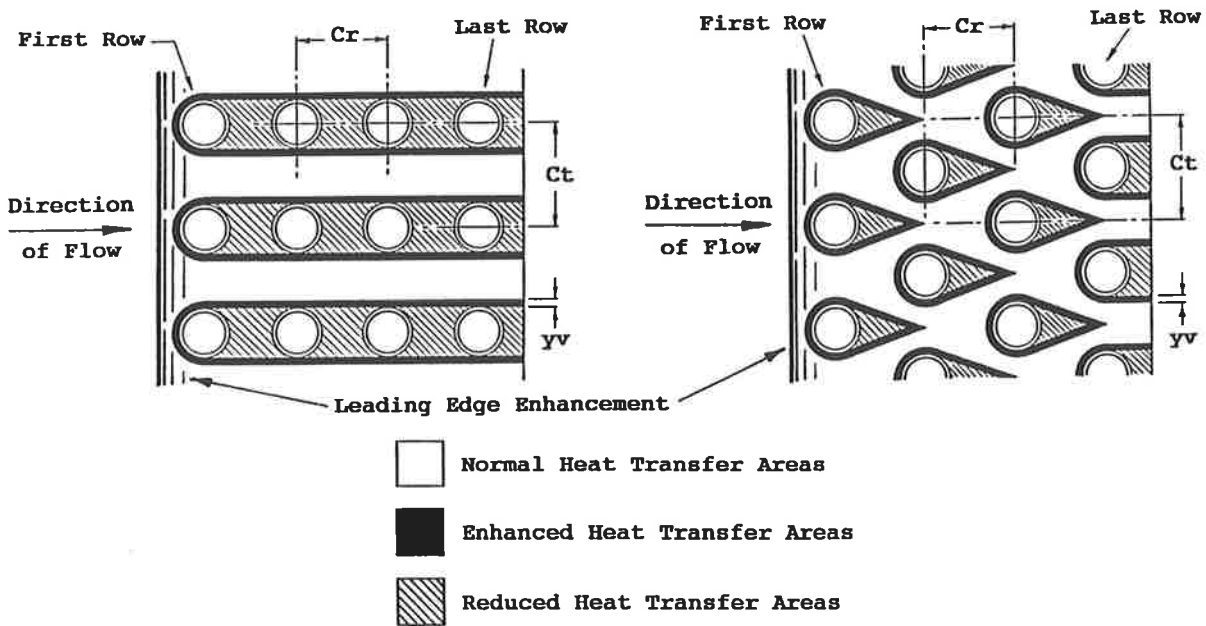
Fig.B.1 - Heat transfer areas on continuous plate fins for In-line and Staggered arrangements.

B.2 DIMENSIONS OF FIN ELEMENTS

The isotherms in the fins are in approximately concentric circular patterns and the fins need therefore to be divided into concentric elements to allow proper modelling of the temperature gradient within the fins. For this reason it is more convenient to work with circular fins; continuous plate fins are therefore converted into circular fins of equivalent heat transfer area.

Fig.B.2 shows two examples of continuous plate fins for tube spacing Ct mm and row spacing Cr mm. By inspection a fin area of $Ct \cdot Cr$ mm² may be assigned to each tube. If R3 is the outer radius of a flat circular plate fin of equal area, then
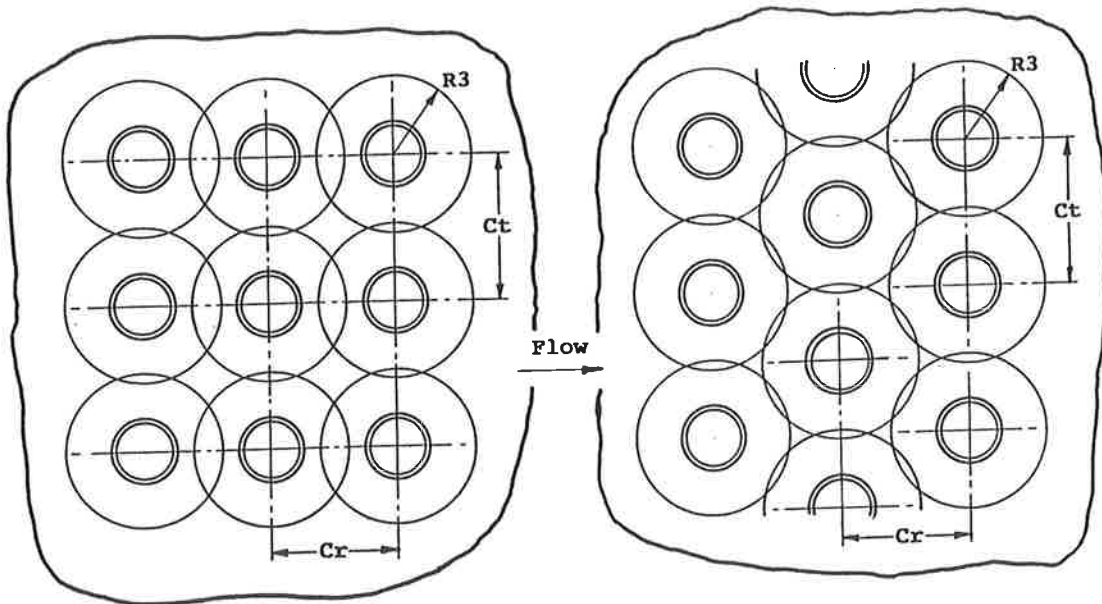
R3 = √(Cr*Ct/π)

(a)   (b)

Fig.B.2 - Conversion of rectangular plate fins
          to circular plate fins of equal area.
          (a) In-line arrangement.
          (b) Staggered arrangement.

$$\pi \cdot R3^2 = Cr \cdot Ct$$

and

$$R3 = \sqrt{(Cr \cdot Ct / \pi)} \quad \text{mm} ,$$

or

$$R3 = \sqrt{(Cr \cdot Ct / \pi)} / 1000. \quad \text{m} . \tag{B.2-1}$$

In Section 4.1 the effective tube outside diameter Do is given by Eq.(4.1-7) in mm, then the tube radius plus fin thickness is defined as

$$R0 = Do / 2000. \quad \text{m} . \tag{B.2-2}$$

Areas of enhanced, normal and reduced heat transfer are to be allocated to the fin elements. To simplify this procedure, let the inner fin element be of the same dimension as the width of the U-shaped vortex, and let the vortices around each tube be yv m wide, then the radius of the outer boundary of the inner element is defined as

$$R1 = R0 + yv \quad \text{m} . \tag{B.2-3}$$

The mean temperature of this small fin element should be close enough to that for the tube so that the tube element can be included as part of the fin's inner element.

Now divide the remaining fin area into two elements of equal area. This will give approximate equal time constants for heat transfer to or from the two outer elements. Thus the outside radius of the intermediate fin element is derived as

$$R2 = \sqrt{((R1^2 + R3^2) / 2)} \quad m \; . \tag{B.2-4}$$

The resultant three fin elements are shown in fig.B.3 below.
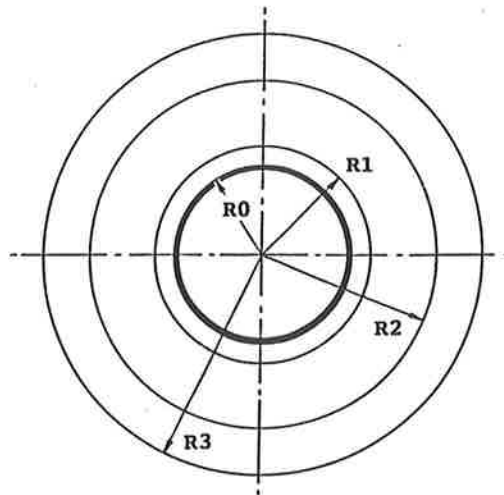
Fig.B.3 - Division of circular-plate fin into
three fin elements.

B.3 AVERAGE HEAT TRANSFER COEFFICIENT

Let

    At(e)   = total heat transfer area of fin element(e) - m²
    Ae(e,c) = enhanced heat transfer area of fin el.(e)   - m²
    Al(e,c) = area of developing laminar flow for el.(e)   - m²
    An(e,c) = normal heat transfer area of fin element(e) - m²
    Ar(e,c) = reduced heat transfer area of fin el.(e)   - m²

where (e) is defined in Table B.3-1 and (c) is defined in Table B.3-2.

e	Fin Element
1	inner fin element
2	intermediate fin element
3	outer fin element

Table B.3-1 - Fin element identification

c	Configuration and Row Identification	
1	first row	- staggered arrangement
2	first row	- in-line arrangement
3	intermediate rows	- staggered arrangement
4	intermediate rows	- in-line arrangement
5	last row	- staggered arrangement
6	last row	- in-line arrangement

Table B.3-2 - Tube configuration and row identification

The enhanced zone fractions of fin element areas to which the vortex enhancement factor applies can be derived for
e = 1 to 3, and c = 1 to 6 as

   Ae(e,c) / At(e) ,

and that for the developing laminar flow enhancement as

   Al(e,c) / At(e) .

The fraction for normal heat transfer is

   An(e,c) / At(e) ,

and that for reduced heat transfer is

   Ar(e,c) / At(e) .

The average heat transfer enhancement factor for each element can then be expressed as

$$Km(e,c) = \frac{Ke \cdot Ae(e,c) + Kl(e,c) \cdot Al(e,c) + An(e,c) + Kr \cdot Ar(e,c)}{At(e)}$$

(B.3-1)

B.4   DEVELOPING LAMINAR FLOW ENHANCEMENT

The developing laminar flow enhancement for flow between parallel plates has been derived in Sect.A.2.4 of Appendix A and is expressed by equations (A.2-16), (A.2-17) and (A.2-11) as a function of x, Dh, Re, and Pr, where

   x = thermal entry length   - m
   Dh = hydraulic diameter = 2·s - m .

Consider the semi-circular area of the equivalent circular fin, as shown in Fig.B.4, for developing laminar flow enhancement, then the combined semi-circular areas of the intermediate and outer elements are

   π (R3² - R1²) / 2   m² .

Let the equivalent thermal entry length for the continuous plate fin be x_{23} m.   Then the equivalent area for the
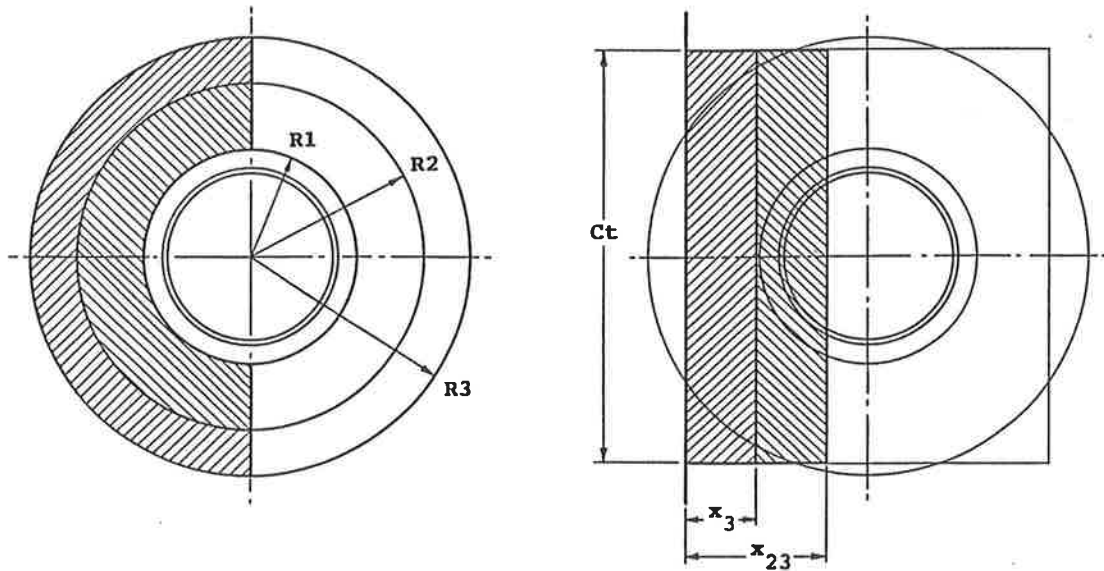
Fig.B.4 - Definition of thermal entry lengths.

continuous plate is

$$x_{23} \cdot Ct / 1000 \qquad m^2 \; ,$$

and the thermal entry length for the intermediate and outer elements combined is

$$x_{23} = 1000 \cdot \pi \, (R3^2 - R1^2) / (2 \cdot Ct) \qquad m \; . \qquad (B.4-1)$$

Now the average developing laminar flow enhancement for the two fin elements is

$$Kl_{23} = \emptyset(x_{23}, \; Dh, \; Re, \; Pr) \qquad\qquad (B.4-2)$$

as defined by equations (A.2-11, 16, 17).

The area of laminar flow enhancement for the outer element (both sides)

$$Al(3,c) = \pi \, (R3^2 - R2^2) \qquad m^2 \qquad\qquad (B.4-3)$$

where c = 1 or 2 .

The equivalent area on the continuous plate fin is

$$x_3 \cdot Ct / 1000 \qquad m^2 \; .$$

Thus for c = 1 or 2

$$x_3 = 1000 \cdot Al(3,c) / (2 \cdot Ct) \qquad m \; , \qquad\qquad (B.4-4)$$

and for c = 1 or 2

$$Kl(3,c) = \emptyset(x_3, Dh, Re, Pr) .$$ (B.4-5)

Also for c = 1 or 2

$$Al(2,c) = \pi (R2^2 - R1^2) \quad m^2$$ (B.4-6)

and for all other values of e and c

$$Al(e,c) = 0 .$$ (B.4-7)

The mean enhancement factor for the two outer elements com-
bined can be expressed in terms of the enhancement factors
for each of these elements as

$$Kl_{23} \cdot (Al(2,c)+Al(3,c)) = Kl(2) \cdot Al(2,c) + Kl(3) \cdot Al(3,c)$$

therefore for c = 1 or 2

$$Kl(2,c) = \frac{Kl_{23} \cdot (Al(2,c)+Al(3,c)) - Kl(3) \cdot Al(3,c)}{Al(2,c)} .$$ (B.4-8)

B.5 INNER FIN ELEMENT HEAT TRANSFER AREAS

B.5.1 Total Heat Transfer Area

Referring to Fig.B.3 the area of one side of the inner fin
element is

$$a1 = \pi \cdot (R1^2 - R0^2) \quad m^2 .$$

The tube outside area is subjected to the same vortex and
hence the same heat transfer coefficients and enhancement
factors could be applied.   For the space between the fins
's' the total heat transfer area is

$$a2 = 2 \cdot \pi \cdot R0 \cdot s \quad m^2 ,$$

and the total heat transfer area for the inner element is
then

$$At(1) = 2 \cdot a1 + a2$$

$$= 2 \cdot \pi \cdot (R1^2-R0^2) + 2 \cdot \pi \cdot R0 \cdot s ,$$

or

$$At(1) = 2 \cdot \pi \cdot (R1^2 - R0^2 + R0 \cdot s) \quad m^2 .$$ (B.5-1)

B.5.2 Staggered and First Row In-Line Arrangements
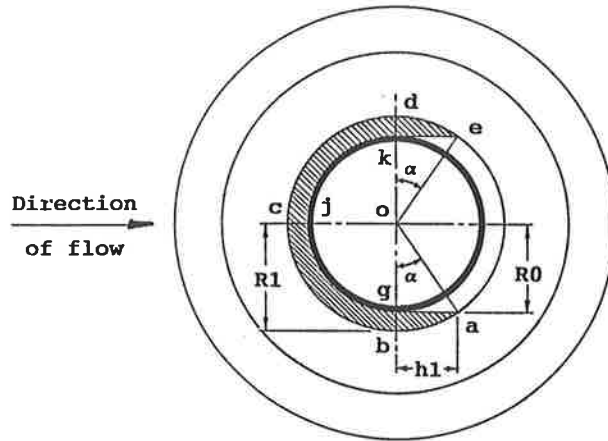
Fig.B.5 – Enhanced heat transfer for inner fin element in staggered tube arrangement or first row in-line arrangement.

In Fig.B.5

$$h1 = \sqrt{(R1^2 - R0^2)} \qquad\qquad (B.5-2)$$

and

$$\tan \alpha = h1/R0 \ ,$$

hence

$$\alpha = atn(h1/R0) \quad \text{radians} \ . \qquad\qquad (B.5-3)$$

Let a3 = Area of quadrant 'abcde' in Fig.B.4, then the angle for that quadrant = $2 \cdot \alpha + \pi$ radians and

$$a3 = (2 \cdot \alpha + \pi)/2 \cdot R1^2 \ .$$

Let a4 = Area for semicircle 'gjk' combined with triangles 'oag' and 'oke', then

$$a4 = \pi/2 \cdot R0^2 + h1 \cdot R0$$
$$= R0 \cdot (\pi/2 \cdot R0 + h1) \ .$$

Let Aef be the area of enhanced region on the fin element (both sides), then

$$Aef = 2 \cdot (a3 - a4)$$
$$= 2 \cdot ((2 \cdot \alpha + \pi)/2 \cdot R1^2 - R0 \cdot (\pi/2 \cdot R0 + h1)) \ ,$$

or

$$Aef = (2 \cdot \alpha + \pi) \cdot R1^2 - R0 \cdot (\pi \cdot R0 + 2 \cdot h1) \ . \qquad (B.5-4)$$

The primary area (tube surface) subjected to heat transfer enhancement is

$$Aet = \pi \cdot R0 \cdot s .$$ (B.5-5)

The total area of heat transfer enhancement then becomes

$$Ae(1,1) = Aef + Aet .$$ (B.5-6)

Also

$$Ae(1,5) = Ae(1,3) = Ae(1,2) = Ae(1,1) .$$ (B.5-7)

The inner fin element, element(1), does not have zones for normal heat transfer hence for m = 1 to 6

$$An(1,m) = 0 .$$ (B.5-8)

B.5.3 In-Line Arrangement for Second and Subsequent Rows
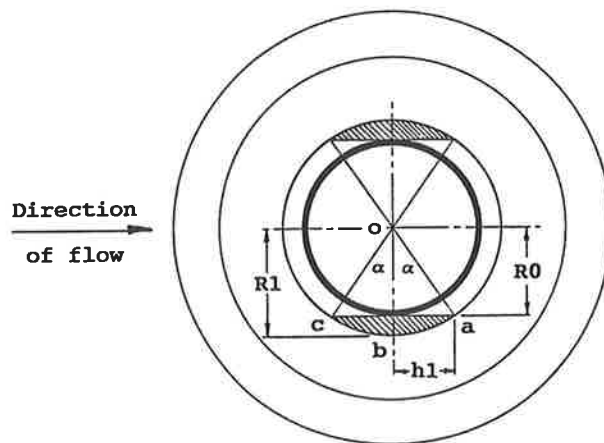
Fig.B.6 - Enhanced heat transfer for inner fin element. Second and subsequent rows in In-line tube arrangements.

In fig.B.6 the area of quadrant

$$'abc' = \alpha \cdot R1^2 ,$$

and area of triangle

$$'aoc' = h1 \cdot R0 ,$$

so that area of segment 'abc' becomes

$$Aseg = \alpha \cdot R1^2 - h1 \cdot R0 .$$ (B.5-9)

The enhanced area on the primary surface will be negligible, ie.

$$ac = 0$$

and the total area for heat transfer enhancement becomes

$$Ae(1,4) = 4 \cdot Aseg$$

or

$$Ae(1,4) = 4 \cdot (\alpha \cdot R1^2 - h1 \cdot R0) \;. \qquad (B.5-10)$$

Also

$$Ae(1,6) = Ae(1,4) \;. \qquad (B.5-11)$$

B.6 INTERMEDIATE FIN ELEMENT HEAT TRANSFER AREAS

B.6.1 Total Heat Transfer Area

The total area (both sides) for the intermediate fin element is

$$At(2) = 2 \cdot \pi \cdot (R2^2 - R1^2) \qquad m^2 \;. \qquad (B.6-1)$$

B.6.2 Staggered Tube Arrangement - all rows except last
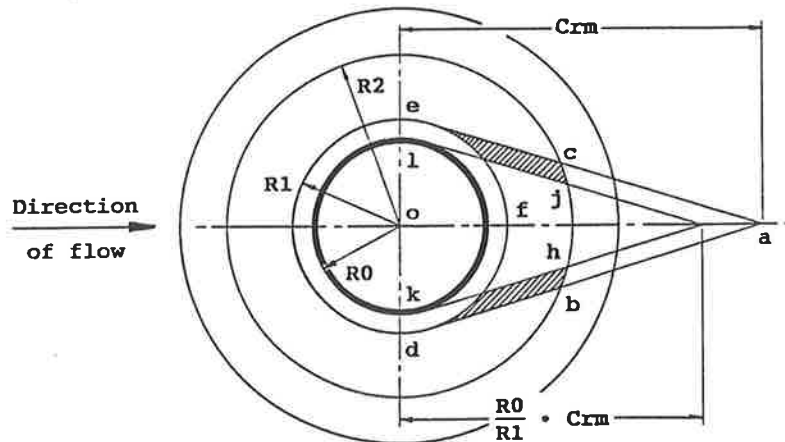
Fig.B.7 - *Enhanced heat transfer for intermediate fin element in a staggered tube arrangement.*

In fig.B.7, length

$$de = 2 \cdot R1 \;.$$

The ratio of triangles

$$abc/ade \approx (Crm-R2)/Crm \approx 1 - R2/Crm \ ,$$

where

$$Crm = Cr/1000 \ , \tag{B.6-2}$$

and distance

$$bc \approx (1 - R2/Crm) \cdot 2 \cdot R1 \ .$$

Therefore

$$de - bc \approx 2 \cdot R1 - (1 - R2/Crm) \cdot 2 \cdot R1$$
$$\approx 2 \cdot R1 \cdot R2 \ / \ Crm \ ,$$

$$\text{Area 'cbde'} \approx (2 \cdot R1 \cdot R2) - ((de-bc)/2) \cdot R2$$
$$\approx (2 \cdot R1 \cdot R2) - (R1 \cdot R2^2 \ / \ Crm)$$
$$\approx (2 - R2/Crm) \cdot (R1 \cdot R2) \ ,$$

Area of semi-circle with radius R1 $= (\pi/2) \cdot R1^2$,
and
area enclosed by R2 $= \pi \cdot R2^2$.

Area of normal heat transfer (one side of fin only)

$$= \text{circle R2} - \text{semicircle R1} - \text{'cbde'}$$
$$= \pi \cdot R2^2 - (\pi/2) \cdot R1^2 - (2-R2/Crm) \cdot R1 \cdot R2 \ .$$

The total area for normal heat transfer (both sides of fin)

$$An(2,3) = 2 \cdot \pi \cdot R2^2 - \pi \cdot R1^2 - 2 \cdot (2-R2/Crm) \cdot R1 \cdot R2 \ . \tag{B.6-3}$$

Area of enhanced region may be approximated as

$$Ae(2,3) \approx 4 \cdot (yv \cdot R2) - 2 \cdot \text{area Aseg} \ ,$$

where area Aseg is defined by Eq.(B.5-9) as

$$Aseg = \alpha \cdot R1^2 - h1 \cdot R0 \ ,$$

hence

$$Ae(2,3) \approx 4 \cdot yv \cdot R2 - 2 \cdot (\alpha \cdot R1^2 - h1 \cdot R0) \ . \tag{B.6-4}$$

Also

$$An(2,1) = An(2,3) - Al(2,1) \ , \tag{B.6-5}$$

and

$$Ae(2,1) = Ae(2,3) \ . \tag{B.6-6}$$

B.6.3 First Row In-Line and Last Row Staggered Arrangements
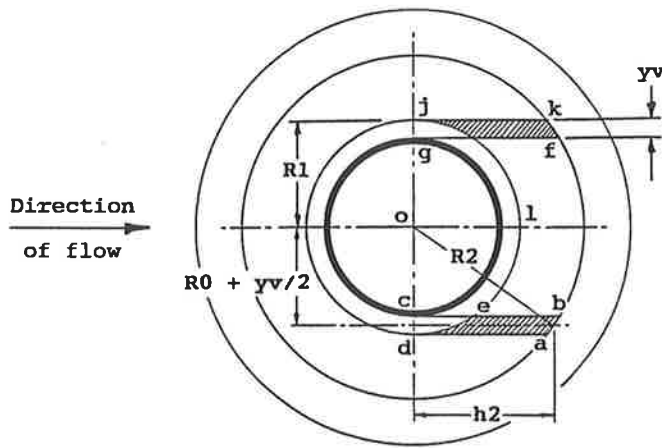
Fig.B.8 - Enhanced heat transfer for intermediate fin element in first row in-line tube arrangement.

In fig.B.8,

$$h2 = \sqrt{(R2^2 - (R0+yv/2)^2)} ,\qquad (B.6-7)$$

and area

$$abcd = yv \cdot h2 .$$

From Eq.(B.5-9), area

$$dce = (\alpha \cdot R1^2 - h1 \cdot R0) / 2 .$$

Therefore total enhanced area (both sides of fin element)

$$Ae(2,5) = 4 \cdot yv \cdot h2 - 2 \cdot Aseg .\qquad (B.6-8)$$

Length

$$ad = \sqrt{(R2^2 - R1^2)}$$

so that area

$$'adjk' \approx 2 \cdot R1 \cdot (R2 + \sqrt{(R2^2-R1^2)}) / 2$$
$$\approx R1 \cdot (R2 + \sqrt{(R2^2 - R1^2)}) .$$

Area of semi-circle

$$'dlj' = \pi/2 \cdot R1^2 ,$$

and

$$\text{Area enclosed by R2} = \pi \cdot R2^2 .$$

Then total area for normal heat transfer (both sides of fin)

$$An(2,5) = 2 \cdot \{\pi \cdot R2^2 - R1 \cdot (R2 + \sqrt{(R2^2 - R1^2)}) - \pi \cdot R1^2/2\} \ ,$$

or

$$An(2,5) = 2 \cdot \pi \cdot R2^2 - 2 \cdot R1 \cdot (R2 + \sqrt{(R2^2 - R1^2)}) - \pi \cdot R1^2. \quad (B.6-9)$$

Also

$$Ae(2,2) = Ae(2,5) \ , \qquad\qquad\qquad (B.6-10)$$

and

$$An(2,2) = An(2,5) - Al(2,2) \ . \qquad\qquad (B.6-11)$$

B.6.4   Second and Subsequent Row – In-Line Arrangement
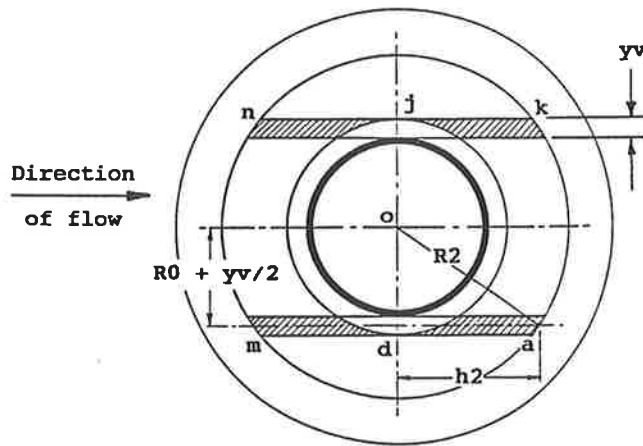
Fig.B.9 – Enhanced heat transfer for intermediate fin element in second and subsequent rows of an in-line tube arrangement.

Fig.B.9 shows double the enhanced area of that derived by Eq.(B.6-8) for Fig.B.8, hence

$$Ae(2,4) = 8 \cdot yv \cdot h2 - 4 \cdot (\alpha \cdot R1^2 - h1 \cdot R0) \ . \qquad (B.6-12)$$

Area

'amnk' = 2 · area 'adjk' in fig.B.8

$$\approx 2 \cdot R1 \cdot (R2 + \sqrt{(R2^2 - R1^2)}) \ .$$

Area enclosed by R2 = $\pi \cdot R2^2$.

Then area for normal heat transfer (both sides of fin)

$$An(2,4) = 2 \cdot \pi \cdot R2^2 - 4 \cdot R1 \cdot (R2 + \sqrt{(R2^2 - R1^2)}) \ . \qquad (B.6-13)$$

Also

$$Ae(2,6) = Ae(2,4) ,$$
(B.6-14)

and

$$An(2,6) = An(2,4) .$$
(B.6-15)

B.7   OUTER FIN ELEMENT HEAT TRANSFER AREAS

B.7.1   Total Heat Transfer Area

The total area for the outer fin element (both sides) is

$$At(3) = 2 \cdot \pi \cdot (R3^2 - R2^2) \quad m^2 .$$
(B.7-1)

B.7.2   Staggered Tube Arrangement – all rows except last
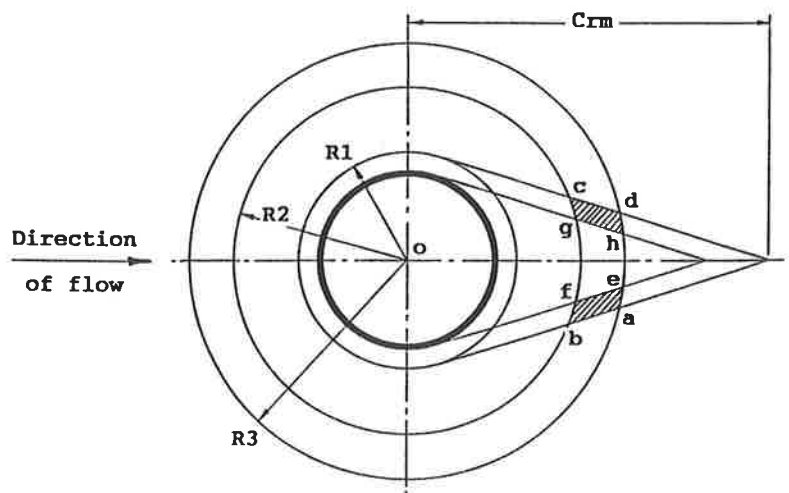
*Fig.B.10 – Enhanced heat transfer for outer fin
element in staggered tube arrangement.*

In fig.B.10,

'bc' $\approx$ 2 $\cdot$ R1 $\cdot$ (Crm-R2)/Crm ,

'ad' $\approx$ 2 $\cdot$ R1 $\cdot$ (Crm-R3)/Crm .

Therefore area

Aabcd $\approx$ (R3-R2) $\cdot$ (ad + bc) / 2

Aabcd $\approx$ R1 $\cdot$ (R3-R2) $\cdot$ (2$\cdot$Crm-R2-R3) / Crm ,
(B.7-2)

and

$$An(3,3) = At(3) - 2 \cdot Aabcd .$$
(B.7-3)

Also

$$An(3,1) = An(3,3) - Al(3,1) .$$

Area

$$'abfe' \approx (R3-R2) \cdot \sqrt{(Crm^2-R1^2)}/Crm \cdot yv ,$$

and

$$Ae(3,3) \approx 4 \cdot yv \cdot (R3-R2) \cdot \sqrt{(Crm^2-R1^2)}/Crm .$$

(B.7-5)

Also

$$Ae(3,1) = Ae(3,3) .$$

(B.7-6)

B.7.3 Last Row Staggered and First Row In-Line Arrangement
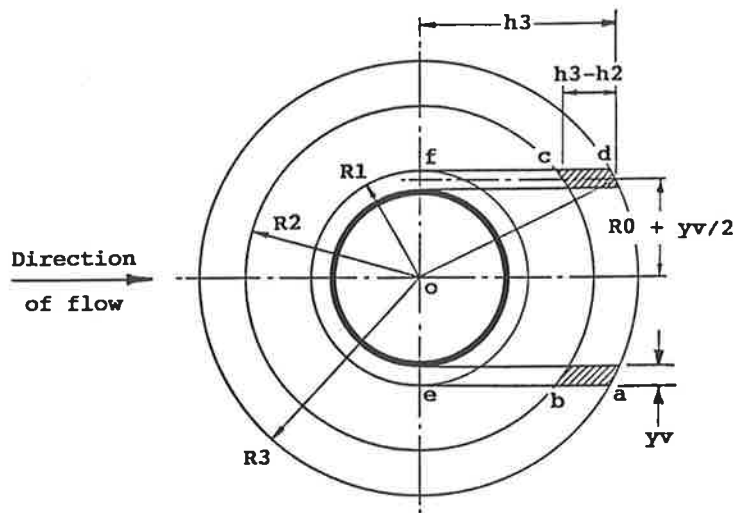
Fig.B.11 – *Enhanced heat transfer for outer fin element in first row in-line, or last row staggered tube arrangement.*

Length 'df' in fig.B.11 is found as

$$df = \sqrt{(R3^2-R1^2)} ,$$

then area

$$Aaefd \approx (df + R3)/2 \cdot 2 \cdot R1 ,$$

or

$$Aaefd \approx R1 \cdot (\sqrt{(R3^2-R1^2)} + R3) .$$

(B.7-7)

Length

$$cf = \sqrt{(R2^2-R1^2)} ,$$

and area

$$A_{befc} \approx (cf + R2)/2 \cdot 2 \cdot R1 ,$$

or

$$A_{befc} \approx R1 \cdot (\sqrt{(R2^2 - R1^2)} + R2) , \qquad (B.7-8)$$

hence area

$$abcd = A_{aefd} - A_{befc} , \qquad (B.7-9)$$

and

$$An(3,5) = At(3) - 2 \cdot (A_{aefd} - A_{befc}) . \qquad (B.7-10)$$

Also

$$An(3,2) = An(3,5) - Al(3,2) . \qquad (B.7-11)$$

In fig.B.11,

$$h3 = \sqrt{(R3^2 - (R0 + yv/2)^2)} . \qquad (B.7-12)$$

h2 is defined by Eq.(B.6-7) so that

$$cd = h3 - h2 ,$$

and

$$Ae(3,5) = 4 \cdot (h3 - h2) \cdot yv . \qquad (B.7-13)$$

Also

$$Ae(3,2) = Ae(3,5) . \qquad (B.7-14)$$

B.7.4   Second and Subsequent Rows - In-Line Arrangement
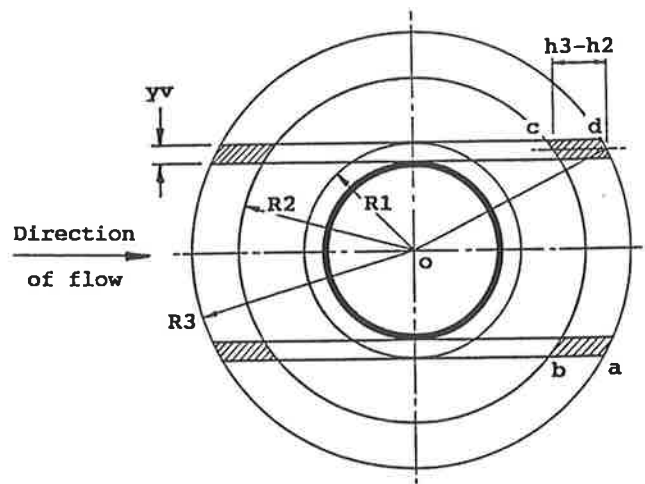
Fig.B.12 - *Enhanced heat transfer for outer fin element in second and subsequent rows of in-line tube arrangements.*

In Section B.7.3, area 'abcd' was defined by Eq.(B.7-9) as

$$abcd = Aaefd - Abefc ,$$

therefore

$$An(3,4) = At(3) - 4 \cdot (Aaefd-Abefc) . \qquad (B.7-15)$$

Also

$$An(3,6) = An(3,4) , \qquad (B.7-16)$$

$$Ae(3,4) = 8 \cdot (h3-h2) \cdot (R1-R0) , \qquad (B.7-17)$$

and

$$Ae(3,6) = Ae(3,4) . \qquad (B.7-18)$$

B.8 REDUCED HEAT TRANSFER AREAS

In Sections B.5, B.6, and B.7 the total heat transfer areas
At(e), the normal heat transfer areas An(e,c), the developing
laminar flow areas Al(e,c), and the enhanced heat transfer
areas Ae(e,c) have been defined.   From this information the
areas of reduced heat transfer are defined for e = 1 to 3,
and c = 1 to 6, as

$$Ar(e,c) = At(e) - An(e,c) - Al(e,c) - Ae(e,c) . \qquad (B.8-1)$$

B.9 SYMBOLS USED IN APPENDIX B

a1, a2	areas defined in Sect. B.5.1	- m²
a3, a4	areas defined in Sect. B.5.2	- m²
Ae(e,c)	enhanced heat transfer area (e,c)	- m²
Al(e,c)	area of developing laminar flow for (e,c)	- m²
An(e,c)	normal heat transfer area (e,c)	- m²
Ar(e,c)	reduced heat transfer area (e,c)	- m²
At(e)	total heat transfer area for fin el.(e)	- m²
Cr	row spacing	- mm
Crm	row spacing	- m
Ct	tube spacing	- mm
Dh	hydraulic diameter	- m
Do	tube outside diameter	- mm
h1	dimension in Fig.B.5	- m
h2	dimension in Fig.B.8	- m
h3	dimension in Fig.B.11	- m
Ke	vortex enhancement factor	
Kl_{23}	average dev.lam.flow enhancement for 2&3	
Kl(e,c)	dev.lam.flow enhancement for element(e,c)	
Km(e,c)	mean heat tran. enhancement for el.(e,c)	
Kr	reduced heat transfer factor	
Pr	Prandtl number	
R0	tube outside radius plus fin thickness	- m
R1	outer boundary rad. for inner fin element	- m
R2	outer boundary rad. for interm. fin el.	- m
R3	outer radius of equivalent circular fin	- m
Re	Reynolds number	
s	space between fins = Channel height	- m
x	thermal entry length	- m
x_{23}	thermal entry length for intermediate and outer fin elements.	- m
x_3	thermal entry length for outer element	- m
xf	fin thickness	- mm
xl	distance from leading edge of plate fin	- m
xp	tube wall thickness	- mm
yv	width of vortex	- m

Greek Symbols

α	angle defined in Figs.B.5, B.6	- radians

Array Dimensions

c	tube configuration number
e	fin element identification,
	1 = inner element
	2 = intermediate fin element
	3 = outer fin element

APPENDIX C

CORRELATION OF AIR SIDE HEAT TRANSFER WITH TEST DATA

CONTENTS

C.1 GENERAL

Four separate areas of heat transfer have been identified in
Appendix B as:

- Fully developed laminar flow (normal) heat transfer
- Developing laminar flow heat transfer enhancement
- Vortex enhanced heat transfer
- Reduced heat transfer

The fully developed laminar flow heat transfer is character-
ised by a Nusselt number which is determined by the direction
of heat transfer, and the shape and aspect ratio of the duct
conducting the flow, but independent upon the Reynolds number
within the laminar flow region. Gilbert[14] suggested that
the fully developed laminar flow behaves like that found in
channels. Fig.C.1 shows the velocity profiles for laminar
flow in channels or rectangular tubes. The effect of these
velocity profiles is that the local heat transfer coeffi-
cients vary around the periphery and approach zero at the
corners. Hence the Nusselt number dependence upon aspect
ratio. However, in the case of flow over plate fins the flow
profiles are bounded by vortices which enhance heat transfer
at the extremities rather than the reduction found in rect-
angular tubes. At this stage it is still uncertain whether
the fully developed laminar flow Nusselt number should be
based upon flow through infinite parallel plates or upon flow
through rectangular channels bounded by the fins and
vortices.
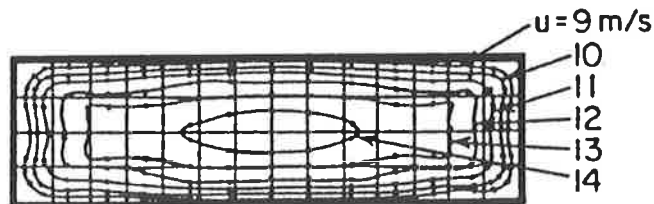
Fig.C.1 - Velocity profiles in a rectangular duct.
(Rohsenow[31])

When the air stream approaches the leading edges of the plate
fins it takes some distance for the flow characteristic to
develop. This developing laminar flow region is subjected
to heat transfer enhancement and has been well defined in
Appendix A as a function of channel dimensions, Reynolds and
Prandtl numbers. Since this region is not as yet influenced
by the tubes, the leading edge heat transfer enhancement will
be calculated using the hydraulic diameter and Reynolds
number for infinite parallel plates.

It has been shown[14] that the vortices around the tubes and
trailing along the fins produce significant heat transfer
enhancement. However, the effect has not as yet been
quantified and neither has the vortex width been defined.

Saboya et al[32,33,34] have shown that the areas shaded by the tubes have considerably reduced heat transfer coefficients. For the analysis described in this Appendix these heat transfer coefficients have been neglected.

Thus at this stage the fully developed channel flow heat transfer coefficients, the vortex enhancement factors, and the vortex widths still need to be defined. Tests have been conducted and analysed for coils with different fin spacings over a range of face velocities in an attempt to resolve these parameters.

Heat transfer from a unit area of dry coil surface to or from an air stream is a function of local temperature difference and heat transfer coefficient. It is the aim of the analysis described in this Appendix to derive the heat transfer coefficients for each of the above mentioned areas. Hence the driving temperature difference must be known in each case.

Therefore this part of the analysis was restricted to single row coils in order to enable the prediction of the local coil surface temperatures.

C.2 TESTS ON 6 FINS PER INCH COIL

C.2.1 Physical Parameters

Heat transfer data for a 1-row coil was extracted from an experimental program conducted by Sekhar[37]. The tests employed a coil manufactured by F.Muller and Sons Pty.Ltd. and the relevant physical data were observed[37] as shown in Table C.1

Coil height,	Clht	457	mm
Coil size parallel to tubes,	Clwi	760	mm
Tube outside diameter,	Dp	16.3	mm
Tube wall thickness,	xp	0.65	mm
Fin thickness,	xf	0.19	mm
Fin pitch,	FP	4.110	mm
Tube spacing within coil row,	Ct	38.10	mm
Fin depth,	Cr	35.05	mm
Number of rows,	Nrow%	1	
Number of fins,	Nfin%	180	
Total number of tubes per row,	Nt%	12	
Number of parallel circuits,	Ncirc%	2	
Number of tubes fed,	Npt%	6	

Table C.1 - Physical dimensions of 6fpi 1-row coil.
    (Sekhar[37])

For the heat transfer analysis the following parameters were derived from the data in Table C.1 and summarised in Table C.2.

Coil face area,

$$Af = Clht \cdot Clwi/1.E+6 = 457 \cdot 760/1.E+6 = 0.347 \text{ m}^2 .$$

Tube inside diameter,

$$Di = Dp - 2 \cdot xp = 16.3 - 2 \cdot 0.65 = 15.0 \text{ mm} .$$

The fins are flared around the tube outside surface so that the effective tube outside diameter,

$$Do = Dp + 2 \cdot xf = 16.3 + 2 \cdot 0.19 = 16.68 \text{ mm} .$$

The space between the fins,

$$s = FP - xf = 4.11 - .19 = 3.92 \text{ mm} \quad \text{or} \quad .00392 \text{ m} .$$

The space between the tubes,

$$a = Ct - Do = 38.1 - 16.68 = 21.42 \text{ mm} \quad \text{or} \quad .02142 \text{ m} .$$

The equivalent circular plate fin radius,

$$R3 = \sqrt{(Cr \cdot Ct/\pi)} = \sqrt{(35.05 \cdot 38.1/\pi)} = 20.62 \text{ mm or } .02062 \text{ m} .$$

The internal heat transfer area,

$$Api = \frac{\pi \cdot Di \cdot Nt \cdot Clwi}{1.0E+06} = \frac{\pi \cdot 15.0 \cdot 12 \cdot 760}{1.0E+06} = .4298 \text{ m}^2 .$$

Primary heat transfer area,

$$Aprim = \pi \cdot Do \cdot Nt\% \cdot (Clwi - Nfin\% \cdot xf)/1.0E+06$$
$$= \pi \cdot 16.68 \cdot 12 \cdot (760 - 180 \cdot .19)/1.0E+06 = .4564 \text{ m}^2 .$$

Face area,	Af	0.347	m²
Tube inside diameter,	Di	15.0	mm
Effective tube outside dia.,	Do	16.68	mm
Space between fins	s	3.92	mm
Space between tubes	a	21.42	mm
Equiv.circ.plate fin radius	R3	20.62	mm
Internal heat transfer area,	Api	0.4298	m²
Primary heat transfer area,	Aprim	0.4564	m²
Fin heat transfer area,	Afin	4.8254	m²
Total area for water flow,	Afw	.001060	m²

Table C.2 - Derived physical parameters for 6fpi 1-row coil.

Fin heat transfer area,

$$Afin = 2 \cdot (Cr \cdot Ct - \pi \cdot Do^2/4) \cdot Nfin\% \cdot Nt\% / 1.0E+06$$
$$= 2 \cdot (35.05 \cdot 38.1 - \pi \cdot 16.68^2/4) \cdot 180 \cdot 12 / 1.0E+06$$
$$= 4.8250 \ m^2 \ .$$

Total area for water flow,

$$Afw = \pi \cdot Di^2 \cdot Npt\% / 4 \cdot 0E+06$$
$$= \pi \cdot (15.0)^2 \cdot 6 / 4 \cdot 0E+06 = 0.001060 \ m^2 \ .$$

C.2.2 Dry Coil Tests at Various Air Flow Rates

This stage of the analysis was restricted to dry coil operation only with the aim of correlating the observed heat transfer rates with the proposed method of establishing heat transfer coefficients and enhancement factors.

The air entering and leaving conditions, the air flow rates, and the chilled water flow rates and temperatures were recorded by Sekhar[37] as shown in Table C.3.

Test Code		D2904	D2892	D2891	D2901	D2902	D2903
Atm. pressure, Pat	kPa	101.456	101.118	101.118	101.456	101.456	101.456
Entering db Temp., t	°C	54.90	44.63	50.70	48.70	34.30	29.80
Entering dew point,	°C	11.90	13.75	19.20	9.50	4.75	3.40
Leaving db Temp.	°C	30.65	31.00	39.15	39.65	28.07	25.00
Leaving dew point	°C	11.90	13.75	19.20	9.50	4.75	3.40
Air flow rate, Fa	l/s	141.0	278.0	435.0	570.0	738.0	952.0
Air face velocity	m/s	0.406	0.801	1.254	1.643	2.127	2.744
Ent.water temp.,Tr	°C	14.9	11.3	17.15	18.74	8.74	7.6
Water flow rate, Mw	l/s	1.78	1.57	1.57	1.57	1.57	1.57

Table C.3 - Summary of dry tests for 6fpi 1-row coil over a range of air flow rates. (Sekhar[37])

C.2.3 Analysis of Test Results

Sub-program AIRGPROP from library GASPARMS[42] was used to compute the thermal conductivities and viscosities for air as a function of temperature.

The psychrometric program[43] PSYCHRO, which is based on the methods and sub-programs described in Section 6.0, was used to compute the air enthalpies and the specific volumes of the air entering the coil for the six tests listed.

The sensible heat flow rate was then be established as

$$Qa = \frac{dH \cdot Fa}{1000 \cdot v} \quad kW \; . \tag{C.2-1}$$

Sub-program H2OLPROP in library GASPARMS[42] gives the viscosity, thermal conductivity, specific heat, and Prandtl number for liquid water as a function of its temperature.

The specific volume for water, vf can be extracted from steam tables and as shown in Table C.4 it has negligible temperature dependence for the range under consideration. Hence the records of water flow rates expressed in l/s can also be read as mass flow rates in kg/s. The water flow rates were chosen such that the water temperature rise would be minimal in an effort to obtain almost uniform coil temperature. Thus any attempt to calculate the heat transfer at the water side would not be accurate. Thus, rather than measuring the water temperature rise, it was calculated from the sensible heat flow at the air side of the coil. The water temperature rise can be expressed as:

$$dTw = \frac{Qa}{Mw \cdot Cp} \quad K \; , \tag{C.2-2}$$

and the water velocity as

$$Vw = Mw / 1000 / Afw \quad m/s \; . \tag{C.2-3}$$

The water mass flow rate is,

$$Gw = Mw / Afw \quad kg/m^2s \tag{C.2-4}$$

or

$$Gw = Vw \cdot 1000 \quad kg/m^2s \; . \tag{C.2-5}$$

The Reynolds number is defined as

$$Re = Dh \cdot G / \mu \; ,$$

Thus

$$Re = 15.0 \cdot Gw / (\mu \cdot 1000) \; . \tag{C.2-6}$$

The Nusselt number for fully developed turbulent flow is given by Eq.(A.3-10), and Eq.(A.3-16) gives the heat transfer enhancement for developing turbulent flow.

The internal heat transfer coefficient can be derived from Eq.(A.2-1) as

$$hi = \frac{Nu \cdot k}{Dh} \quad W/m^2K \; , \tag{C.2-7}$$

Since

$$Qa \cdot 1000 = hi \cdot Api \cdot \delta T \; ,$$

the temperature gradient across the internal film can be established as

$$dTi = \frac{Qa \cdot 1000}{hi \cdot Api} \; K \; , \qquad\qquad (C.2-8)$$

and the primary surface temperature at any point can then be established as the water temperature at that point plus the temperature gradient across the internal film. The temperature gradient across the tube wall can be neglected. Thus the primary coil surface temperature ranges from Tr+dTi to Tr+dTi+dTw.

For counterflow the mean temperature difference between air and water is given as

$$dTm = \frac{(t1 - tr2) - (t2 - tr1)}{\ln\left[\dfrac{t1 - tr2}{t2 - tr1}\right]} \; . \qquad\qquad (C.2-9)$$

Threlkeld[40] has shown that this equation may also be applied to cross flow heat transfer problems. The aim of this analysis is to derive the external heat transfer coefficient ho, therefore the mean temperature difference with respect to the coil external surface temperature is of greater interest. Since the coil surface temperature is almost uniform the heat transfer across the face area is also nearly uniform so that the internal fluid temperatures in Eq.(C.2-9) may be replaced by the surface temperatures

tr1 = Tr+dTi , and

tr2 = Tr+dTi+dTw .

Eq.(C.2-9) may be generalised as

$$dTm = \frac{ABS(t1 - tr2) - ABS(t2 - tr1)}{\ln\left[\dfrac{ABS(t1 - tr2)}{ABS(t2 - tr1)}\right]} \qquad\qquad (C.2-10)$$

to make it valid for heating as well as for cooling.

In a heat transfer process the fins have a significant temperature gradient in a radial direction. This will reduce the rate of heat transfer. In order to establish the mean heat transfer coefficient this temperature gradient must be taken into account. For the purpose of this analysis the fin efficiency of Gardner[10] has been used.

The fin efficiency Ø is defined[40] as

$$\text{Ø} = \frac{\text{mean fin temp. - fluid temp.}}{\text{temp. at fin base - fluid temp.}} \qquad\qquad (C.2-11)$$

Test Code	D2904	D2892	D2891	D2901	D2902	D2903
Entering db Temp., t °C	54.90	44.63	50.70	48.70	34.30	29.80
Thermal cond. E-02 W/mK	2.816	2.743	2.786	2.772	2.669	2.636
Viscosity, μ E-05 Pa s	1.980	1.933	1.961	1.952	1.885	1.864
Entering enth. kJ/kg	77.88	70.39	87.47	68.20	48.17	42.36
Leaving enth. kJ/kg	53.09	56.44	75.54	58.93	41.84	37.49
Enth.diff., dH kJ/kg	24.79	13.95	11.93	9.27	6.33	4.87
Spec.volume, v cu.m/kg	0.941	0.916	0.940	0.922	0.877	0.864
Air flow rate, Fa l/s	141.0	278.0	435.0	570.0	738.0	952.0
Actual face vel. m/s	0.406	0.800	1.252	1.641	2.125	2.741
Air flow rate, Ma kg/s	0.150	0.303	0.463	0.618	0.842	1.102
Sensible heat, Qa kW	3.715	4.234	5.521	5.731	5.327	5.366
Ent.water temp.,Tr °C	14.9	11.3	17.15	18.74	8.74	7.6
Water flow rate, Mw l/s	1.78	1.57	1.57	1.57	1.57	1.57
Viscosity, μ E-03 Pa s	1.126	1.244	1.060	1.017	1.339	1.385
Therm.Cond., kw W/m K	0.5950	0.5890	0.5986	0.6011	0.5846	0.5827
Spec.Heat, Cpw kJ/kg K	4.189	4.193	4.186	4.185	4.198	4.199
Prandtl number, Pr(w)	7.925	8.854	7.415	7.083	9.614	9.983
Specific volume, l/kg	1.001	1.000	1.001	1.002	1.000	1.000
Water temp.rise, dTw K	0.498	0.643	0.840	0.872	0.808	0.814
Water velocity, Vw m/s	1.678	1.481	1.480	1.478	1.481	1.481
Reynolds No., Re(w)	22371	17859	20950	21831	16584	16033
Nusselt No., developed	170.77	148.24	157.30	159.78	144.28	142.51
Nusselt No., enhanced	171.24	150.04	157.35	159.78	146.84	145.40
Int.film res.E-04 m²K/W	1.472	1.697	1.573	1.566	1.747	1.771
Tube wall grad., dTi K	1.273	1.672	2.045	2.088	2.166	2.211
Mean prim.surf.t., tpo	16.422	13.294	19.615	21.264	11.310	10.218
driving dTm K	24.461	23.937	24.928	22.666	19.751	17.105

Table C.4 - Derived mean surface temperatures for 6fpi 1-row coil.

Gardner[10] evaluated the fin efficiencies for various extended surfaces as functions of fin dimension, fin conductivity, and fin surface heat transfer coefficient. Fig.C.2 shows the efficiencies for a circular-plate fin of uniform thickness in which

$$\emptyset = f \{ L \sqrt{(ho/(kf \cdot y))} \} , \qquad (C.2-12)$$

and where

kf = conductivity of fin material and for aluminium

kf = 203.0 W/m K ,

y = ½ fin thickness = .19/2 = .095 mm ,

L = R3 - R0 .
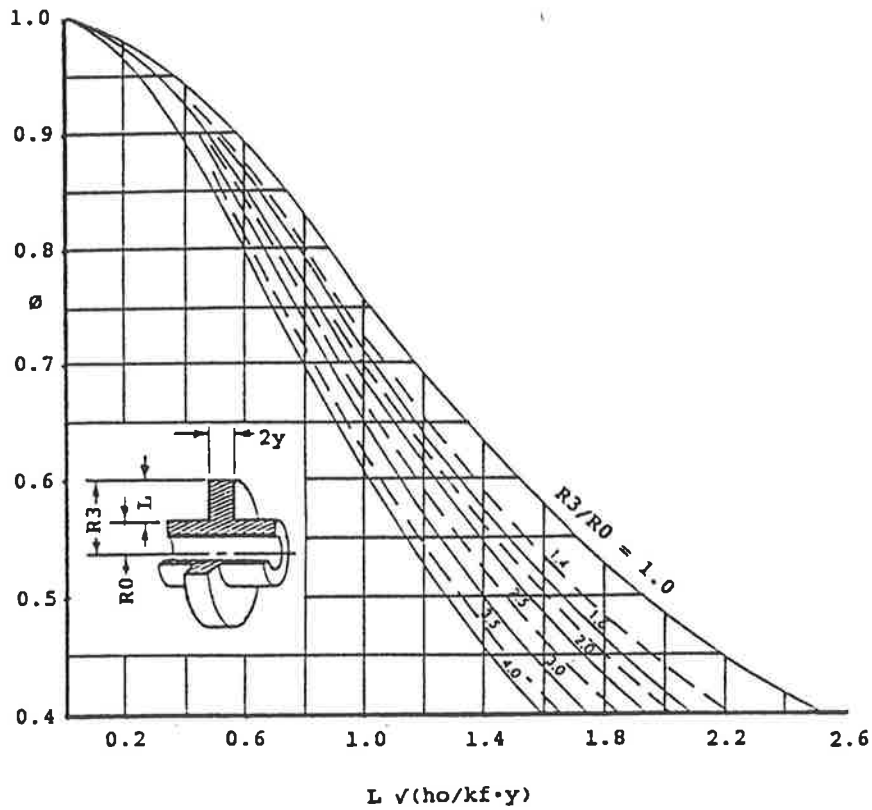
Fig.C.2 - Efficiency of Annular Fins of Constant
Thickness. (ARI Standard 410-81[2])

But

$$RO = Do/2 = 16.68/2 = 8.34 \text{ mm} .$$

Thus

$$L = 20.62 - 8.34 = 12.28 \text{ mm} .$$

Flow visualisation experiments conducted by Gilbert[14]
suggested that flow through finned tube heat exchangers
behaved as flow through channels with dimensions a and s mm.
However, these channels are not bounded by smooth walls but
by vortices as shown in Fig.B.1. The width of these vortices
were found to be approximately 10% of the tube outside dia-
meter. Thus the laminar flow between the fins is bounded by
the space s between the tubes reduced by the vortex width on
either side.

Gilbert[14] conducted his tests for relatively wide fin spacing.   It is not unreasonable to assume that the vortex width will also be influenced by the fin spacing when this is relatively small.

At this stage of the analysis it is still uncertain whether the heat transfer calculations should be based upon the Nusselt number for well developed laminar flow between infinite parallel plates or upon that for laminar flow within the rectangular area bounded by the fins and vortices.   Hence external heat transfer coefficients have been analysed for both cases and for vortex widths of

$$yv = 0.1 \cdot Do / 1000. \quad m \qquad\qquad (C.2\text{-}13)$$

and

$$yv = s / 2. \quad m \quad . \qquad\qquad (C.2\text{-}14)$$

C.2.4 Analysis for Infinite Parallel Plate Fins

Tables C.5 and C.6 show the results of the analysis for Eqs.(C.2-13) and (C.2-14) respectively using the laminar flow Nusselt number for infinite parallel plates.

For well developed laminar flow between infinite parallel plates, the Nusselt number for constant temperature is found from Table A.4 as

$$Nu(T)_\infty = 7.541 \ .$$

For infinite parallel plates spaced at $s = 3.92$ mm the hydraulic diameter

$$Dh = 2 \cdot 3.92 = 7.84 \text{ mm} = .00784 \text{ m} \ .$$

From Table C.4 the mean thermal conductivity for the six tests can be established as 2.737E-02 W/m K.   Re-arranging Eq.(A.2-1),

$$ho = \frac{Nu_\infty \cdot ka}{Dh} = \frac{7.541 \cdot 2.737E\text{-}02}{0.00784} = 26.33 \text{ W/m}^2\text{K} \ .$$

Thus the parameter

$$L \sqrt{(ho/(kf \cdot y))} = \frac{12.28}{1000.} \sqrt{(26.33/(203.0 \cdot .095E\text{-}03))} = .454 \ ,$$

and the fin ratio R3/R0 = 20.62/8.34 ≐ 2.472 .

From Fig.C.2, the fin efficiency ∅ = 0.90 .

The rate of heat transfer from the external coil surface is expressed as

Qa = ho (Aprim + Ø·Afin) dTm

= ho (.4564 + .9·4.825) dTm

= ho · 4.799 · dTm ,

so that

ho = Qa/(4.799·dTm) W/m²K ,

and the mean Nusselt number is then derived as

$$Num = \frac{Dh \cdot ho}{ka} = \frac{.00784 \cdot ho}{ka} .$$

The mean heat transfer enhancement can be simply expressed by the ratio Num/Nu∞, and the vortex enhancement factor Ke was then computed by iteration using Eq.(B.3-1) to match the

Test Code	D2904	D2892	D2891	D2901	D2902	D2903
Re (inf. par. plates)	179.1	371.4	558.5	750.2	1056	1399
Re (Do)	677.4	1406	2113	2839	3997	5296
Ext.heat tran.coef. ho	31.647	36.858	46.151	52.687	56.201	65.370
Thermal cond. E-02 W/mK	2.816	2.743	2.786	2.772	2.669	2.636
Mean Nusselt No., Num	8.811	10.535	12.987	14.901	16.509	19.442
Ratio Num/Nu∞	1.168	1.397	1.722	1.976	2.189	2.578
Vortex Enhancement Ke	3.220	4.364	6.235	7.682	8.682	11.076
Vortex Nusselt no. Nuv	24.28	32.91	47.02	57.93	65.47	83.52

Table C.5 - Derived heat transfer parameters for 6fpi 1-row coil dry tests over a range of face velocities, flow over infinite parallel plates and vortex width of Do/10.

Test Code	D2904	D2892	D2891	D2901	D2902	D2903
Re (inf. par. plates)	179.1	371.4	558.5	750.2	1056	1399
Re (Do)	677.4	1406	2113	2839	3997	5296
Ext.heat tran.coef. ho	31.647	36.858	46.151	52.687	56.201	65.370
Thermal cond. E-02 W/mK	2.816	2.743	2.786	2.772	2.669	2.636
Mean Nusselt No., Num	8.811	10.535	12.987	14.901	16.509	19.442
Ratio Num/Nu∞	1.168	1.397	1.722	1.976	2.189	2.578
Vortex Enhancement Ke	2.966	3.987	5.662	6.953	7.853	9.993
Vortex Nusselt no. Nuv	22.37	30.07	42.70	52.43	59.22	75.36

Table C.6 - Derived heat transfer parameters for 6fpi 1-row coil dry tests over a range of face velocities, flow over infinite parallel plates and vortex width of s/2.

ratio Num/Nu∞.   Now the vortex heat transfer can also be
expressed by a Nusselt number as

Nuv = Ke · Nu(T)∞   (C.2-15)

```
┌─────────────────────────────────────────────────────────────────────────┐
│ Processed data from file E:MULLER6.DAT                                    │
│                                                                           │
│ Coil Fin Data                    Fin Element Areas                        │
│                                                                           │
│ Radius R0  =  8.34 mm            Inner Element    3.977 sq.cm             │
│ Radius R1  = 10.01 mm            Intermediate    10.207 sq.cm             │
│ Radius R2  = 16.21 mm            Outer Element   10.207 sq.cm             │
│ Radius R3  = 20.62 mm                                                     │
│ Tube pitch = 38.10 mm                                                     │
│ Row pitch  = 35.05 mm                                                     │
│ Fin space  =  3.92 mm                                                     │
└─────────────────────────────────────────────────────────────────────────┘
```

Test Code	D2904	D2892	D2891	D2901	D2902	D2903
Coil Face Velocity m/s	0.41	0.80	1.25	1.64	2.12	2.74
Mean Air Velocity m/s	0.76	1.49	2.34	3.06	3.96	5.11
Air Mass Flow Rate kg/m²s	0.804	1.629	2.484	3.321	4.517	5.918
Reynolds No.(Channel flow)	261.8	543.0	816.5	1097	1544	2046
Reynolds No.(entering coil)	179.1	371.4	558.5	750.2	1056	1399
Inner Element enh. factor	1.813	2.457	3.510	4.325	4.888	6.236
Intermediate enh. factor	0.971	1.055	1.243	1.392	1.528	1.745
Outer element enh. factor	1.115	1.327	1.504	1.645	1.798	1.985
Vortex enh. factor Ke	3.220	4.364	6.235	7.682	8.682	11.076
Reduced heat tran. factor	0.000	0.000	0.000	0.000	0.000	0.000
Entering enh. outer el.	1.396	1.743	1.973	2.158	2.396	2.611
Entering enh. int. el.	1.056	1.081	1.223	1.338	1.486	1.619
Mean enh.1-row coil Num/Nu∞	1.168	1.397	1.722	1.976	2.189	2.578

*Table C.7 - Summary of iteration procedure for deriving Ke
in Table C.5.   (yv=Do/10 for 6fpi 1-row coil,
flow over infinite parallel plates)*

C.2.5 Analysis for Channel Flow and Vortex Width of Do/10.

Table C.8 shows the results of the analysis for Eq.(C.2-13).
Thus for this analysis the vortex width,

yv = 0.1 · 16.68 = 1.668 mm or .001668 m ,

and the channel aspect ratio is 3.92/(21.42-3.336) = .217 .

For well developed laminar flow within a channel with aspect
ratio of .217 and for cooling application, the Nusselt number
for constant temperature is found by Eq.(A.2-4) as

Nu(T)∞ = 4.668 .

But

$$Nu = \frac{ho \cdot Dh}{ka} \quad ,$$

where for the channel in question

$$Dh = 4 \cdot rh = \frac{2 \cdot (21.42-3.336) \cdot 3.92}{21.42-3.336 + 3.92} = 6.443 \text{ mm} .$$

Now for a mean thermal conductivity of 2.737E-02 W/m K.

$$ho = \frac{Nu\infty \cdot ka}{Dh} = \frac{4.668 \cdot 2.737E-02}{0.006443} = 19.83 \text{ W/m}^2\text{K} .$$

Thus the parameter

$$L \sqrt{(ho/kf \cdot y)} = \frac{12.28}{1000.} \sqrt{(19.83/(203.0 \cdot .095E-03))} = .394 \quad ,$$

and the fin ratio R3/R0 = 20.62/8.34 = 2.472 .

From Fig.C.2, the fin efficiency ∅ = 0.92, and the rate of heat transfer from the external coil surface is expressed as

$$Qa = ho \ (Aprim + ∅ \cdot Afin) \ dTm$$
$$= ho \ (.4564 + .92 \cdot 4.825) \ dTm$$
$$= ho \cdot 4.895 \cdot dTm \quad ,$$

so that

$$ho = Qa/(4.895 \cdot dTm) \quad \text{W/m}^2\text{K} ,$$

and the mean Nusselt number is then derived as

$$Num = \frac{Dh \cdot ho}{ka} = \frac{.006443 \cdot ho}{ka} \quad .$$

Test Code	D2904	D2892	D2891	D2901	D2902	D2903
Re (channel flow)	261.8	543.0	816.5	1097	1544	2046
Re (D0)	677.4	1406	2113	2839	3997	5296
Ext.heat tran.coef. ho	31.062	36.135	45.246	51.654	55.099	64.088
Thermal cond. E-02 W/mK	2.816	2.743	2.786	2.772	2.669	2.636
Mean Nusselt No., Num	7.099	8.488	10.464	12.006	13.301	15.665
Ratio Num/Nu∞	1.521	1.818	2.242	2.572	2.849	3.356
Vortex Enhancement Ke	5.894	7.553	10.174	12.197	13.682	16.970
Vortex Nusselt no. Nuv	27.51	35.26	47.49	56.94	63.87	79.22

Table C.8 - Derived heat transfer parameters for 6fpi 1-row coil dry tests over a range of face velocities, channel flow and vortex width of Do/10.

C.2.6   Analysis for Channel Flow and Vortex Width of *s/2*.

For this analysis the vortex width,

   yv = *s/2.* = 3.92/2. = 1.96 mm   or   .00196 m ,

and the channel aspect ratio is 3.92/(21.42-3.92) = .224 .

For well developed laminar flow within a channel with aspect ratio of .224 and for cooling application, the Nusselt number for constant temperature is found by Eq.(A.2-4) as

   $Nu(T)_\infty$ = 4.614

For the channel in question

   $$Dh = 4 \cdot rh = \frac{2 \cdot (21.42-3.92) \cdot 3.92}{21.42-3.92 + 3.92} = 6.405 \text{ mm} .$$

For the previously established mean thermal conductivity of 2.737E-02 W/mK

   $$ho = \frac{Nu_\infty \cdot ka}{Dh} = \frac{4.614 \cdot 2.737E\text{-}02}{0.006405} = 19.72 \text{ W/m}^2\text{K} ,$$

and the parameter

   $$L \sqrt{(ho/(kf \cdot y))} = \frac{12.28}{1000.} \sqrt{(19.72/(203.0 \cdot .095E\text{-}03))} = .393 .$$

From Fig.C.2 for R3/R0=2.472 the fin efficiency ∅=0.92, and the heat transfer from the external coil surface

   ho = Qa/4.895/dTm   W/m²K   ,

and the mean Nusselt number is then derived as

Test Code	D2904	D2892	D2891	D2901	D2902	D2903
Re (channel flow)	260.3	539.8	811.7	1090	1535	2034
Re (D0)	677.4	1406	2113	2839	3997	5296
Ext.heat tran.coef. ho	31.026	36.135	45.246	51.654	55.099	64.088
Thermal cond. E-02 W/mK	2.816	2.743	2.786	2.772	2.669	2.636
Mean Nusselt No., Num	7.057	8.438	10.402	11.935	13.223	15.572
Ratio Num/Nu∞	1.529	1.829	2.254	2.587	2.866	3.375
Vortex Enhancement Ke	5.405	6.899	9.250	11.074	12.419	15.372
Vortex Nusselt no. Nuv	24.94	31.83	42.68	51.10	57.30	70.93

   Table C.9 - Derived heat transfer parameters for 6fpi 1-row coil dry tests over a range of face velocities, channel flow and vortex width of s/2.

$$Num = \frac{Dh \cdot ho}{ka} = \frac{.006405 \cdot ho}{ka} \quad .$$

The results are listed in Table C.9.

C.3 TESTS ON 10 FINS PER INCH COIL

C.3.1 Physical Parameters

Heat transfer data for another 1-row coil with a different fin spacing was extracted from a subsequent experimental program conducted at the Holden Test Rig of the University of Adelaide. The coil investigated was also manufactured by F.Muller and Sons Pty.Ltd. and the relevant physical data were observed as shown in Table C.10. The parameters shown in Table C.11 were derived in the manner described in section C.1.1 of this Appendix.

Coil height,	Clht	457	mm
Coil size parallel to tubes,	Clwi	760	mm
Tube outside diameter,	Dp	16.3	mm
Tube wall thickness,	xp	0.65	mm
Fin thickness,	xf	0.19	mm
Fin pitch,	FP	2.508	mm
Tube spacing within coil row,	Ct	38.10	mm
Fin depth,	Cr	35.05	mm
Number of rows,	Nrow%	1	
Number of fins,	Nfin%	303	
Total number of tubes per row,	Nt%	12	
Number of parallel circuits,	Ncirc%	2	
Number of tubes fed,	Npt%	6	

Table C.10 - Physical dimensions of 10fpi 1-row coil.

Face area,	Af	0.347	m²
Tube inside diameter,	Di	15.00	mm
Effective tube outside dia.,	Do	16.68	mm
Space between fins	s	2.318	mm
Space between tubes	a	21.42	mm
Equiv.circ.plate fin radius	R3	20.62	mm
Internal heat transfer area,	Api	0.4298	m²
Primary heat transfer area,	Aprim	0.4417	m²
Fin heat transfer area,	Afin	8.1220	m²
Total area for water flow,	Afw	.001060	m²

Table C.11 - Derived physical parameters for 10fpi
1-row coil.

C.3.2 Dry Coil Tests at Various Air Flow Rates

As for the 6 fpi coil, the analysis of the 10 fpi coil was restricted to dry operation only. The air entering and leaving conditions, the air flow rates, and the chilled water flow rates and temperatures were recorded as shown in Table C.12.

Test No.		T01	T02	T03	T04	T05	T06
Atm. pressure, Pat	kPa	102.242	102.242	102.242	102.242	102.441	102.441
Entering db Temp., t	°C	39.52	42.66	38.52	39.41	39.54	34.87
Entering dew point,	°C	17.15	19.7	18.4	17.35	21.7	20.8
Leaving db Temp.	°C	20.74	28.25	26.29	29.34	31.08	27.72
Leaving dew point	°C	17.15	19.7	18.4	17.35	21.7	20.8
Air mass flow rate	kg/s	.1707	.3045	.4099	.5701	.6683	.7347
Air face velocity	m/s	.440	.795	1.055	1.469	1.730	1.870
Ent.water temp.,Tr	°C	14.3	19.45	16.09	17.24	19.67	17.15
Water flow rate, Mw	l/s	1.718	1.712	1.722	1.724	1.710	1.700
Test No.		T07	T08	T09	T10	T11	T12
Atm. pressure, Pat	kPa	102.242	102.235	102.235	102.235	102.235	102.235
Entering db Temp., t	°C	36.95	35.06	35.12	35.17	35.23	35.32
Entering dew point,	°C	15.7	13.2	13.55	13.7	13.65	13.65
Leaving db Temp.	°C	29.10	27.86	28.40	28.96	29.35	29.76
Leaving dew point	°C	15.7	13.2	13.55	13.7	13.65	13.65
Air mass flow rate	kg/s	.8481	.9471	1.0497	1.1601	1.2567	1.3385
Air face velocity	m/s	2.163	2.397	2.657	2.936	3.180	3.391
Ent.water temp.,Tr	°C	16.15	14.87	15.22	15.74	16.25	16.63
Water flow rate, Mw	l/s	1.724	1.724	1.712	1.714	1.725	1.713

Table C.12 - Summary of dry tests for 10fpi 1-row coil over a range of air flow rates.

C.3.3 Analysis of Test Results

The parameters listed in Table C.13 were derived in a similar manner as that described in sub-section C.2.3.

Test No.	T01	T02	T03	T04	T05	T06
Entering db Temp., t C	39.52	42.66	38.52	39.41	39.54	34.87
Thermal cond. E-02 W/mK	2.707	2.729	2.699	2.706	2.707	2.673
Viscosity, E-05 Pa s	1.9092	1.9237	1.9046	1.9087	1.9093	1.8876
Entering enthalpy kJ/kg	71.11	79.92	72.71	71.41	81.58	74.45
Leaving enthalpy kJ/kg	51.81	65.05	60.12	61.06	72.82	67.06
Enth.diff., dH kJ/kg	19.30	14.87	12.59	10.35	8.76	7.39
Spec.volume, v cu.m/kg	0.895	0.907	0.894	0.895	0.899	0.884
Air flow rate, Ma kg/s	0.1707	0.3045	0.4099	0.5701	0.6683	0.7347
Air flow rate, Fa l/s	152.78	276.18	366.45	510.24	600.80	649.47
Actual face vel. m/s	0.440	0.795	1.055	1.469	1.730	1.870
Sensible heat, Qa kW	3.295	4.528	5.161	5.901	5.854	5.429
Ent.water temp.,Tr C	14.3	19.45	16.09	17.24	19.67	17.15
Water flow rate, Mw l/s	1.718	1.712	1.722	1.724	1.710	1.700
Viscosity, E-03 Pa s	1.144	0.9991	1.090	1.058	0.9936	1.060
Therm.Cond., kw W/m K	0.5940	0.6022	0.5969	0.5987	0.6025	0.5986
Spec.Heat, Cpw kJ/kg K	4.189	4.184	4.187	4.186	4.184	4.186
Prandtl number, Pr(w)	8.070	6.942	7.649	7.395	6.899	7.415
Water temp.rise, dTw K	0.458	0.632	0.716	0.818	0.818	0.763
Water velocity, Vw m/s	1.620	1.615	1.624	1.626	1.613	1.603
Reynolds No., Re(w)	21243	24241	22344	23059	24348	22684
Nusselt No., developed	164.79	172.91	168.11	170.20	173.11	168.07
Nusselt No., enhanced	165.53	172.91	168.26	170.20	173.11	168.07
Int.film res.E-04 m²K/W	1.526	1.441	1.494	1.472	1.438	1.491
Tube wall grad., dTi K	1.170	1.518	1.794	2.021	1.959	1.883
Mean prim.surf.t., tpo	15.699	21.284	18.241	19.670	22.038	19.415
driving dTm K	12.224	12.974	13.345	14.206	12.897	11.589

Test No.	T07	T08	T09	T10	T11	T12
Entering db Temp., t C	36.95	35.06	35.12	35.17	35.23	35.32
Thermal cond. E-02 W/mK	2.688	2.675	2.675	2.675	2.676	2.676
Viscosity, E-05 Pa s	1.8973	1.8885	1.8888	1.8890	1.8893	1.8897
Entering enthalpy kJ/kg	65.67	59.42	60.05	60.35	60.33	60.41
Leaving enthalpy kJ/kg	57.61	52.06	53.17	53.98	54.31	54.73
Enth.diff., dH kJ/kg	8.06	7.36	6.88	6.37	6.02	5.68
Spec.volume, v cu.m/kg	0.886	0.879	0.879	0.879	0.879	0.880
Air flow rate, Ma kg/s	0.8481	0.9471	1.0497	1.1601	1.2567	1.3385
Air flow rate, Fa l/s	751.42	832.50	922.69	1019.73	1104.64	1177.88
Actual face vel. m/s	2.163	2.397	2.657	2.936	3.180	3.391
Sensible heat, Qa kW	6.836	6.971	7.222	7.390	7.565	7.603
Ent.water temp.,Tr C	16.15	14.87	15.22	15.74	16.25	16.63
Water flow rate, Mw l/s	1.724	1.724	1.712	1.714	1.725	1.713
Viscosity, E-03 Pa s	1.089	1.127	1.116	1.101	1.086	1.075
Therm.Cond., kw W/m K	0.5970	0.5949	0.5955	0.5963	0.5971	0.5977
Spec.Heat, Cpw kJ/kg K	4.187	4.189	4.188	4.188	4.187	4.187
Prandtl number, Pr(w)	7.635	7.932	7.849	7.729	7.613	7.528
Water temp.rise, dTw K	0.947	0.965	1.007	1.030	1.047	1.060
Water velocity, Vw m/s	1.626	1.626	1.615	1.617	1.627	1.616
Reynolds No., Re(w)	22406	21650	21703	22034	22478	22547
Nusselt No., developed	168.37	166.23	165.84	166.87	168.62	168.27
Nusselt No., enhanced	168.50	166.77	166.29	167.15	168.72	168.27
Int.film res.E-04 m²K/W	1.491	1.512	1.515	1.505	1.489	1.491
Tube wall grad., dTi K	2.372	2.452	2.546	2.588	2.621	2.638
Mean prim.surf.t., tpo	18.995	17.805	18.269	18.843	19.394	19.798
driving dTm K	13.742	13.415	13.286	13.051	12.743	12.608

Table C.13 - Derived mean surface temperatures for 10fpi 1-row coil.

C.3.4 Analysis for Infinite Parallel Plate Fins

Tables C.14 and C.15 show the results of the analysis for Eqs.(C.2.13) and (C.2.14) respectively in which the laminar flow Nusselt number of 7.541 for infinite parallel plates was used.

For infinite parallel plates spaced at s = 2.318 mm the hydraulic diameter

Dh = 2 • 2.318 = 4.636 mm or .004636 m .

From Table C.13 the mean thermal conductivity for the 12 tests is 2.691E-02 W/mK. Then from Eq.(A.2-1),

$$ho = \frac{Nu\infty \cdot ka}{Dh} = \frac{7.541 \cdot 2.691E\text{-}02}{.004636} = 43.77 \ W/m^2K \ .$$

Thus the parameter

$$L \ \sqrt{(ho/(kf \cdot y))} = \frac{12.28}{1000.} \ \sqrt{(43.77/(203.\cdot.095E\text{-}03))} = .585 \ .$$

From Fig.C.2 and for R3/R0=2.472 the fin efficiency Ø=0.85 .

Test No.	T01	T02	T03	T04	T05	T06
Re (inf. par. plates)	129.1	228.6	310.9	431.4	505.5	561.8
Re (Do)	827	1463	1990	2761	3235	3619
Ext.heat tran.coef. ho	36.699	47.516	52.653	56.554	61.798	63.780
Thermal cond. E-02 W/mK	2.707	2.729	2.699	2.706	2.707	2.673
Mean Nusselt No., Num	6.285	8.072	9.044	9.689	10.584	11.062
Ratio Num/Nu∞	0.833	1.070	1.199	1.285	1.404	1.467
Vortex Enhancement Ke	1.000	2.725	3.585	4.208	4.983	5.356
Vortex Nusselt no. Nuv	7.54	20.55	27.03	31.73	37.58	40.39

Test No.	T07	T08	T09	T10	T11	T12
Re (inf. par. plates)	645.4	724.7	802.7	886.7	960.2	1023
Re (Do)	4130	4638	5137	5674	6145	6549
Ext.heat tran.coef. ho	67.727	70.748	74.007	77.092	80.825	82.101
Thermal cond. E-02 W/mK	2.688	2.675	2.675	2.675	2.676	2.676
Mean Nusselt No., Num	11.681	12.261	12.826	13.361	14.002	14.223
Ratio Num/Nu∞	1.549	1.626	1.701	1.772	1.857	1.886
Vortex Enhancement Ke	5.831	6.292	6.750	7.178	7.754	7.881
Vortex Nusselt no. Nuv	43.97	47.45	50.90	54.13	58.47	59.43

Table C.14 - Derived heat transfer parameters for 10fpi 1-row coil dry tests over a range of face velocities, flow over infinite parallel plates and vortex width of Do/10.

The rate of heat transfer from the external coil surface is

$$Qa = ho \ (Aprim + \emptyset \cdot Afin) \ dTm$$
$$= ho \ (.4417 + .85 \cdot 8.122) \ dTm$$
$$= ho \cdot 7.345 \cdot dTm$$

This re-arranges to

$$ho = Qa/(7.345 \cdot dTm) \quad W/m^2K \quad .$$

The mean Nusselt number is then derived as

$$Num = \frac{Dh \cdot ho}{ka} = \frac{.004636 \cdot ho}{ka}$$

Test No.	T01	T02	T03	T04	T05	T06
Re (inf. par. plates)	129.1	228.6	310.9	431.4	505.5	561.8
Re (Do)	827	1463	1990	2761	3235	3619
Ext.heat tran.coef. ho	36.699	47.516	52.653	56.554	61.798	63.780
Thermal cond. E-02 W/mK	2.707	2.729	2.699	2.706	2.707	2.673
Mean Nusselt No., Num	6.285	8.072	9.044	9.689	10.584	11.062
Ratio Num/Nu∞	0.833	1.070	1.199	1.285	1.404	1.467
Vortex Enhancement Ke	1.022	3.289	4.433	5.278	6.289	6.778
Vortex Nusselt no. Nuv	7.71	24.80	33.43	39.80	47.43	51.11
Test No.	**T07**	**T08**	**T09**	**T10**	**T11**	**T12**
Re (inf. par. plates)	645.4	724.7	802.7	886.7	960.2	1023
Re (Do)	4130	4638	5137	5674	6145	6549
Ext.heat tran.coef. ho	67.727	70.748	74.007	77.092	80.825	82.101
Thermal cond. E-02 W/mK	2.688	2.675	2.675	2.675	2.676	2.676
Mean Nusselt No., Num	11.681	12.261	12.826	13.361	14.002	14.223
Ratio Num/Nu∞	1.549	1.626	1.701	1.772	1.857	1.886
Vortex Enhancement Ke	7.400	8.000	8.611	9.167	9.922	10.089
Vortex Nusselt no. Nuv	55.80	60.33	64.94	69.13	74.82	76.08

Table C.15 - Derived heat transfer parameters for 10fpi 1-row coil dry tests over a range of face velocities, flow over infinite parallel plates and vortex width of s/2.

C.3.5 Analysis for Channel Flow and Vortex Width of Do/10.

This part of the analysis was based on the same procedure as that described in section C.2.5 of this Appendix and the results are as shown in Table C.16.

The vortex width

$$y_v = D_o/10 = 16.68/10 = 1.668 \text{ mm or } .001668 \text{ m} .$$

This leaves a channel aspect ratio of

$$2.318 / (21.42 - 3.336) = 0.128 .$$

The Nusselt number for well developed laminar flow for this aspect ratio and for cooling is found by Eq.(A.2-4) as

$$Nu(T)_\infty = 5.521 ,$$

and the hydraulic diameter

$$D_h = \frac{2 \cdot (21.42 - 3.336) \cdot 2.318}{21.42 - 3.336 + 2.318} = 4.109 \text{ mm} .$$

For a mean thermal conductivity of 2.691E-02 W/mK

$$h_o = \frac{Nu_\infty \cdot k_a}{D_h} = \frac{5.521 \cdot 2.691E-02}{.004109} = 36.16 \quad W/m^2K ,$$

Test No.	T01	T02	T03	T04	T05	T06
Re (channel flow)	203.6	360.4	490.2	680.1	796.9	885.8
Re (Do)	827	1463	1990	2761	3235	3619
Ext.heat tran.coef. ho	35.901	46.485	51.510	55.326	60.456	62.395
Thermal cond. E-02 W/mK	2.707	2.729	2.699	2.706	2.707	2.673
Mean Nusselt No., Num	5.449	6.999	7.842	8.401	9.177	9.592
Ratio Num/Nu∞	0.987	1.268	1.420	1.522	1.662	1.737
Vortex Enhancement Ke	2.297	4.390	5.442	6.203	7.153	7.625
Vortex Nusselt no. Nuv	12.68	24.24	30.05	34.25	39.49	42.10
Test No.	**T07**	**T08**	**T09**	**T10**	**T11**	**T12**
Re (channel flow)	1018	1143	1265	1398	1514	1613
Re (Do)	4130	4638	5137	5674	6145	6549
Ext.heat tran.coef. ho	66.256	69.212	72.400	75.418	79.070	80.318
Thermal cond. E-02 W/mK	2.688	2.675	2.675	2.675	2.676	2.676
Mean Nusselt No., Num	10.128	10.631	11.121	11.585	12.141	12.333
Ratio Num/Nu∞	1.834	1.926	2.014	2.098	2.199	2.234
Vortex Enhancement Ke	8.225	8.814	9.383	9.917	10.627	10.808
Vortex Nusselt no. Nuv	45.41	48.66	51.80	54.75	58.67	59.67

Table C.16 - Derived heat transfer parameters for 10fpi 1-row coil dry tests over a range of face velocities, channel flow and vortex width of Do/10.

and the parameter

$$L \sqrt{(ho/(kf \cdot y))} = \frac{12.28}{1000.} \sqrt{(36.16/(203...095E-03))} = .532 \quad .$$

From Fig.C.2 and for R3/R0=2.472 the fin efficiency $\emptyset$=0.87 .

Thus

$$Qa = ho \cdot (Aprim + \emptyset \cdot Afin) \cdot dTm$$
$$= ho \cdot (.4417 + .87 \cdot 8.122) \cdot dTm$$
$$= ho \cdot 7.508 \cdot dTm$$

so that

$$ho = Qa / (7.508 \cdot dTm) \quad W/m^2K \quad .$$

The mean Nusselt number is then

$$Num = \frac{Dh \cdot ho}{ka} = \frac{0.004109 \cdot ho}{ka} \quad .$$

C.3.6 Analysis for Channel Flow and Vortex width of $s/2$.

For this analysis the vortex width

$$yv = s / 2. = 2.318/2. = 1.159 \text{ mm} = .001159 \text{ m} ,$$

so that the channel aspect ratio is

$$2.318/(21.42-2.318) = .121 \quad .$$

For well developed laminar flow within a channel with aspect ratio of .121 and for cooling application, the Nusselt number for constant temperature is found by Eq.(A.2-4) as

$$Nu(T)\infty = 5.604 ,$$

and the hydraulic diameter

$$Dh = \frac{2 \cdot (21.42 - 2.318) \cdot 2.318}{21.42 - 2.318 + 2.318} = 4.134 \text{ mm} \quad .$$

Now for the mean thermal conductivity of 2.691E-02 W/m K ,

$$ho = \frac{Nu\infty \cdot ka}{Dh} = \frac{5.604 \cdot 2.691E-02}{0.004134} = 36.48 \text{ W/m}^2K ,$$

and the parameter

$$L \sqrt{(ho/(kf \cdot y))} = \frac{12.28}{1000.} \sqrt{(36.48/(203...095E-03))} = 0.534 \quad .$$

Again from Fig.C.1 the fin efficiency is found as ∅=0.87, so that the heat transfer coefficient remains as

$$ho = \frac{Qa}{7.508 \cdot dTm} \quad W/m^2K \quad ,$$

but the mean Nusselt number is now

$$Num = \frac{Dh \cdot ho}{ka} = \frac{.004134 \cdot ho}{ka} \quad .$$

Test No.	T01	T02	T03	T04	T05	T06
Re (channel flow)	204.8	362.6	493.2	684.3	801.8	891.2
Re (Do)	827	1463	1990	2761	3235	3619
Ext.heat tran.coef. ho	35.901	46.485	51.510	55.326	60.456	62.395
Thermal cond. E-02 W/mK	2.707	2.729	2.699	2.706	2.707	2.673
Mean Nusselt No., Num	5.483	7.042	7.890	8.452	9.233	9.650
Ratio Num/Nu∞	0.978	1.257	1.408	1.508	1.648	1.722
Vortex Enhancement Ke	2.633	5.378	6.756	7.756	9.000	9.611
Vortex Nusselt no. Nuv	14.76	30.14	37.86	43.46	50.44	53.86

Test No.	T07	T08	T09	T10	T11	T12
Re (channel flow)	1024	1150	1273	1406	1523	1623
Re (Do)	4130	4638	5137	5674	6145	6549
Ext.heat tran.coef. ho	66.256	69.212	72.400	75.418	79.070	80.318
Thermal cond. E-02 W/mK	2.688	2.675	2.675	2.675	2.676	2.676
Mean Nusselt No., Num	10.190	10.696	11.189	11.655	12.215	12.408
Ratio Num/Nu∞	1.818	1.909	1.997	2.080	2.180	2.214
Vortex Enhancement Ke	10.389	11.148	11.900	12.589	13.511	13.733
Vortex Nusselt no. Nuv	58.22	62.47	66.69	70.55	75.72	76.96

Table C.17 - Derived heat transfer parameters for 10fpi 1-row coil dry tests over a range of face velocities, channel flow and vortex width of s/2.

C.4 CORRELATION BETWEEN TEST DATA

The results as listed in Tables C.5, C.6, C.8, C.9, C.14, C.15, C.16, and C.17 are graphically represented in Figures C.3 to C.10. Ke and Nuv are plotted for vortex widths Do/10 and *s/2* against Reynolds numbers based on infinite parallel plates, channel flow, and tube outside diameter with the aim to establish some correlation between the two sets of tests.
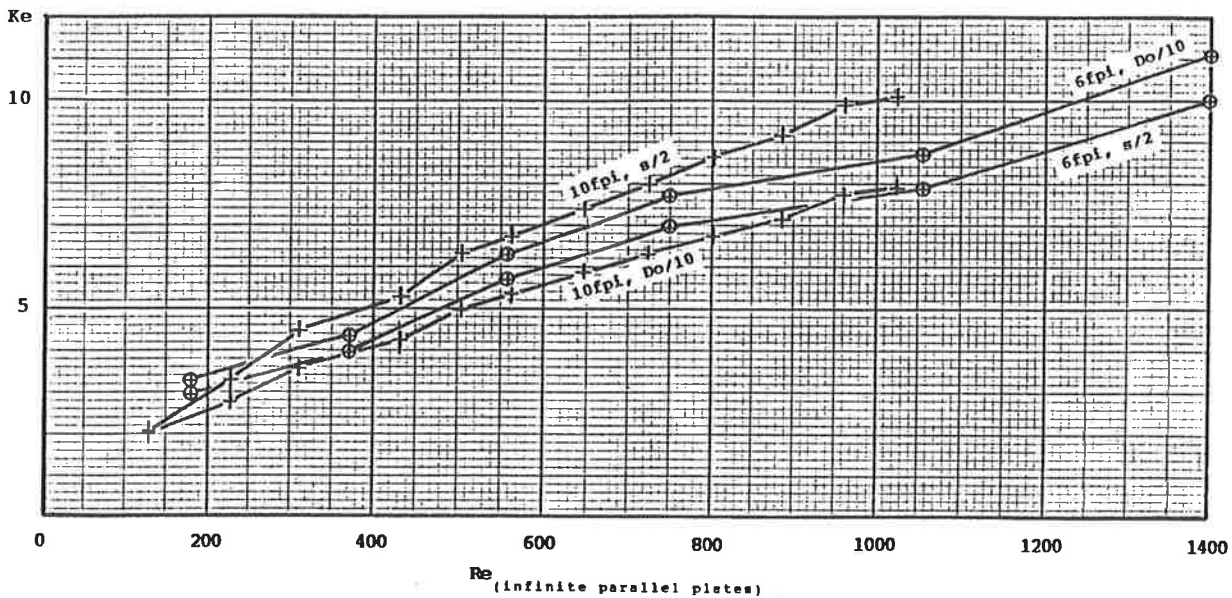
Fig.C.3 - Plot of vortex enhancement factor Ke against Reynolds number based on infinite parallel plates.

Fig.C.4 - Plot of vortex enhancement factor Ke against Reynolds number based on tube outside diameters. Nu(T)∞ for infinite parallel plates.

By inspection, Reynolds numbers based on fin spacing give the better correlation over those based on tube diameter and hence the latter is no further pursued.

Fig.C.5 - Plot of vortex Nusselt number Nuv against Reynolds number based on infinite parallel plates.
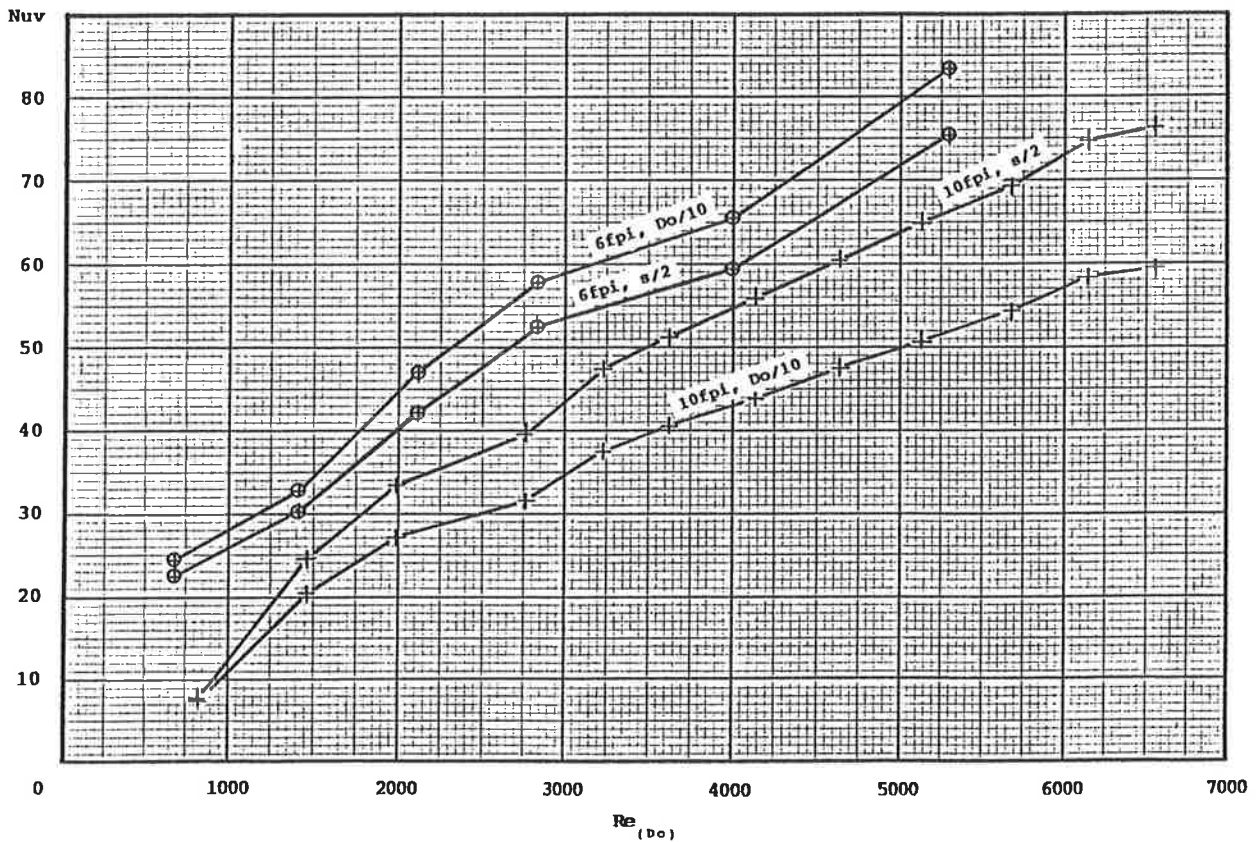
Fig.C.6 - Plot of vortex Nusselt number Nuv against Reynolds number based on tube outside diameter. Nu(T)∞ for infinite parallel plates.
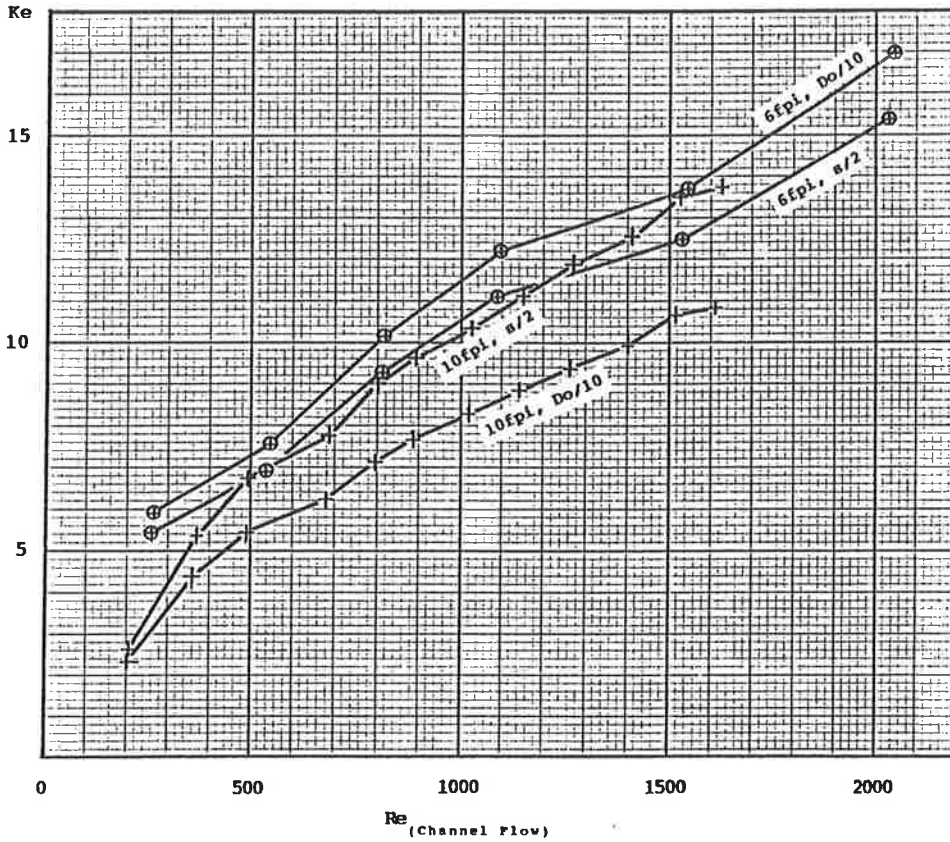
Fig.C.7 - Plot of vortex enhancement factor Ke against
Reynolds number based on channel flow.
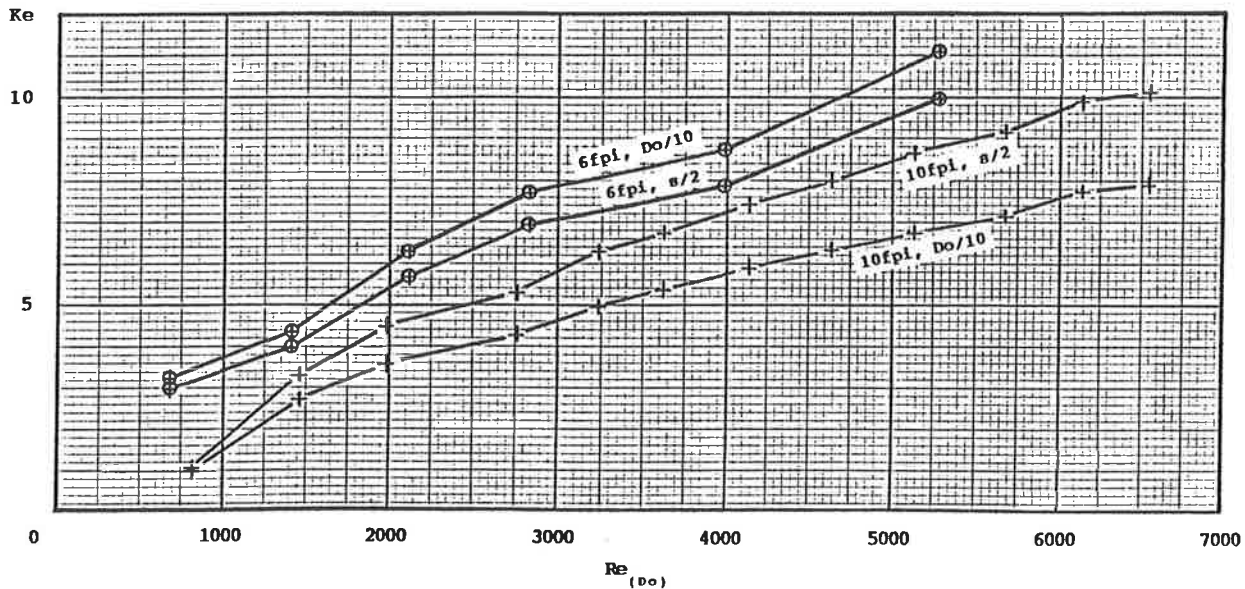

Fig.C.8 - Plot of vortex enhancement factor Ke against
Reynolds number based on tube outside diameter.
$Nu(T)_\infty$ for channel flow.

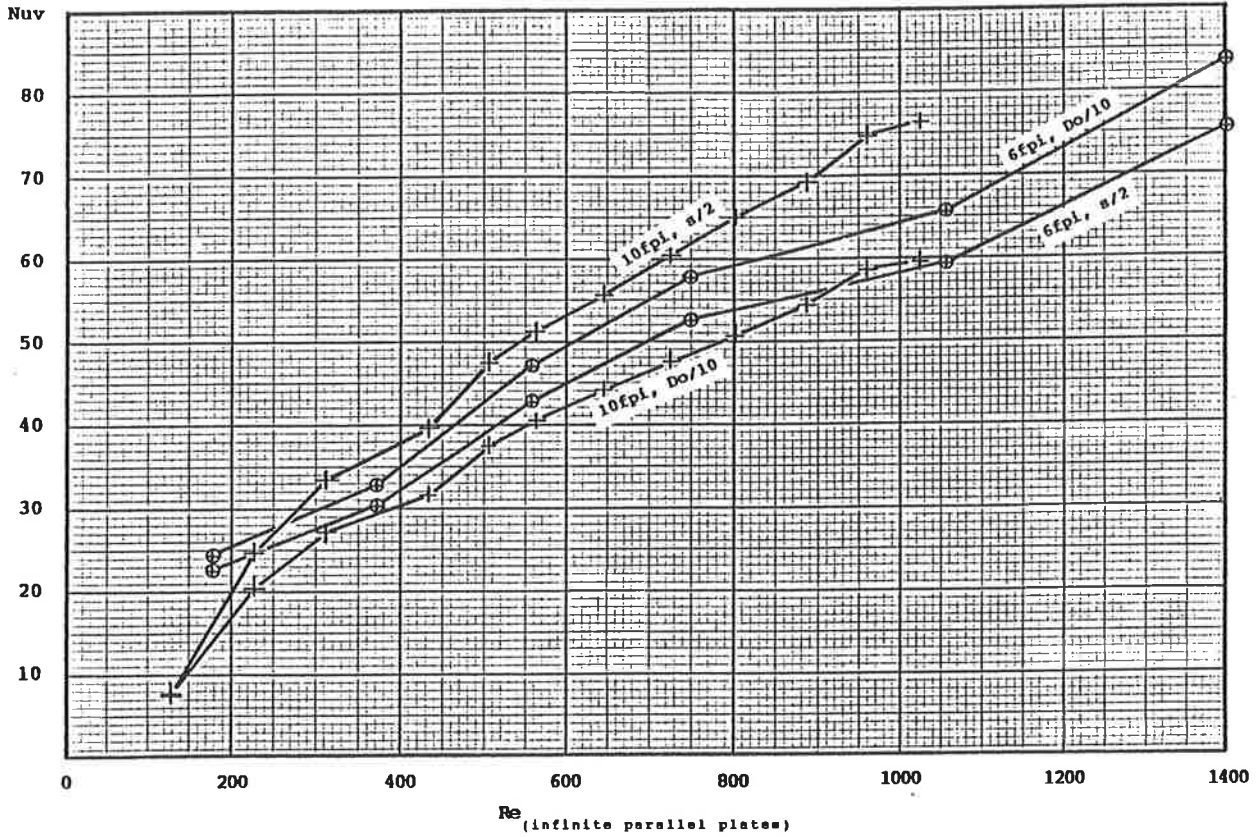*Fig.C.9 - Plot of vortex Nusselt number Nuv against Reynolds number based on channel flow.*

Fig.C.10 - Plot of vortex Nusselt number Nuv against Reynolds number based on tube outside diameter. Nu(T)∞ for channel flow.

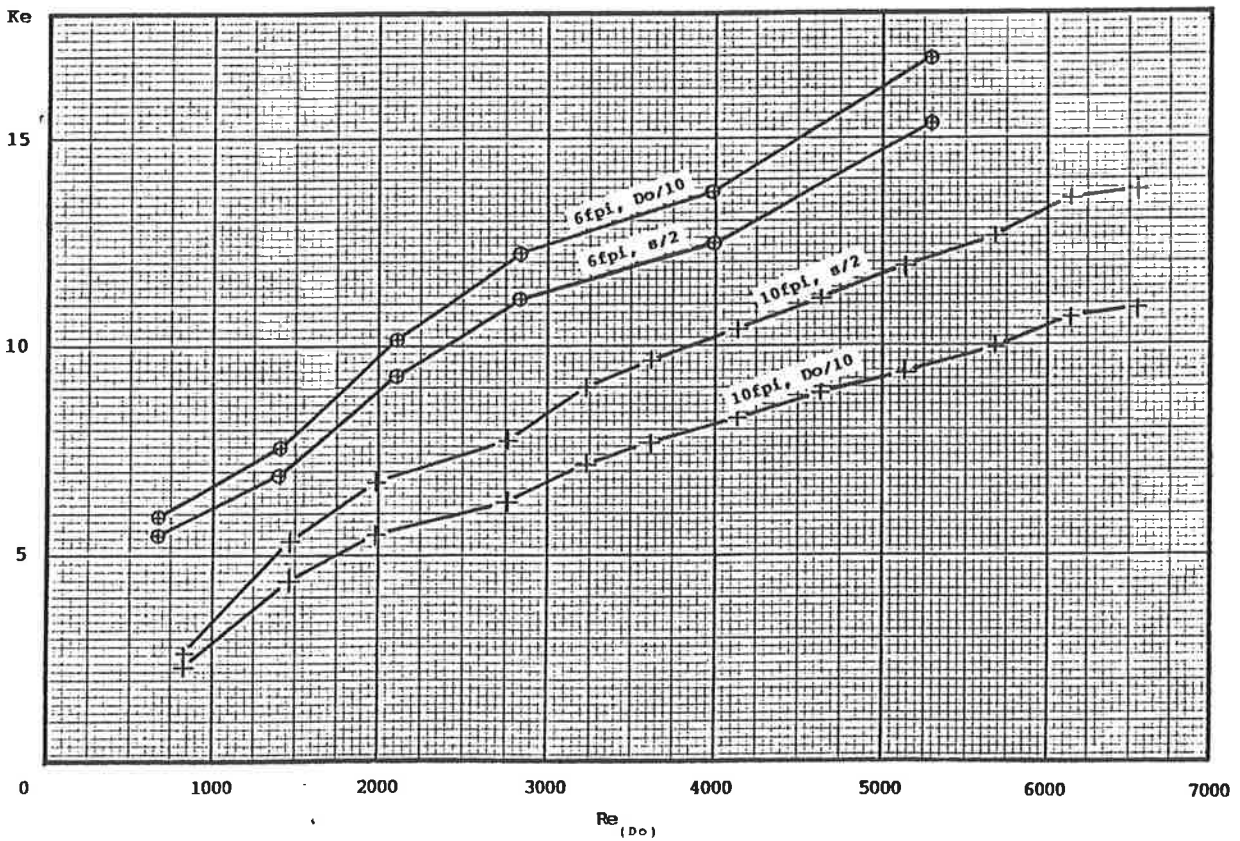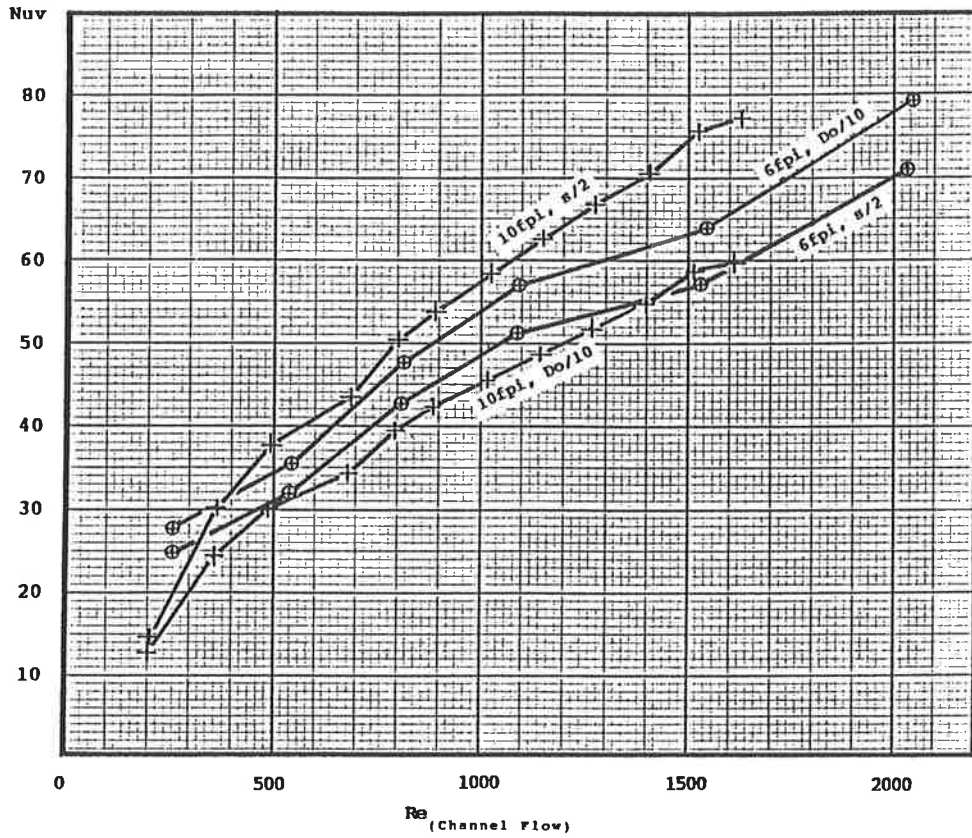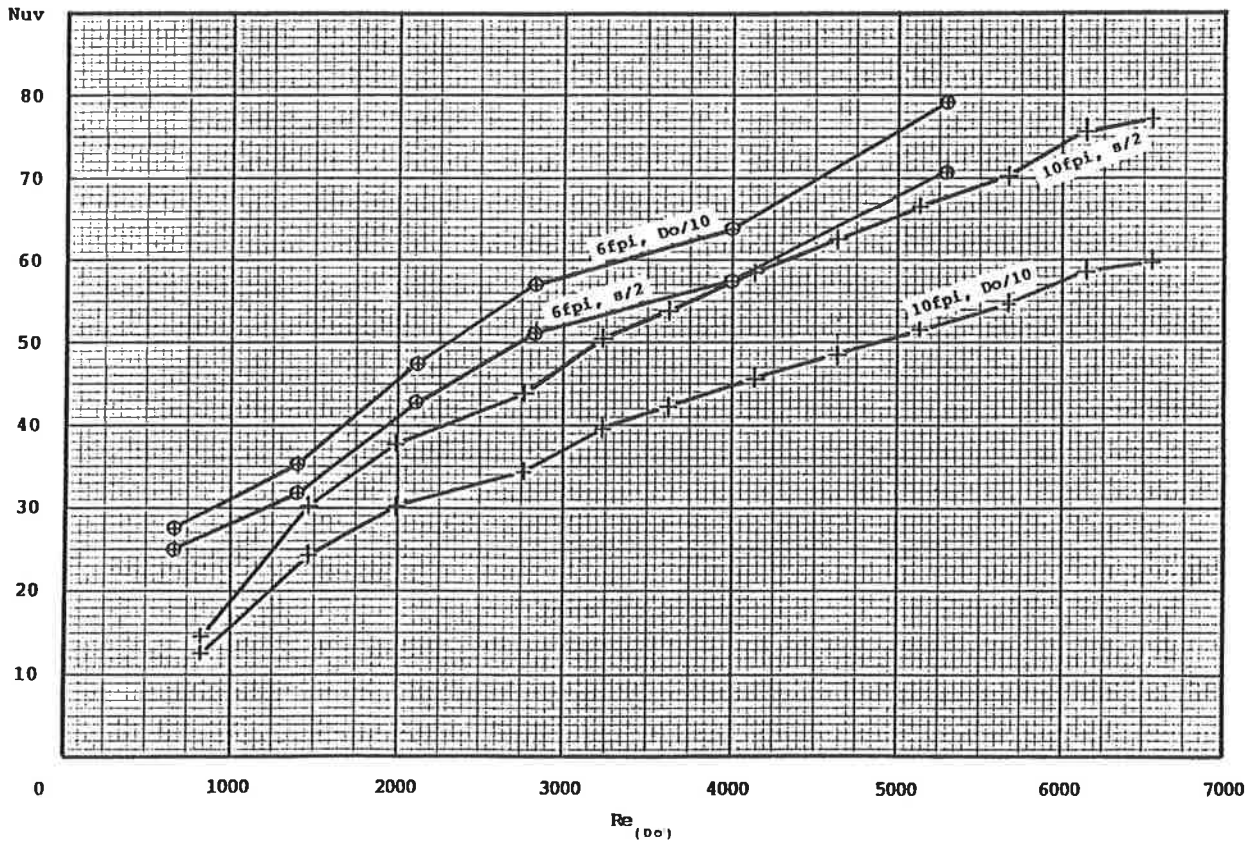Visually there is little to choose between the plots in figures C.3, C.5, C.7, and C.9. Regression modelling showed strong correlation of each set of test results with a curve of the general form of

$$Y = a \cdot X^b$$

In an attempt to quantify the correlation between the test results for the two coils, the test results were combined to give a single correlation coefficient for each pair of test results. Since only 6 test results were available for the 6fpi coil, only every second test for the 10fpi coil was considered for this exercise to ensure equal weighting for the two coils.

Table C.18 shows the results of the linear regression analysis with program CURFIT[a] on the test results shown in Fig.C.3 for the 6fpi coil and vortex width of $s/2$. Table C.19 summarises the analysis for the plots in figures C.3, C.5, C.7, and C.9 and tends to favour the relation in Fig.C.7. There is very little difference between the correlation coefficients of equations <1>, <5>, and <7>. However, equations <1> and <7> have unacceptable offsets at low Reynolds numbers whereas equation <5> goes through the origin and has also the smallest deviations. Equation <5> is thus derived as

```
 ┌─────────────────────────────────────────────────────────────────────────┐
 │  C U R F I T            ───────      LINEAR      REGRESSION    MODELLING  │
 │  G.J.Van Aken      -  Australian Construction Services        Ver.03-04-91│
 │                                                                           │
 │                                                                           │
 │   Filename: c3ke6                                                         │
 │   Average value of independent variable X  =  7.1903E+02                  │
 │   Average value of dependent variable    Y  =  6.2357E+00                 │
 │   Number of (X,Y) pairs                      =  6                         │
 │                                                                           │
 │  No.    Curve          r         a          b         s.e.(b)     F(1,4)  │
 │                                                                           │
 │  <1> Y=a+b•X       0.99063   2.1543E+00   5.6762E-03  3.9127E-04  2.1E+02 │
 │  <2> Y=a+b/X       0.86300   8.9151E+00  -1.2308E+03  3.6026E+02  1.2E+01 │
 │  <3> Y=1/(a+b•X)   0.90768   3.1834E-01  -1.7945E-04  4.1486E-05  1.9E+01 │
 │  <4> Y=a•EXP(b•X)  0.96134   2.8894E+00   9.5954E-04  1.3742E-04  4.9E+01 │
 │  <5> Y=a•X^b       0.99227   1.2688E-01   5.9841E-01  3.7423E-02  2.6E+02 │
 │  <6> Y=a+b•X^2     0.94830   3.9425E+00   3.3419E-06  5.5923E-07  3.6E+01 │
 │  <7> Y=a+b•SQR(X)  0.99185  -1.2505E+00   2.9247E-01  1.8782E-02  2.4E+02 │
 │  <8> Y=X/(a•X+b)   0.97412   8.4948E-02   4.7938E+01  5.5623E-00  7.4E+01 │
 │                                                                           │
 │  <N>ew curve analysis                                                     │
 │  <C>hange range of analysis                                              │
 │  <Q>uit program          For which curve are details required?           │
 └─────────────────────────────────────────────────────────────────────────┘
```

Table C.18 - Linear regression analysis on Ke vs Re for 6fpi coil and vortex width of s/2.

[a] CURFIT is a linear regression analysing program developed by the author. It establishes the best fit for eight different curves and computes the coefficient of correlation, standard error of estimate, and the F(1,n-2) distribution for each curve.

```
<1>  Y = a + b • X
Fig.      r           a            b          F(1,10)  max. deviations   range

C.3    0.98965    1.8718E+00   5.9473E-03    4.8E+02   +18.58%   -8.28%   26.86%
C.5    0.98965    1.4117E+01   4.4848E-02    4.8E+02   +18.59%   -8.28%   26.87%
C.7    0.98898    3.9524E+00   5.9094E-03    4.5E+02   +13.34%   -6.14%   19.48%
C.9    0.98989    1.7883E+01   2.6544E-02    4.9E+02   +13.24%   -8.38%   21.62%


<5>  Y = a • X^b
Fig.      r           a            b          F(1,10)  max. deviations   range

C.3    0.98704    9.3349E-02   6.4086E-01    3.8E+02   +11.32%  -12.53%   23.85%
C.5    0.98703    7.0420E-01   6.4080E-01    3.8E+02   +11.32%  -12.54%   23.86%
C.7    0.98896    2.2127E-01   5.5475E-01    4.5E+02    +8.18%  -10.44%   18.62%
C.9    0.98535    1.0716E+00   5.4424E-02    3.3E+02    +8.89%  -11.34%   20.23%


<7>  Y = a + b √ X
Fig.      r           a            b          F(1,10)  max. deviations   range

C.3    0.99031   -1.6208E+00   2.9983E-01    5.1E+02    +9.47%  -19.36%   28.83%
C.5    0.99031   -1.2220E+01   2.2610E+00    5.1E+02    +9.49%  -19.37%   28.86%
C.7    0.99261   -1.2137E+00   3.6353E-01    6.7E+02    +6.96%  -13.94%   20.90%
C.9    0.98952   -5.0871E+00   1.6252E+00    4.7E+02    +8.89%  -15.26%   24.15%
```

Table C.19 - Summary of linear regression analysis on combined test results in figures C.3, C.5, C.7, and C.9.

$$Y = 0.22127 \cdot X^{.55475 \pm (.02629)} \qquad\qquad (C.4\text{-}1)$$

```
Filename: c7ke

                  Average        Std.Dev.from Regression
Ind Var: X      1.0323E+03
Dep Var: Y      1.0053E+01       5.4520E-02

Curve 5    Y = a * X^b        a = 2.21267E-01
                              b = 5.54748E-01   se(b) = 2.6287E-02

        Number of (X,Y) pairs     =  12
        Correlation coefficient   = 0.988963
        F(1,10)                   = 445.6

Co-ord.    X            Y obs.        Y est.        Residual      % Diff

    1    2.6030E+02   5.4050E+00   4.8406E+00   -5.6442E-01   -10.44
    2    3.6260E+02   5.3780E+00   5.8178E+00    4.3976E-01     8.18
    3    5.3980E+02   6.8990E+00   7.2547E+00    3.5569E-01     5.16
    4    6.8430E+02   7.7560E+00   8.2750E+00    5.1895E-01     6.69
    5    8.1170E+02   9.2500E+00   9.0970E+00   -1.5297E-01    -1.65
    6    8.9120E+02   9.6110E+00   9.5810E+00   -2.9994E-02    -0.31
    7    1.0900E+03   1.1074E+01   1.0713E+01   -3.6067E-01    -3.26
    8    1.1500E+03   1.1148E+01   1.1037E+01   -1.1142E-01    -1.00
    9    1.4060E+03   1.2589E+01   1.2338E+01   -2.5065E-01    -1.99
   10    1.5350E+03   1.2419E+01   1.2954E+01    5.3505E-01     4.31
   11    1.6230E+03   1.3733E+01   1.3361E+01   -3.7208E-01    -2.71
   12    2.0340E+03   1.5372E+01   1.5143E+01   -2.2874E-01    -1.49
```

Table C.20 - Detailed analysis by CURFIT on test results for 6fpi,s/2 and 10fpi,s/2 curves from Fig.C.7.

The full results for Eq.(C.4-1) have been derived by CURFIT as shown in Table C.20.
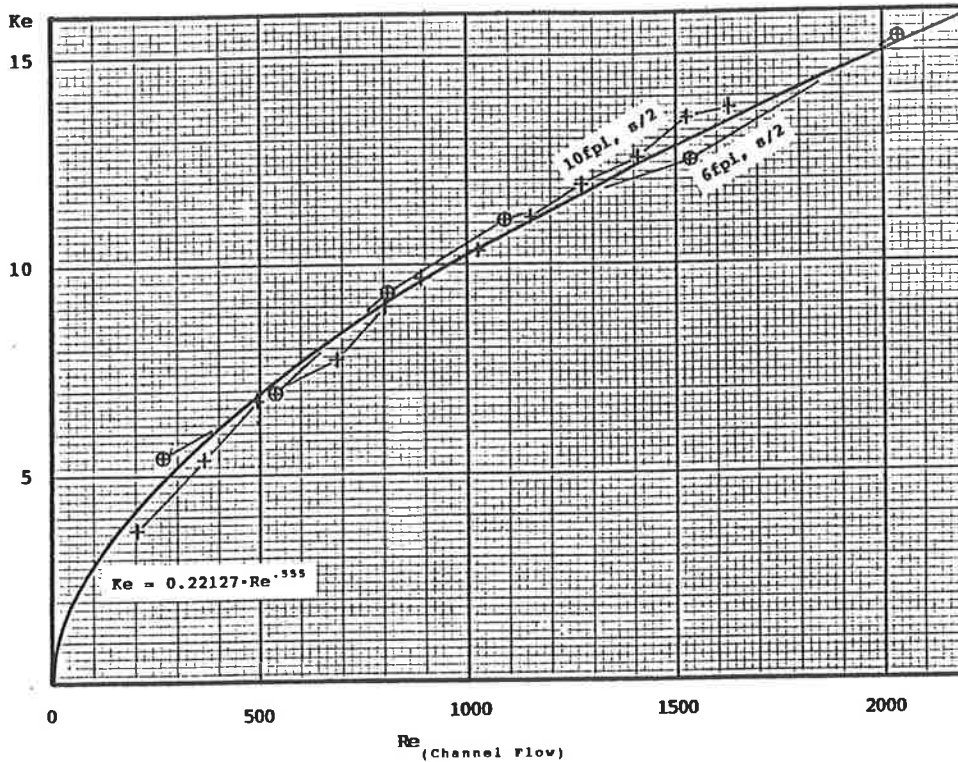
Fig.C.11 - *Plot of Eq.(C.4-2) with plots of vortex enhancement factors Ke for 6fpi and 10fpi coils, and s/2 vortex widths against Reynolds number based on channel flow.*

Fig.C.11 compares the test results for the two coils with equation

$$Ke = 0.22127 \cdot Re_{(channel)}^{.555}$$ (C.4-2)

It shows a promising correlation. However, it must be remembered that the test results were derived from fin efficiencies based on uniform heat transfer which is not strictly correct. Hence the validity of Eq.(C.4-2) remains to be tested in the transient simulation model.

C.5 SYMBOLS USED IN APPENDIX C

a	Space between tubes (Ct-Do)	- mm
Af	Face area	- m²
Afin	Fin heat transfer area	- m²
Afw	Total area for water flow	- m²
Api	Internal heat transfer area	- m²
Aprim	Primary heat transfer area	- m²
Clht	Coil height	- mm
Clwi	Coil size parallel to tubes	- mm
Cpw	Specific Heat for water	- kJ/kg K
Cr	Fin depth	- mm
Ct	Tube spacing within coil row	- mm
dH	Enthalpy difference	- kJ/kg
Dh	Hydraulic diameter	- m
Di	Tube inside diameter	- mm
Do	Effective tube outside dia.	- mm
Dp	Tube outside diameter	- mm
dTi	Total tube wall temperature gradient	- K
dTm	Log mean temperature difference	- K
dTw	Water temperature rise	- K
Fa	Air flow rate	- l/s
FP	Fin pitch	- mm
Gw	Water mass flow rate	- kg/m²s
hi	Internal heat transfer coefficient	- W/m²K
ho	External heat transfer coefficient	- W/m²K
ka	Thermal conductivity for air	- W/m K
Ke	Vortex enhancement factor	
kf	Thermal conductivity of fin material	- W/m K
kw	Thermal conductivity for water	- W/m K
L	Fin depth (R3-RO)	- mm
Ma	Air mass flow rate	- kg/s
Mw	Water flow rate	- l/s
Ncirc%	Number of parallel circuits	
Nfin%	Number of fins	
Npt%	Number of tubes fed	
Nrow%	Number of rows	
Nt%	Total number of tubes per row	
Nu	Nusselt number	
Num	Mean Nusselt number (Dh·ho/ka)	
Nu(T)∞	Nusselt number for well developed flow and constant temperature	
Nuv	Vortex Nusselt number	
Pat	Atmospheric pressure	- kPa
Pr	Prandtl number	
Qa	Sensible heat flow rate	- kW
R0	Effective tube outside radius	- mm
R3	Equivalent circular plate fin radius	- mm
Re	Reynolds number (Dh·G/μ)	
s	Space between fins (FP-xf)	- mm
t	Entering dry bulb Temperature	- °C
tpo	Mean primary surface temperature	- °C
Tr	Entering water temperature	- °C
v	Specific volume	- cu.m/kg

Vw	Water velocity	- m/s
xf	Fin thickness	- mm
xp	Tube wall thickness	- mm
y	Half fin thickness	- mm
yv	vortex width	- m

| μ | Viscosity | - Pa s |
| ∅ | Fin thermal efficiency | |

APPENDIX   D

SOFTWARE LIBRARIES

CONTENTS

Page

D.1 SOFTWARE LIBRARY OVERVIEW

Main program COILSIM and auxiliary program COILPAR have been linked with a number of sub-program libraries of which the extracts are listed in Sections D.2 to D.7 of this Appendix. Only the sub-programs used for programs COILSIM and COILPAR and those used for developing this thesis are listed.

The sub-program libraries consist of:

1. **COILSIM**
   Finned Tube Heat Exchanger Sub-Programs specifically developed for programs COILSIM and COILPAR.

2. **MISC**
   Miscellaneous Utility Sub-Programs. This library contains all the screen handling and general purpose mathematical routines.

3. **DYNSIM**[44]
   General Purpose Dynamic System Simulation Procedure. This library contains all the file handling and housekeeping routines associated with general purpose simulation and was developed as a design aid for the analysis of engineering systems.

4. **GASPARMS**[42]
   Gas Parameter Sub-Programs developed for applications to compressor plant, fluid reticulation, steam plant, refrigeration, heat transfer, and combustion processes.

5. **PSYCHRO**[43]
   Psychrometric Sub-Programs primarily developed for dynamic simulation by computer such as the application within COILSIM. The library has subsequently been linked into a main line program by the same name to replace the use of psychrometric charts.

6. **FLOWPARS**
   Fluid Flow Parameter Sub-Programs used for convective heat transfer calculations and for the development of Appendix A of this thesis.

D.2 Sub-Program Library 'COILSIM'

COILHEAD(Col%(),F%,Rel$,Ver$)
        Clears screen and writes title heading for COILSIM
        simulation program.

COILINTR(Col%(),Da$)
        Brief introduction to program COILSIM. (first panel)

SELCOILD(Col%(),Da$,Path$,Fil$,CDF%)
        Selects coil data file in specified Path and checks
        for its existence.

CRPARFIL(kc,ka,kt,Cc,Ca,Ct,Sc,Sa,St,hc,ha,ht,Kr,yw)
        Reads data file COILSIM.DAT to determine its exis-
        tence.   If it does not exist, it will be created
        with the default values set by the arguments.
        Arguments are set in main program COILPAR.

COILPARM(Col%(),Da$,Pm$,Fm$,kc,Cc,Sp,hp,kfin,Cfin,Sfin,hfin,_
        Kr,yw)
        Reads thermo-physical properties of coil materials
        from COILSIM.DAT.

COILFOOT(Col%(),FT%,Q%)
        Screen foot notes for program COILSIM.

COILDIMS(Col%(),Da$,Ti$,CFil$,Path$,Fil$,Prt$,CDF%)
        Edits and saves coil dimensions and parameters.

DEVCLPAR(Filn$,Test$,hp,hfin,Af,s,Dh,NuT,NuH,Ur,Di,Api,Vcc,_
        Ncir,Acr,R(),Cm())
        Develops coil parameters and computes fin element
        heat capacities.

SETFLOPA(Col%(),Ta,RH,Af,Ur,v,Dh,Mu,Acr,Di,Uf,Fa,Rea,Fdir$,_
        Tr,Vr,Fr,Rer)
        Interactively selects air and water quantities.

FINAREAS(T$,R(),Cx,Cr,s,Rea,Pr,Ke,Kr,Kl2,Kl3,At(),Km())
        Computes heat transfer areas of fin elements and
        their mean enhancement factors.

PROCOILD(R(),Ct,Cr,s,At(),Uf,Ur,v,Rea,Rent,Km(),Ke)
        Displays processed coil data when COILSIM is in Test
        mode.

HTRANH2O(Tr,Ta,Di,Gw,EnL,Rfi,Pr,Re,Nu(),Ui())
        Heat transfer coefficients for water inside tubes.

TCFINELS(R(),kfin,xf,Nt%,Nfin%,Cm(),TCf())
        Heat transfer time constants between fin elements.

Sub-Program Library 'COILSIM' *(continued)*

TCH2OFIN(Test$,Fr,Acr,Clwi,Tr,Ta,Di,Rfi,Api,Vcc,Cm(),Trf(),_
       Tfr())
       Heat transfer time constants between tubes and water.

TCAIRFIN(hn,Km(),Cm(),Rfo,At(),Uod(),Tfa())
       Heat transfer time constants between fin elements and air stream.

TCONSMIN(Test$,TCf(),Trf(),Tfr(),Tfa(),Clwi,Vr,DTmax)
       Establishes the minimum time constant for heat transfer and consequently the maximum integration interval.

CHWREDIS(C$,Fdir$,Nrow%,Clwi,Vr,Tr,DT,Tr(),Tout,Nc%)
       Chilled Water redistribution between coil rows for various circuit configurations.

HTCOEFFS(Pat,Ts,Uod,yw,Sb,Cp,hw,Uow)
       Heat Transfer Coefficients for wet fins.

DISPEXPS(Tr,Cw,Vcc,Cwr,DT,Ef(),Efad())
       Displays temperature iteration parameters.

PRNTHEAD(Fil$,BF$,Rel$,Ver$,Da$,Ti$)
       Prints Heading for COILSIM Coil Data Files.

PRNTOUTP(Col%(),Prt%,Prt$,FILE$,FPAR$,CoilPrt$)
       Print output option panel.

COILCRGT(Col%(),Da$)
       COILSIM program information and Copyright statement.

D.2.1 Symbols used in Sub-Program library 'COILSIM'

Acr	Total internal area/row for fluid flow	- m²
Af	Face area of coil	- m²
Api	Inside surface area of tubes per row	- m²
At(e)	Total area of fin elements(e)	- m²
Ca	Specific heat of aluminium	- kJ/kg K
Cc	Specific heat of copper	- kJ/kg K
CDF%	Coil data file status, 0=create new file, 1=existing file.	
Cfin	Specific heat of fin material	- kJ/kg K
Cm(e)	Heat cap. of fin elements(e) per row	- J/K
Col%(2,6)	Colour codes for the monitor derived from MISC	
Cr	Centre distance between rows	- mm
Ct	Specific heat of alternative material	- kJ/kg K
Cx	Centre distance between tubes	- mm
Dh	Hydraulic diameter	- m
Di	Tube inside diameter	- mm
F%	Flag for screen footer, 0=no footing, 1=surround for foot notes.	
Fa	Air flow rate	- l/sec
Fdir$	Fluid flow direction: <C>ounter flow <P>arallel flow	
Fil$	Filename without path or extension identification.	
Filn$	Complete data filename with path and extension.	

Fm$	fin material: <A>luminium
	                        <C>opper
	                        <O>ther, def'd in COILPAR	

Fr	Water flow rate	- l/s
FT%	Screen foot note identifyer.	
Gw	Mass velocity of fluid in pipes	- kg/m² s
ha	Heat capacity of aluminium	- J/cc K
hc	Heat capacity of copper	- J/cc K
hfin	Heat capacity of fin material	- J/cc K
hp	Heat capacity of tube material	- J/cc K
ht	Heat capacity of alternative material	- J/cc K
ka	Thermal conductivity for aluminium	- W/m K
kc	Thermal conductivity for copper	- W/m K
Ke	Vortex enhancement factor	
kfin	Thermal conductivity of fin material	- W/m K
Km(e,c)	Mean enhancement factors.	
Kr	Reduced heat transfer factor for fins.	
kt	Thermal conductivity for alt. material	- W/m K
Mu	Dynamic viscosity (also Pa s or N s/m²)	- kg/m s
Ncir	Number of parallel circuits per row.	
NuH	Nusselt number for constant heat rate.	
NuT	Nusselt number for constant surface temp.	
Path$	Path description.	

Pm$	tube material: <A>luminium
	                          <C>opper
	                          <O>ther, def'd in COILPAR	

Pr	Prandtl number = Cp μ/k (dimensionless)	
Q%	ASCII value of upper case key stroke.	

Symbols used in Sub-Program library 'COILSIM' *(continued)*

R(e)	Outer boundary rad. for fin element(e)	- m
Rea	Reynolds No. for air (Channel flow)	
Rent	Reynolds No. for air (entering coil)	
Rel$	Program release date.	
RH	Relative humidity	- %
s	space between fins = Channel height	- m
Sa	Specific gravity of aluminium	- g/cc
Sc	Specific gravity of copper	- g/cc
Sfin	Specific gravity of fin material	- g/cc
Sp	Specific gravity of tube material	- g/cc
St	Specific gravity of alt. material	- g/cc
T$	Tube arrangement: <I>n line <S>taggered	
Ta	Air dry bulb temperature	- C
Test$	Flag for program test mode.	
Tr	Water temperature entering tubes	- C
Uf	Face velocity	- m/s
Ur	Mean air flow velocity ratio.	
v	Specific volume	- cu.m/kg
Vcc	Volume of fluid inside tubes per row	- cu.cm
Ver$	Program version identification.	
Vr	Water velocity inside tubes	- m/s
yw	film thickness of water	- mm

D.3 Sub-Program Library 'MISC'

TONE(PC%,MS%)
>   Sound generator using the system timer

EDITKEY(FC%(),RC%)
>   Keystroke arbitrator for BASIC and BASCOM

EDITCODE(Col%(),RC%,C%,Qi%,Nx%)
>   Processes return code from EDITKEY

SETCOLOR(Col%())
>   Stores and passes colour combinations

FOOTPANL
>   Establishes surround for foot notes.

DISPTEXT(Col%(),F$)
>   Displays ASCII Text Files on the screen. Page
>   breaks (Ctrl-L) for the printer are ignored on the
>   screen. Page breaks for the screen are triggered by
>   the null character CHR$(255).

FXPOLYNO(XJ,PB#(),N%,YJ)
>   Computes the numerical value of f(X) for any X from
>   Polynomial coefficients using the Horner's scheme.

POLYDEG4(A,B,C,D,E,Xp,Yp)
>   Solves polynomial equations up to 4th degree.
>   A - E = Polynomial coefficients
>   Xp   = Independent variable
>   Yp   = Dependent (calculated) variable

MISCFOOT(Col%(),FT%,Q%)
>   General screen footing display.

QUITPROG(Col%(),Q%)
>   Controls 'Quit Program' with verification.

DATETIME(Da$,Ti$)
>   Sets the Date and Time from the Computer Clock.

TESTPATH(Col%(),Pname$,PS%)
>   Tests the validity of the Path specification and its
>   availability.

SELPATHN(Col%(),Path$,Nx%)
>   Selects Drive and/or path name for data files and
>   checks its validity.

CHKDRIVE(Col%(),DR$,DSTAT%)
>   Checks the validity of the drive specification in
>   sub-program SELPATHN. Allows drive id. from A to T.

CHECKFIL(File$,Op%,JF%)
        Checks the existence and access of a given data file
        for a given path.

SELDATFL(Col%(),Rs$(),Path$,Fi$,Ext$,Fd$,Sel%,JF%,Nx%)
        Interactively selects a data filename for a speci-
        fied path and checks for its existence.   Path name
        will be established and tested in SELPATHN.

STORFILN(Fil$,OF$,NF$)
        Stores Old and New Path and filenames, OF$ and NF$
        in a nominated data file Fil$.

D.3.1   Symbols used in Sub-Program library 'MISC'

Symbol	Description
C%	Numeric keypad identification from EDITKEY.
Col%(2,6)	Colour codes for the monitor set by SETCOLOR.
Da$	Computer date.
DR$	Drive specification.
DSTAT%	Disk drive status (Error code).
DT%	Duration for TONE.
Ext$	Filename extension identification.
F$	Text file name.
Fi$	Filename without path or extension identification.
File$	Path and/or filename.
FT%	Screen foot note identifyer.
JF%	Returned error code.
N%	Degree of polynomial.
NF$	New filename.
Nx%	Sub-program return code: 0=Continue, 1=Quit procedure.
OF$	Old filename.
Op%	File operator code: 1=Open for O/P, 2=Open for I/P, 3=Open printer port.
Path$	Path description.
PB#(25)	Polynomial coefficients (double precision).
PC%	Period count for TONE (determines frequency).
Pname$	Drive and/or path name.
Q%	ASCII value of upper case key stroke.
RC%	Return code from EDITKEY.
Ti$	Computer time.
XJ	Input variable to polynomial routines FXPOLYNO and POLYDEG4.
YJ	Output from polynomial routines FXPOLYNO and POLYDEG4.

D.4 Sub-Program Library 'DYNSIM'

DFILNAME(Col%(),Sel%,Path$,Fil$,FILE$,FPAR$)
>   Interactively sets and checks path specification and
>   data filenames for DYNSIM simulation procedure.

INTEGPAR(Col%(),RK%,TIME,DTmax,DT,PT,TL,IM)
>   Sets integrating parameters for DYNSIM simulation
>   procedure.

OPDATFIL(FILE$,FPAR$,NC%)
>   Opens data files for DYNSIM simulation procedure.

SIMULSCR(Col%(),TL,ND%,VND$())
>   Sets screen display during simulation procedure.

RANDATST(TIME,DT,PT,IM,SD%,CNT%,ND%,NC%,BD(),BN())
>   Random-Access data storage for DYNSIM simulation
>   procedure.   Writes data in previously created
>   Random-Access Data Files which can be subsequently
>   analysed by using the Simulation Analysing Programs.

EXITROUT(Col%(),NC%,CNT%,DT,PT,TIME,TL,Nx%)
>   Exit procedure for DYNSIM.

RDDYNCTR(PC$,FC$,Path$,File$)
>   Reads control data file PC$+FC$+".CTR".

WRDYNCTR(PC$,FC$,Path$,File$)
>   Writes control data to file PC$+FC$+".CTR"

D.4.1 Symbols used in Sub-Program library 'DYNSIM'

A#(25)	Polynomial coefficients for FXCHEBYS or FXPOLYNO
A to E	Single precision polynomial coeff's for POLYDEG4
B(50)	Variable array
BD(6)	Variables selected for display during simulation
BN(32)	Variables selected for data storage
BF$	Filename (without path or extension id.)
CNT%	Simulation storage counter
Col%(2,6)	Colour codes for the monitor derived from MISC
ConFil$	Data file storing controller settings
D%(6)	Variable selected for display during simulation
Da$	Computer date
DR$	Drive identification for data files
DT	Integration interval
DTmax	Maximum integration interval
EO	General sub-program exit value.
	(also used for passing on previous output)
E1-E3	Local input values
F%	Screen footing status, 1=on, 0=off
FILE$	Data storage filename
FPAR$	Parameter filename
IM	Order of integration time
NC%	Number of variables to be stored
NCon%	Number of PID Controllers in simulated system
ND%	Number of variables for display during simulation
NI%	Integration loop counter
NVAR%	Number of variables identified for storage
Path$	Path description
P1-P5	Local parameters (real values)
P1%-P5%	Local parameters (integer values)
PT	Data storage interval
Rel$	Release date
RK%	Order of integration, 1, 2, or 4
SD%	Display interval during simulation
Sel%	
T%(32)	Variables to be stored
TIME	Simulation time
Titl$	Program title up to 46 characters long
TL	Maximum simulation time set by user
Ver$	Version identification
VN$(50)	Variable names up to 8 characters long
VND$(6)	Names of variables selected for display during simulation
VNN$(32)	Names of variables selected for storage
X	Input variable to FXCHEBYS, FXPOLYNO, or POLYDEG4
Y	Output from FXCHEBYS, FXPOLYNO, or POLYDEG4

D.5   Sub-Program Library 'GASPARMS'

INTOHM11(Tred,Ohm11)
>   Computes the integral $\Omega(1,1)*$ which is used for cal-
>   culating the Transport Coefficients for the Lennard-
>   Jones (6-12) potential.

TRANCOEF(Tred,Fmu,Fk,FDf)
>   Interpolates the functions for calculating the
>   higher approximations to the Transport Coefficients
>   of pure substances for the Lennard-Jones (6-12)
>   Potential.

DFH2OAIR(Tgas,Pgas,Dfad)
>   Diffusion Coefficient for Water Vapour in Air - m^2/s

CPAIRGAS(Tgas,Pgas,Cp)
>   Specific Heat of air in gaseous state as a function
>   of temperature and pressure. (90K to 5000K).

CPH2OGAS(Tgas,Cp)
>   Specific Heat of water vapour (dry steam) for the
>   temperature range of 100K to 5000K.

AIRGPROP(t,Mu,kt,Cp,Cv,gamma,Pr)
>   Real-Gas thermodynamic properties of air at atmos-
>   pheric pressure for the temp. range of 85K to 1000K.

H2OGPROP(t,Mu,kt,Cp,Cv,gamma,Pr)
>   Thermodynamic properties of dry steam at atmospheric
>   pressure for the temperature range of 373K to 1000K.

H2OLPROP(t,Mu,kt,Cp,Pr)
>   Thermodynamic properties of water for the tempera-
>   ture range of 273K to 647K.

D.5.1   Symbols used in Sub-Program library 'GASPARMS'

Cp	specific heat at constant pressure	- kJ/kg K
Cv	specific heat at constant volume	- kJ/kg K
Dfad	diffusion coefficient for water vapour in air	- m^2/s
FDf	functions for the higher approximation to Df	
Fk	functions for the higher approximation to k	
Fmu	functions for the higher approximation to Mu	
gamma	specific heat ratio Cp/Cv	
kt	thermal conductivity	- W/m K
Mu	coefficient of viscosity (dynamic)	- Pa s
	(alternative units are kg/m s and N s/m^2)	
Ohm11	Integral $\Omega(1,1)*$	
Pgas	gas pressure	- kPa
Pr	Prandtl number = Cp·Mu/kt (dimensionless)	
T	absolute temperature	- K
t	temperature	- °C
Tgas	gas temperature	- K
Tred	reduced temperature $T* = kT/\epsilon$	- K

D.6 Sub-Program Library 'FLOWPARS'

KARMANIK(Re,f)
> Karman-Nikuradse Fanning friction factor relation for fully developed turbulent flow in smooth circular tubes.

FCIRCDEV(Re,f,ft)
> Fanning friction factor for fully developed laminar or turbulent flow in smooth circular tubes. In the range of 2100 < Re < 4000, ft is interpolated as f(ln(Re)).

FRECTDEV(Re,a,s,f,ft,fRn)
> Fanning friction factor for fully developed laminar or turbulent flow in smooth rectangular tubes. In the range of 2100 < Re < 4000, ft is interpolated as f(ln(Re)).

FCIRCENT(Re,x,Di,f,ft,fRn)
> Fanning friction factor for developing laminar or turbulent flow in smooth circular tubes. In the range of 2100 < Re < 4000, ft is interpolated as f(ln(Re)).

FRECTENT(Re,x,a,s,f,ft)
> Fanning friction factor for developing laminar or turbulent flow in smooth rectangular tubes. In the range of 2100 < Re < 4000, ft is interpolated as f(ln(Re)).

CURVEFAC(Re,Di,R,kcur,ktran)
> Fanning Friction Factor Ratio for curved tubes.

NUCIRDEV(Re,Pr,NuT,NuH,Nu)
> Nusselt numbers for fully developed laminar or turbulent flow in smooth circular tubes.

NURECLAM(a,s,NuT,NuH,Nu)
> Nusselt numbers for fully developed laminar flow in smooth rectangular ducts and parallel plates.

NURECTUR(Re,Pr,NuT,NuH,Nu)
> Nusselt numbers for turbulent flow in smooth rectangular ducts.

NURECDEV(Re,Pr,a,s,NuT,NuH,Nu)
> Nusselt numbers for fully developed laminar or turbulent flow in smooth rectangular ducts and between parallel plates.

NUXTLAMC(x,Dh,Re,Pr,xplus,Nux)
> Local Nusselt number for laminar flow, constant surface temperature in thermal entry length of smooth circular tubes.

Sub-Program Library 'FLOWPARS' *(continued)*

NUMTLAMC(x,Dh,Re,Pr,xplus,Num)
     Mean Nusselt number for laminar flow, constant sur-
     face temperature in thermal entry length of smooth
     circular tubes.

NUXHLAMC(x,Dh,Re,Pr,Nuinf,xplus,Nux)
     Local Nusselt number for laminar flow, constant heat
     rate in thermal entry length of smooth circular
     tubes.

NUXTLAMP(x,Dh,Re,Pr,xplus,Nux)
     Local Nusselt number for laminar flow, constant sur-
     face temperature in thermal entry length of smooth
     parallel plates.

NUMTLAMP(x,Dh,Re,Pr,xplus,Num)
     Mean Nusselt number for laminar flow, constant sur-
     face temperature in thermal entry length of smooth
     parallel plates.

NUCURTUB(Re,Di,R,Pr,Nu,Nutran)
     Nusselt numbers for fully developed laminar or tur-
     bulent flow in smooth circular curved tubes.

ENCIRLAM(x,Dh,Re,Pr,xplus,ke)
     Heat transfer enhancement for laminar flow in ther-
     mal entry length of smooth circular tubes.

ENCIRTUR(x,Dh,Re,Pr,ke)
     Heat transfer enhancement for turbulent flow in
     thermal entry length of smooth circular tubes.

ENRECLAM(a,s,x,Re,Pr,xplus,ke)
     Heat transfer enhancement for laminar flow in ther-
     mal entry length of smooth rectangular ducts or
     parallel plates.

D.6.1 Symbols used in Sub-Program Library 'FLOWPARS'

a	channel or duct width (set to 0 for infinite parallel plates at spacing s)	- m
Dh	hydraulic diameter	- m
Di	tube inside diameter	- m
f	Fanning friction factor	
ft	mean friction factor for transient flow	
fRn	product f · Re	
kcur	friction factor ratio in curved tube	
ke	enhancement factor Num/Nu∞	
ktran	transient fric. fac. ratio in curved tube	
Nu	Nusselt number = h Dh / k	
NuH	Nusselt number for constant heat rate	
NuT	Nusselt number for constant surface temp.	
Nux	local Nusselt number at x	
Num	mean Nusselt number over distance x	
Nuinf	Nu∞ = Nusselt number for developed flow	
Nutran	mean Nusselt number for transient flow	
Pr	Prandtl number = Cp μ/k (dimensionless)	
R	radius of curvature at centre line	- m
Re	Reynolds number = Dh G/μ (dimensionless)	
s	space between fins or Channel height	- m
x	distance from pipe or duct entry	- m
xplus	x^+ = 2·(x/Dh)/(Re·Pr)	

D.7 Sub-Program Library 'PSYCHRO'

PSYCHEAD(Col%(),F%,Rel$,Ver$)
    Clears screen and writes title heading for
    Psychrometric Program.

PSYCFOOT(Col%(),FT%,Q%)
    Foot notes for program PSYCHRO

PSKEEKEY(tsat,Psat)
    Computes water vapour pressure Psat for temperature
    tsat with the Keenan and Keyes empirical equation
    for the temperature range of 0.01 to 374.15°C.

PSATASME(Tsat,Psat)
    Computes water vapour pressure Psat for temperature
    Tsat with the ASME equation for the temperature
    range of 273.16 to 647.30K (0.01 to 374.15°C).

PSATHYWE(Tsat,Psat)
    Computes water vapour pressure Psat for temperature
    Tsat with the Hyland and Wexler empirical equations
    for the temperature range of 173.15 to 473.15K.
    (-100 to 200°C)

PSATH2O(tsat,Psat)
    Computes the saturation vapour pressure Psat for
    water at given temperature tsat by using the follow-
    ing sub-programs:
        PSATHYWE for tsat = -120 to 0.0°C
        PSKEEKEY for tsat = 0.01 to 177°C
        PSATASME for tsat = 177 to 374.15°C

ENTWATFG(t,hf,hfg,hg)
    Computes the specific enthalpies for water substance.

ENHANCFS(P,t,fs)
    Computes the Enhancement factor fs as a function of
    total pressure p and temperature t by empirical
    equations. The application of fs allows an exact
    solution for Ws.

DEWPOINT(Pw,td)
    Establishes the dewpoint temperature td in °C as a
    function of the water vapour partial pressure Pw kPa

MOISTAIR(P,t,W,h,ha,Cp)
    Enthalpy and specific heat of moist air.

SATURAIR(t,Pat,Ws,va,vas,vs,ha,has,hs,Cps)
    Thermodynamic properties of saturated moist air.

Sub-Program Library 'PSYCHRO'   *(continued)*

DRYWETMP(t,tw,P,W,RH,v)
> Moist air properties from dry bulb and wet bulb
> temperatures, and total mixture pressure.   When W<0
> then tw is out of range.

DRYDETMP(t,td,P,W,RH,v)
> Moist air properties from dry bulb and dewpoint
> temperatures, and total mixture pressure.

DRYTMPRH(t,RH,P,W,v)
> Moist air properties from dry bulb temperature, rel-
> ative humidity, and total mixture pressure.

WETBULBT(t,RH,P,tw)
> Wet bulb temperature from dry bulb temperature and
> relative humidity.

PSYCHROS(Col%(),Pn$,Pt,Ta,Tw,td,RH,W,Ws,v,rho,h,Cp,Pws,Pw)
> Calculates properties of air/water vapour mixtures
> at any atmospheric pressure.

ELEVATIO(Col%(),Alt)
> Displays tables of elevations for selected
> locations.

ENTHSATN(Ts,Pat,hs,Ws,Cp)
> Enthalpy and Specific Heat of moist air at
> Saturation Temperature.

LEWISREL(tm,Pat,alpha,Df,Le)
> Lewis relation for water vapour in air.

ENTHWDRY(h,W,Ta)
> Computes dry bulb temperature Ta C from enthalpy
> and humidity ratio.

HUMDRYRH(Pat,W,Ta,RH)
> Computes relative humidity from atmospheric
> pressure, humidity ratio, and dry bulb temperature.

HUMRATIO(Tao,Ts,Pat,Wrow,hrow,delth,Wx)
> Ratio dh/dW

D.7.1 Symbols used in Sub-program Library 'PSYCHRO'

Cp	spec. heat of moist air at con.press.	- kJ/kg K	
Cps	spec. heat of moist air at saturation	- kJ/kg K	
fs	Enhancement factor for humidity calcs.		
h	specific enthalpy for moist air	- kJ/kg	
ha	specific enthalpy for dry air	- kJ/kg	
has	hs - ha	- kJ/kg	dry air
hf	specific enthalpy for saturated liquid	- kJ/kg	
hfg	latent heat of evaporation = hg - hf	- kJ/kg	
hg	specific enthalpy for saturated vapour	- kJ/kg	
hs	enthalpy of moist air at saturation	- kJ/kg	dry air
P	total mixture pressure	- kPa	
p	total mixture pressure	- Pa	
Pat	atmospheric pressure	- kPa	
Psat	saturation vapour pressure	- kPa	
Pw	water vapour partial pressure	- kPa	
RH	relative humidity	- %	
t	dry bulb temperature	- °C	
td	dew point temperature	- °C	
tw	wet bulb temperature	- °C	
Tsat	temperature at saturation pressure	- K	
tsat	temperature at saturation pressure	- °C	
v	specific volume of moist air	- m^3/kg	dry air
va	specific volume of dry air	- m^3/kg	
vas	vs - va	- m^3/kg	dry air
vs	spec.vol. of moist air at saturation	- m^3/kg	dry air
W	humidity ratio	- kg/kg	dry air
Ws	humidity ratio at saturation	- kg/kg	dry air